Propulsion System Integration of a Parallel Through The Road Hybrid Electric Vehicle

Propulsion System Integration of a Parallel Through The Road Hybrid Electric Vehicle

By

Andrew R. George, B.Eng.

A Thesis

Submitted to the School of Graduate Studies

in Partial Fulfilment of the Requirements for the Degree

Master of Applied Science

McMaster University

Lay Abstract

As Hybrid Electric Vehicles continue to grow in market share, the Advanced Vehicle Technology Competition series seeks to challenge and train students in this booming industry. The current competition in this series is the EcoCAR Mobility Challenge, where students must re-engineer a 2019 Chevrolet Blazer into a hybrid vehicle over four years. The vehicle is to incorporate new autonomous technologies, as well as be targeted at a car sharing application. The McMaster University Engineering EcoCAR team has entered into this competition.

This thesis describes the detailed mechanical design of the new vehicle. This begins by examining the selected hybrid layout, or architecture. Then the design process of individual systems is shown, with emphasis on how each system meets the McMaster team goals. Then the current state of the vehicle is shown, and delays due to COVID-19 are discussed. Finally, a testing plan is proposed, to ensure all systems can meet their design goals.

Abstract

This thesis outlines the mechanical design and integration of a P0/P4 Parallel Through-the-Road Hybrid Electric Vehicle. The vehicle is McMaster University's entrant into the EcoCAR Mobility Challenge, the current offering of the long running Advanced Vehicle Technology Competition series. The competition challenges students to electrify a 2019 Chevrolet Blazer, while meeting the needs of a car sharing platform.

The design of the McMaster vehicle will be explored, starting with a walkthrough of the architecture selection process performed in the first year of competition. The design process of both powertrains will be examined, starting with component selection and working up to assembly integration. Particular attention will be paid to the rear electrified powertrain, which has been designed from the ground up for this purpose, including custom single speed gear reduction.

The current integration status of the vehicle will be shown. Timeline delays due to the COVID-19 pandemic will be discussed, as well as next steps to move towards complete vehicle integration. A vehicle testing plan will be put forward, using the cutting edge systems available at the McMaster Automotive Resource Center.

Acknowledgments

This research was undertaken, in part, thanks to funding from the Canada Research Chair in Transportation Electrification and Smart Mobility, Natural Sciences and Engineering Research Council of Canada (NSERC), McMaster Engineering EcoCAR Mobility Challenge Program, and General Motors (GM).

Thank you to my supervisor Dr. Emadi for giving me this opportunity, and helping me reach my full potential here at McMaster.

Thank you to the EcoCAR team for six years of amazing experiences. I wish all of the members luck in their future endeavors. Good luck to Shiva, Colleen, Ethan, and Sam as they take up the mantle, I am excited to see what you do with it.

Thank you to my family and friends for their ongoing and relentless support. In particular my parents, Gerry and Pat George, for the support they have given me throughout my entire life. I would not have made it here without you.

List of Acronyms

AAM American Axle & Manufacturing

ACC Adaptive Cruise Control

ANL Argonne National Laboratory

AVTC Advanced Vehicle Technology Competition

AWD All Wheel Drive

BAS Belted Alternator Starter

BCM Body Control Module

BEV Battery Electric Vehicle

BSG Belted Starter Generator

CAD Computer Aided Design

CAFE Corporate Average Fuel Economy

CAN Controller Area Network

CAV Connected and Automated Vehicle

CI Compression Ignition

CMM Coordinate Measurement Machine

CNC Computer Numerical Control

CUV Crossover Utility Vehicle

CV Constant Velocity

DOE Department of Energy

ECM Engine Control Module

E&EC Emissions and Energy Consumption

EMC EcoCAR Mobility Challenge

EM Electric Motor

EPA Environmental Protection Agency

ESS Energy Storage System

ETRS Electronic Transmission Range Selection

EV Electric Vehicle

FEA Finite Element Analysis

FEAD Front End Accessory Drive

FWD Front Wheel Drive

GHG Green House Gas

GM General Motors

GTHA Greater Toronto Hamilton Area

HESS Hybrid Energy Storage System

HEV Hybrid Electric Vehicle

HTSR Heat Treated Stress Relieved

HV High Voltage

HVAC Heating, Ventilation, and Air Conditioning

I4 Inline-4

ICE Internal Combustion Engine

ISG Integrated Starter Generator

ISO International Organization for Standardization

IVM Initial Vehicle Motion

IWM In-Wheel Motor

LKA Lane Keeping Assist

LSD Limited Slip Differential

LV Low Voltage

MaaS Mobility as a Service

MARC McMaster Automotive Resource Centre

MSU Mississippi State University

NA Naturally Aspirated

NDA Non Disclosure Agreement

NiMH Nickel-Metal Hydride

NVH Noise, Vibration, and Harshness

OEM Original Equipment Manufacturer

PCM Propulsion Controls and Modeling

PEU Petroleum Energy Usage

PHEV Plug-in Hybrid Electric Vehicle

PSI Propulsion System Integration

PTU Power Transfer Unit

RDU Rear Drive Unit

SAE Society of Automotive Engineers

SUV Sport Utility Vehicle

TCM Transmission Control Module

TTR Through-The-Road

UW University of Wisconsin

V2X Vehicle-to-Everything

VTS Vehicle Technical Specifications

WOT Wide Open Throttle

WTW Well to Wheel

Table of Contents

List of Figures

List of Tables

Chapter 1

Introduction

1.1 Hybrid Electric Vehicles: Current Status & Future Trends

As the world's population becomes increasingly aware of and active towards reducing climate change, increased conversion to Electric Vehicles (EVs) is one of the main avenues to reduce Green House Gas (GHG) emissions. According to the US Environmental Protection Agency (EPA), 29% of GHG emissions in 2017 came from the transportation sector, of which 59% was from light duty vehicles [1]. This shows the large impact consumer vehicles have on global GHG emissions, and the effect a large scale move towards electric and hybrid vehicles could have.

EV is somewhat of an unspecific term, and so more specific categories are used to differentiate different levels of vehicle electrification. Hybrid Electric Vehicles (HEVs) are powered by both a conventional Internal Combustion Engine (ICE) and one or more Electric Motors (EMs). They do not possess the battery capacity to have a dedicated electric only driving mode. The ICE and EM work together to power the vehicle, resulting in increased fuel economy. Plug-in Hybrid Electric Vehicles (PHEVs) are simply HEVs with a large enough battery capacity to justify an electric only driving mode, and therefore can be plugged in to charge in order to prevent charging via the ICE. This allows them to function as pure EVs over short trips, and as HEVs over longer ones. This significantly increases the potential fuel savings of the vehicle. Battery Electric Vehicles (BEVs) operate exclusively via EMs, powered via an on-board battery. This entirely eliminates fuel consumption from the vehicle, making the type of electricity generation the driving force behind GHG emissions.

Over recent years, sales of EVs worldwide have increased. Measured by percentage of total vehicle sales in the United States, HEVs have increased to 2.4% in 2019 from 2.0% in 2018 [2], [3]. BEVs and PHEVs together are down slightly to 1.9% from 2.1%. In Canada, 2018 marked a massive increase of BEV and PHEV sales to 2.2% from 1.0% the previous year [4]. HEVs increased to 1.3% from 1.1% [4].

These increases in hybrid and EV adoption are due in part to the increase in model options on the market. There are now 43 HEV and 57 BEV or PHEV models offered on the U.S. market [2]. This increase in choice allows a wider market segment to meet their transportation requirements with a hybrid or electric vehicle. Major automakers continue to expand these electrified vehicle ranges. General Motors (GM) has committed 20 new models by 2023 [5], while Ford has committed 40 by 2022 [6].

A major reason for this increase in hybrid and EV models is increasing emissions standards across the world. In 2012 the Obama administration implemented stricter Corporate Average Fuel Economy (CAFE) standards, resulting in a 54.5 mpg (4.3 L/100km) target by 2025 [7]. Two major ways to improve the average fleet economy are to electrify more vehicle models into hybrids, and to add more pure BEVs. The Trump administration loosened these standards to 40.4 mpg (5.8 L/100km) by 2025

[8]. In response, California along with 22 other states have sued the EPA in an attempt to retain their current rights to set state specific fuel efficiency standards [9]. Canada defines its standards in grams of CO_2 per mile produced by a vehicle [10]. Canada has up to this point maintained its standards to be equivalent to those of the older and stricter USA CAFE standards. During the midterm review of the Canadian standards, several regulated companies suggested Canada maintain alignment with current US standards [11]. They argue the Canadian market cannot remain competitive if regulations differ from the US, as economies of scale for technology improvements to meet these requirements do not work in the small Canadian market. Other organizations argue that in terms of the global marketplace, maintaining higher standards keeps Canada competitive due to the increased demand for lower emission vehicles, and encourages new technologies to be developed in Canada. It was also suggested that Canada could align its standards with other stringent markets, such as California or Europe. Thirteen states and the District of Columbia have directly followed California's emissions standards, and together account for 43% of the US automotive market [12]. Combined with Canada this makes up 51.5% of the combined Canada-US market. This should represent a large enough demand to justify the production of low-emission vehicles by major automakers.

As vehicles become more electrified they are also becoming more connected, leading to the rise of Connected and Automated Vehicles (CAVs). These vehicles are usually defined by using Society of Automotive Engineers (SAE) Levels of Autonomy which range from 0 to 5. A vehicle at level 0 has no autonomous features, up to a level 5 which is a fully autonomous vehicle [13]. Current production vehicles with these features can achieve between level 2 and 3 autonomy. This usually takes the form of Adaptive Cruise Control (ACC), Lane Keeping Assist (LKA) and Park Assist as the main features. These technologies are not limited to EVs, however these vehicles do have inherent advantages for autonomy implementation. EMs can be controlled with a much higher level of precision as compared to ICEs, which allows easier integration with sensor systems. As the autonomy of vehicles increases, the desire for more connectivity also increases. This is where Vehicle-to-Everything (V2X) communication technology becomes important. Future vehicles will be able to communicate with other vehicles, infrastructure, cloud services and more. Together with autonomous driving this will revolutionize how vehicles are used.

Leveraging the above technology, vehicles have begun shifting towards a Mobility as a Service (MaaS) model. Specific to the automotive industry this is a model where vehicles are not privately owned, but can be used when needed. Companies such as Uber and Lyft are examples of ride-hailing services, essentially replacing taxis in their function [14]. Ride-sharing services look to emulate carpooling, and can be seen in specific offerings such as UberPool and Lyft Shared. Car-sharing is seen in companies such as Car2Go and Zipcar. These operate as short term car rentals, allowing consumers to have access to a car without the associated maintenance and storage costs. Looking into the future, these car-sharing services would be fully integrated into a larger MaaS system, allowing consumers to interact with all transport modes via a single app [15]. This would truly revolutionize the transportation system.

1.2 EcoCAR Competition & Thesis Objectives

This research was completed as a result of McMaster University's involvement in the EcoCAR Mobility Challenge (EMC). The EMC is the 12$^{\text{th}}$ competition in the long running Advanced Vehicle Technology Competition (AVTC), sponsored by the US Department of Energy (DOE). This competition series began in 1988 with the Methanol Marathon [16]. The competitions serve to stimulate students to pursue careers in the automotive industry, push the boundaries of innovative automotive technologies, and bridge the gap between theoretical classroom and hands-on experience. This is accomplished through automotive industry partners, that allow students access to real world scenarios and constraints. The McMaster Engineering EcoCAR team consists of over 100 mainly undergraduate students, ranging across the majority of engineering disciplines and all years of study. The MAC team is divided into three competition required sub-teams, Propulsion System Integration (PSI), Propulsion Controls and Modeling (PCM), and CAV. MAC then chooses to further split PSI into mechanical and electrical sub-teams.

The current EMC competition is centered around the redesign of a 2019 Chevrolet Blazer. The competition is headline sponsored by the DOE, GM and Mathworks, and managed by Argonne National Laboratory (ANL). Over the four year long competition, 12 North American schools are tasked to redesign the Chevrolet Blazer into a hybrid vehicle targeted at a car sharing application, including the design of SAE Level 2 autonomous features. This brings together the expected future trends of the automotive industry into one project. Hybrid technology, MaaS applications, and CAV features are all large components of this student competition. EMC is the second AVTC competition the MAC team has competed in. The first was the EcoCAR 3 competition, which similarly was a four year competition to redesign a 2016 Chevrolet Camaro. Results from the competition will be further discussed in Section 2.3.

The new Chevrolet Blazer is marketed by GM as a mid-size Sport Utility Vehicle (SUV), however it is more accurately categorized as a Crossover Utility Vehicle (CUV). This is due to its unibody construction, as opposed to the body on frame construction of traditional SUVs [17]. This lends relevancy to the current automotive market. As of September 2017 CUVs have outsold cars and continue to rise in market share [18]. Cars in this context is a class that includes sedans, hatchbacks and sports cars.

Year 1 of the EMC focused on architecture selection, which will be reviewed in Chapter 3. Year 2 of the competition focused on powertrain design and integration, with the goal of complete integration by May 2020. This entails the design of all mechanical and electrical systems to meet the chosen architecture. The systems must then be manufactured, tested, and integrated into the vehicle. Vehicle controls for these systems must be developed for basic functionality. Goals for the end of Year 2 are for all propulsion systems to safely produce torque, to pass vehicle inspection and attempt all dynamic events at competition. The mechanical design and integration of the vehicle is the subject of this thesis. The objectives of the thesis are simply a subset of the competition goals, to design, manufacture and integrate the mechanical components of the hybrid propulsion system, along with all auxiliary systems, into the vehicle.

1.3 Thesis Organization

This thesis begins with a literature review of existing research on parallel Through-The-Road (TTR) architectures. This review is followed by an investigation into existing real world implementations of this architecture. This will include a discussion on the advantages and disadvantages of this architecture in terms of mass market vehicles.

Following this, McMaster's performance in the EcoCAR 3 competition will be reviewed, in order to identify lessons learned to apply to this new competition. Then there will be a discussion and analysis of the EMC rules and recommendations. Together these will be used to construct design guidelines for the vehicle.

Chapter 3 will serve as a summary of all the work done over Year 1 of the EMC as it pertains to this thesis. This will include an explanation of the architecture selection process, an analysis of the target market, Vehicle Technical Specifications (VTS), and an overview of the final architecture chosen by the team.

The next chapter will discuss the design process for the front ICE powertrain of the vehicle. Component justifications and mounting solutions will be discussed. Additionally, the integration plan for the 12 V Belted Alternator Starter (BAS) will be discussed at a high level.

Moving to the rear powertrain, a deep dive into the design of all components will be conducted. This includes the design of all powerflow components from the EM to the wheels, excluding the differential. Finite Element Analysis (FEA) at component and system levels will be used to justify the design.

Chapter 6 will discuss the vehicle integration up until May of 2020 for both the front and rear powertrain components. Timeline delays due to COVID-19 will be discussed, with recommendations for integration going forward.

A proposed vehicle testing plan will be developed. This will involve in-house testing utilizing dynamometers from the McMaster Automotive Resource Centre (MARC), as well as dynamic vehicle testing on-site and at competition events. The testing plan seeks to strike a balance between being thorough and the aggressive EcoCAR timeline.

Chapter 2

Background and Literature Review

2.1 Hybrid & Motor Placement Nomenclature

There are many possible combinations of EMs and ICEs inside of a hybrid vehicle. For this reason nomenclature exists to identify and differentiate vehicle architectures by powerflow and motor position. First an industry accepted nomenclature system for EM placement inside of a hybrid architecture will be shown. Then the difference between series and parallel hybrid architectures will be explained.

EM placement inside a hybrid vehicle is usually described by the relative position as compared to other powertrain components. This nomenclature system uses Position 0 through 4, abbreviated P0 through P4 [19], [20]. All positions can be seen in Figure 2.1. The positions describe where the power of the EM enters the traditional ICE powertrain. Therefore the EM can have its own gear reduction which does not effect the position it is designated.

P0 motors are connected to the ICE via a belt, and integrated into the Front End

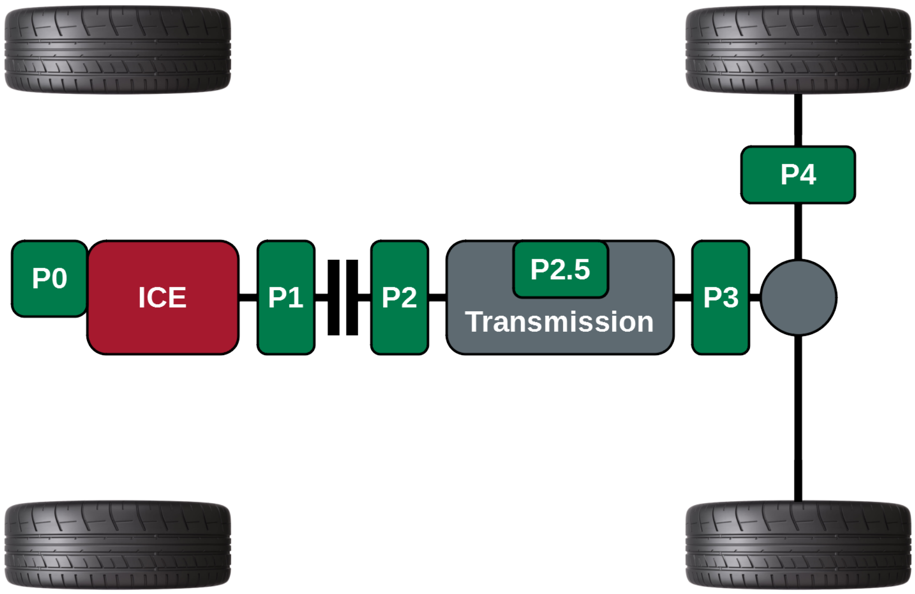

Figure 2.1: Electric motor Position 0 to Position 4 (P0 to P4) nomenclature.

Accessory Drive (FEAD). These motors are typically used for start-stop functionality and limited electrical assist. These motors are usually referred to as a BAS, Belted Starter Generator (BSG), or Integrated Starter Generator (ISG).

P1 motors are connected to the crankshaft of the ICE. This includes the front or rear of the engine. Importantly this motor is situated before the transmission coupling, be it a torque converter or clutch, in terms of powerflow. The direct connection means the EM speed is directly correlated to ICE speed.

P2 motors are connected to the transmission input shaft. The main difference to a P1 motor is that P2 motors are situated after the transmission coupling. This allows the engine to be disconnected from the transmission, and for the EM to still provide tractive power.

The P2.5 position is a newer developement, and describes a transmission with integrated EM. This allows vehicle electrification with no modification to the rest of the powertrain. Hybrid transmissions can provide electric boost, start-stop, and pure electric driving modes. An example of this kind of transmission is the Volvo 7DCTH [21].

P3 motors are connected at any point between the transmission output shaft and the differential input shaft. This placement limits the motor speed similar to the P1 position. The motor is correlated to the speed of the drive shaft. This position is extremely uncommon in Front Wheel Drive (FWD) vehicles, where the differential is often built into the transmission.

Finally, P4 motors are attached directly to the wheel axles. This generally means one EM is required per wheel. In the case of a TTR hybrid where the EM is isolated on its own axle, this motor is always a P4, even if one motor powers both wheels through a differential. This is because the position number is related to the powerflow of the ICE. These motors are also speed limited, by wheel speed, similar to the P1 and P3 placements.

A series hybrid uses the ICE exclusively as a generator, then an EM to drive the wheels, as can be seen in Figure 2.2. The ICE can be run at its optimal efficiency point at all times, and can be switched off when the battery is charged [22]. However, the two energy conversions necessary are a source of inefficiency.

A parallel hybrid uses an ICE and an EM to provide tractive power, as can be seen in Figure 2.3. This architecture allows many possible operation modes by combining the power sources in different amounts [22]. This includes pure electric, combined, and pure combustion driving modes. This architecture also has more variations in terms of motor placement as compared to the series architecture.

The series and parallel architectures can be combined to form series-parallel architectures. This involves the use of multiple EMs as well as at least one clutch in order to disconnect and combine the powerflows in more complicated ways. There are also power-split architectures, which use planetary gear sets to actively combine multiple

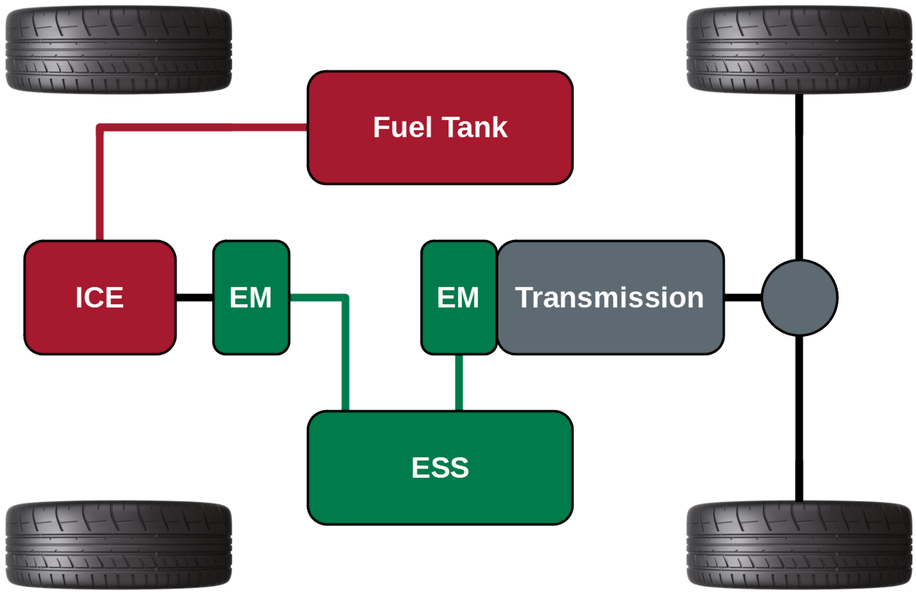

Figure 2.2: Example of a series hybrid architecture.

input sources. The architecture to be defined and examined in the following section is a parallel TTR architecture.

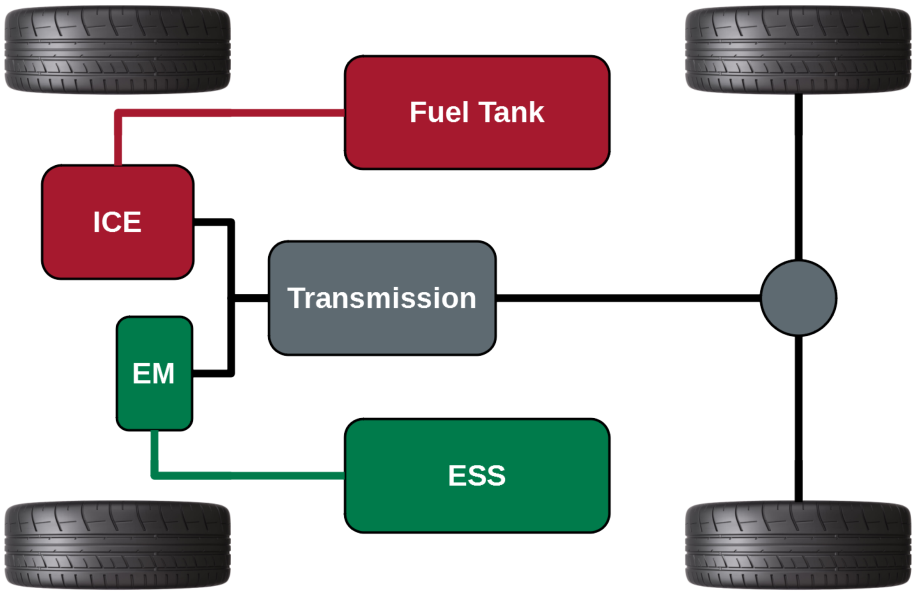

Figure 2.3: Example of a parallel hybrid architecture.

2.2 Parallel Through-The-Road Hybrid Electric Powertrains

2.2.1 Research and Academia

Current literature on TTR hybrids is somewhat limited as other architectures are still the norm in most production vehicles. The most common theme in current literature is to investigate the conversion of two-wheel drive combustion vehicles to hybrid vehicles by electrifying the non-driven axle. Most of the following researchers suggest aftermarket TTR hybrid conversions as a stepping stone to a larger hybrid fleet. Importantly, converted HEVs would ease pressure on existing grid infrastructure compared to a highly PHEV and BEV heavy fleet. In a study by the Pacific Northwest National Laboratory, it was found that the US grid had a technical potential for 73% PHEV adoption among light duty vehicles, using 2002 statistics [23]. If the charging period is limited to between 6pm and 6am, this drops to a potential for 43% conversion. The study assumed PHEVs with only a 33 mile range. Gong et al. studied the effect of PHEVs and EVs on the expected lifetime of local distribution transformers [24]. The study showed that unregulated charging can drastically raise the temperature and therefore reduce the lifetime of these transformers, and increased market penetration for these plug-in vehicles only increases the extra charging load. It is shown that smart charging strategies would be necessary to mitigate these problems in order for a high market penetration of plug-in vehicles to be viable.

Researchers Zulkifli et al. present a definition of the parallel TTR architecture, defining it as having an ICE and EM operating on different drive shafts [25]. They identify the architecture as a torque coupled drivetrain, where the torque from both sources are added together, while the speed of each source cannot be individually controlled as the front and rear tires must spin at the same speed. They also present five distinct operating modes possible within the architecture, which are listed below.

Operating Modes of a TTR Architecture Vehicle [26]–[28]

1. ICE alone delivers power to the load
2. EM alone delivers power to the load
3. Both the ICE and EM deliver power to the load
4. EM obtains power from the load
5. ICE delivers power to the load, and the load delivers power to the EM

Several design considerations for the vehicle control system were also identified, specific to the TTR architecture [26]–[28]. The most significant is that charging can only occur while the vehicle is moving. This prevents charging opportunities at idle, such as at stop lights in city drive cycles, reducing the charging capability as compared to a more traditional hybrid architecture. Zulkifli et al. are focused on the conversion of existing vehicles using In-Wheel Motors (IWMs), and so the remaining design considerations are specific to that use case. When converting an existing vehicle, there is no opportunity to downsize the ICE as would normally be part of a hybrid architecture design. This limits the possible fuel savings. Additionally the use of IWMs limits the torque and power potential of the electric powertrain, due to the physical motor constraints.

Pisanti et al. present a dynamic programming optimized energy management system, using the HySolarKit aftermarket IWM system and a FIAT Punto as the model [29]. They report that the conversion of this vehicle reduces fuel consumption as compared to the stock vehicle, but less so than a native HEV would. Speed constraints of IWMs and lack of downsizing of the ICE due to converting an existing vehicle are cited as reasons for the lower efficiency gains compared to a native HEV. These findings agree with those of Zulkifli et al. above. A further study by Rizzo et al. examines the implementation of a fuzzy logic control system which predicts driver intention and driving conditions using only OBD data [30]. This was tested with a real world Fiat Punto fitted with the HySolarKit, showing functionality of the basic control scheme.

Galvagno et al. used mathematical modeling to perform a drivability analysis of the TTR architecture [31]. The addition of a second powertrain introduces a second set of natural frequencies, which must be accounted for in vehicle design. This second set of natural frequencies contributes to a more complex time history during acceleration testing. However, it was found that the overall amplitude of the natural frequency response was lower, making the HEV more comfortable then the FWD car.

Finesso et al. created a software tool to optimize the EM and battery size in TTR hybrids based on powertrain cost, including fuel costs, over 160 000 km lifetime [32]. Two HEVs of different degrees of hybridization were compared to a conventional vehicle. All vehicles had Compression Ignition (CI) engines, and the two HEVs were constrained to match the same performance targets as the conventional vehicle. It was found that the component cost of the HEV powertrains were higher as expected, but the overall costs were lower by up to $1300 when fuel cost was considered [32]. Other interesting findings include the dependence of the fuel economy improvements on different factors. It was found that operating Mode 5 as described above where the EM regenerates energy while the ICE propels the vehicle results in a maximum 2% improvement in fuel consumption. Conversely, the optimization of the current transmission gear, as opposed to a simple shift strategy based on vehicle velocity and power, resulted in a minimum of 3% gain, up to a maximum of 12.7% depending on drive cycle. Lastly they found the EM was oversized by their optimization tool. EM size was predominantly based on vehicle performance requirements, which meant at most points during the tested drive cycles the EM was operating at less optimal points in its efficiency range.

Hall et al. developed and built a TTR vehicle based on a Volkswagen Golf, in order to showcase the Protean PD18 in-wheel motors and MAHLE Powertrain controller used in the project [33]. The vehicle goals were to halve the 0-100 km/h time of the vehicle while reducing CO_2 emissions to less than 50 g/km, with initial testing showing this to be achievable. The vehicle was also fitted with a 350 V, 14 kW h battery pack inside the trunk. This all but eliminates cargo capacity, however was justified on a testing platform vehicle.

Last in this literature review is a group of three papers concerning the design of past AVTC competition vehicles, all with TTR architectures. The first two are 2005 Chevrolet Equinox SUVs, part of the Challenge X competition. The Mississippi State University (MSU) [34] and University of Wisconsin (UW) [35] teams will be examined. Both teams have identical vehicle architectures, using a 1.9 L diesel engine, 65 kW induction motor with integrated powertrain, and 330 V Nickel-Metal Hydride (NiMH) battery pack. This makes them both parallel TTR HEVs. The UW team was able to achieve 36.5 mpg compared to the MSU teams 32 mpg, while also maintaining a Tier 2 Bin 5 emissions level compared to the Tier 2 Bin 8 of MSU. MSU notes that their vehicle was not fitted with a BAS, meaning the contol strategy for the vehicle does not contain engine idle-off or electric vehicle launch capabilities [34]. The UW vehicle does use an engine idle-off strategy, as well as removing the engine alternator and using a high to low DC-DC converter which improved fuel economy by 2.9% [35].

The Purdue University EcoCAR 2 team 2013 Chevrolet Malibu used a parallel TTR PHEV architecture. The vehicle used a 1.7 L diesel engine, 16.2 kW h battery pack, and a Magna E-drive 90 kW motor [36]. The team targeted a charge sustaining fuel economy of 5.6 L/100 km, with a charge depleting range of 96 mi. The battery of this vehicle was placed in the trunk of the vehicle, limiting the cargo capacity to 12 ft^3. The battery also required a temperature range of 10 °C to 35 °C, which necessitated sub-ambient cooling [36]. Therefore a heat exchanger was added to the vehicle's Heating, Ventilation, and Air Conditioning (HVAC) system, in which the battery coolant was circulated.

Interesting similarities to note between these three AVTC vehicles are as follows. All three vehicles used an all-in-one electric driveline solution, with motor and transmission being a single unit. This eliminated the need for powertrain design past the component mounting phase. All teams also took a modular approach to control design due to the modular nature of the TTR powertrain. All vehicles utilize the ICE as a primary power source, with the EM supplying supporting power, when attempting a charge sustaining strategy. All teams also primarily relied upon regenerative braking to charge the battery, instead of operating mode 5 from above.

2.2.2 Existing Implementations

The TTR architecture has become popular with the high-performance automotive market. Vehicles including but not limited to the BMW i8 [37], Acura NSX [38], and Porsche 918 Spyder [39] use a variation of this architecture to achieve All Wheel Drive (AWD) and increased vehicle performance. Each vehicle uses a mid-mounted ICE, meaning it is mounted behind the seats but in front of the rear axle. The front axle of all the vehicles then has additional EMs, one in the BMW and Porsche [37][39], two in the Acura [38]. Each vehicle also has an additional smaller EM on the rear axle, used in parallel with the ICE. This makes the vehicles not strict TTR hybrids, as defined in Section 2.2.1. However it is interesting that these high performance vehicles use an independently powered and electrified front axle instead of a more traditional AWD system. This is most likely due to the increased control possible with EMs over traditional systems, improving traction control capabilities. The Acura solution provides true torque vectoring by using two motors on the front axle, one for each wheel. These vehicles also outline the packaging benefits possible with this architecture. Traditional AWD systems require a driveshaft that runs the length of the vehicle, meaning the driver compartment must be higher up for ground clearance. The independent electric axle allows a lower overall vehicle, which translates to a lower and more stable center of mass.

A more widespread use of this architecture comes from Volvo, who use a similarly modified TTR architecture for all hybrid vehicles built on their Scalable Product Architecture [40]. This includes all 90 and 60 series Volvo vehicles [41]. These vehicles are similar to the performance powertrains listed above. The front axle is powered by a 2.0 L ICE and a small 34 kW EM. The rear axle contains a larger 61 kW EM. Using the two separately powered axles has manufacturing benefits on a modular vehicle platform, where different powertrain components do not have to be developed for different wheelbase vehicles. This allows this hybrid architecture to be used across five models in Volvo's range. This adaptability is a strong case for the use of the TTR architecture for manufacturers wishing to electrify a large range of vehicles quickly.

2.3 McMaster EcoCAR3 Review & Lessons Learned

As mentioned in Section 1.2, the MAC team has competed in one AVTC competition in the past, being the EcoCAR 3 competition from 2014 to 2018. This competition comprised the electrification of a 2016 Chevrolet Camaro over four years, with many similarities in structure to the current EMC competition. This allowed MAC to draw on its previous experience and develop key lessons to use going forward.

First a review of the MAC Chevrolet Camaro architecture. The vehicle was a series-parallel hybrid vehicle with P1 and P2 YASA P400 HC EMs, a 2.0 L Inline-4 (I4) turbocharged GM LTG engine, and a Hybrid Energy Storage System (HESS) consisting of lithium ion batteries and ultra-capacitors. An architecture diagram can be seen in Figure 2.4. The two EMs allow pure electric, series hybrid, and parallel hybrid driving modes, as well as regenerative breaking using the P2 EM. The architecture is also extremely power dense, featuring the highest theoretical performance of any EcoCAR 3 vehicle. Each EM is capable of a continuous 90 kW output, with a peak torque of 370 N m. The student designed HESS uses the high power density of ultra-capacitors to help supply the combined 180 kW electric output, while the energy density of the lithium ion batteries is used to achieve the desired electric and hybrid driving ranges.

The overall complexity of this architecture is very high. The team pursued a

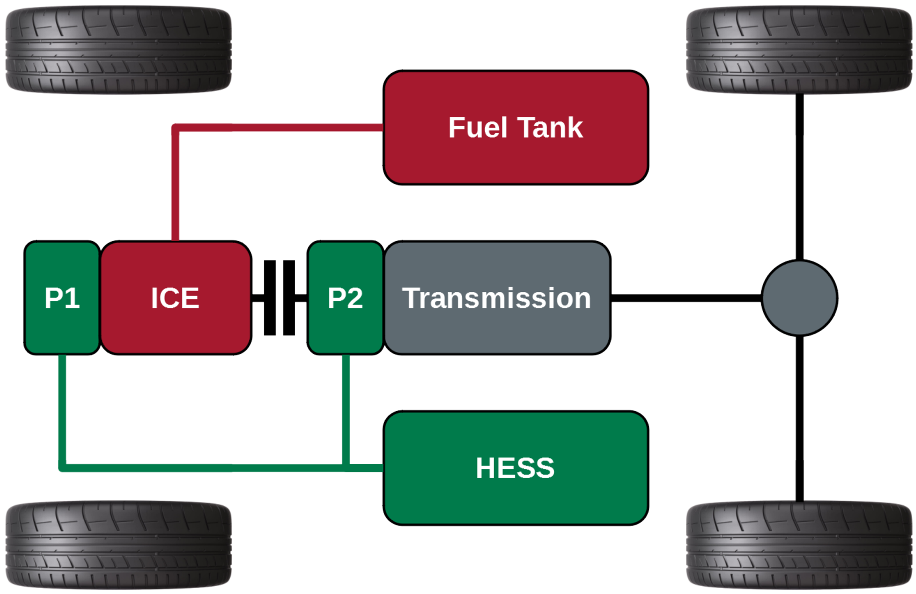

Figure 2.4: McMaster Engineering EcoCAR 3 vehicle architecture.

high-risk high-reward strategy in an attempt to maximise vehicle performance within the muscle car platform. This was partly influenced by the team's past involvement in the SAE Formula Hybrid competition, which is extremely performance oriented. This resulted in an architecture that was difficult to implement, especially for a team new to the structure of the AVTC series. The complex powertrain caused timeline and financial penalties over the four year competition, resulting in the vehicle never reaching its theoretical performance. A review of the EcoCAR 3 competition was conducted at the start of the EMC competition, which included a review of the MAC team as well as strategies and results from all other teams [42], [43]. Main lessons learned as they pertain to vehicle design were as follows.

1. Simpler architectures generally lead to higher overall results.
2. Using components with industry support generally reduced integration time.
3. Using components a team has past experience with generally reduced integration time.
4. Some teams experienced timeline delays as a result of choosing competition

sponsored components.

5. All teams consistently struggled with the design and/or integration of torque coupling and torque transfer components.

6. Team designed components can meet specific requirements more easily than purchased components.

Generally speaking, experienced teams that performed well in the competition chose architectures that were feasible to implement in the tight EcoCAR timeline. This is exemplified by both Ohio State University and Embry-Riddle Aeronautical University, who chose relatively simple architectures [42]. These afforded them faster integration time, which translated to more time available to troubleshoot issues that did arise. These teams placed first and second overall in the EcoCAR 3 competition.

Component selection was also found to be extremely important. Points 2 through 4 above all relate to this issue. Point 2 is most applicable to ICE selection, as GM provides teams with support if they select one of the offered engine variants. The MAC team chose a GM engine that was not supported for the competition, and therefore did not receive CAD models or integration support. This caused the team to use 3D scanning technology and a FaroArm Coordinate Measurement Machine (CMM) to create a CAD model of the engine. This introduced unnecessary complexity into the design process. Point 3 is relevant to teams with past experience in the AVTC series, where re-using components from past vehicles can drastically reduce integration time. Many experienced teams re-used EMs in order to capitalize on past controls experience, which is often one of the largest contributors to integration time. Point 4 would seem to contradict point 2, however speaks more to the delivery timeline then the integration timeline. Certain competition level sponsored components such as EMs and battery packs had limited quantities available to teams. This means that upon architecture selection, some teams did not receive their first choice in components.

Additionally, teams would not know if they had received a component until after architecture selection documents had been finalized and reviewed by the competition. Therefore competition level sponsored components bring uncertainty and possible timeline delays to an architecture. GM was seen as an exception to this rule as discussed above as it related to their engines and transmissions.

Finally points 5 and 6 relate to component design. It was found that all teams had issues with Noise, Vibration, and Harshness (NVH) through the torque transfer components of the driveline. This resulted mainly from team designed components, but also occurred for some teams due to improper alignment of powertrain components. This lead to component failures in some cases. Colorado State University experienced the failure of their clutch and torque converter in Year 3 [42]. The MAC team had several shaft failures, which will be further explored in Section 5.4 during the shaft design for the current vehicle. Additionally the MAC team experienced some powertrain alignment issues, in part due to the very long nature of the powertrain stack. Extra care should therefore be taken in the design and installation of these components to ensure longevity of the vehicle.

It was found that while large and high risk components such as EMs or batteries benefit more from industry support, as noted above, smaller components can greatly benefit from being custom designed for the task at hand. The MAC team found that the use of team designed control boards, something no other team in the competition did, greatly improved overall functionality of the vehicle. The bespoke nature of the boards reduced overall wiring complexity, as well as providing complete documentation for troubleshooting and vehicle inspections. This approach of using team designed components to fulfill specific use cases or requirements extends to other areas of the vehicle, where off the shelf components may over-complicated assemblies.

Overall these lessons learned were extremely valuable in the design of the new vehicle architecture, as well as individual component design. This will be further explored in Chapter 3 where the full architecture selection process from Year 1 of the EMC will be reviewed.

2.4 EcoCAR Mobility Challenge Rules & Limitations

The specific environment of the EMC competition has a large influence on vehicle design, at both the architectural and component level. In this section the main rules and limitations effecting design decisions will be reviewed. This will put many of the decisions made in future chapters into context.

Starting with rules that effect architecture level decisions, EMC specifies the intended market for the final vehicle to be a car-sharing application. This means the vehicle has in effect two customers. The first is the fleet owner, who owns the vehicle and is in charge of maintenance and vehicle upkeep. The second is a car-sharing customer, who would rent the vehicle from the fleet owner via their car-sharing service. This target market has some unique aspects that influence vehicle design. The fleet owner is concerned not only with up-front vehicle cost, but also overall vehicle cost of ownership. The competition specifies a 30000 mile, 18 month vehicle lifetime. At the end of this lifetime the vehicle is assumed to be sold for 75% of its purchase price. This makes the high initial purchase price of some hybrid components easier to overcome through fuel savings over the specified mileage. Cost is calculated via Equations 2.1 to 2.7 below, with variables defined in Table 2.1 [44]. The powertrain cost of the vehicle is specified as the difference to the stock Chevrolet Blazer. This isolates the cost of the powertrain in relation to the rest of the vehicle. The total cost of ownership is then used in scoring certain dynamic events at competition, with lower costs being better.

$$TotalOwnershipCost = PurchasePrice + TotalFuelCost - ResalePrice \tag{2.1}$$

$$PurchasePrice = TeamPropSysCost - StockPropSysCost \tag{2.2}$$

$$PropSysCost = EngCost + MotCost + BattCost \tag{2.3}$$

$$EngCost = 827 + (109 \times NoCyl) + (6.2 \times EngPwr) + (283 \times DI) + (1730 \times Boost) \tag{2.4}$$

$$MotCost = 6 \times MotPower \tag{2.5}$$

$$BattCost = 20 \times BattPower \tag{2.6}$$

$$TotalFuelCost = \frac{FuelPrice \times LifetimeMileage}{FuelEconomy} \tag{2.7}$$

Table 2.1: Variable definitions for competition cost of ownership equations.

Variable	**Description**	**Unit**
BattPower	10 second peak power of battery pack	kW
Boost	Presence of a turbocharger or supercharger	Binary (1/0)
DI	Presence of Direct Injection	Binary (1/0)
EngPwr	Peak power of engine as defined by manufacturer	kW
Fuel Economy	Vehicle fuel economy as measured by Energy Consumption event	mpg
FuelPrice	Price per gallon of fuel as defined by the competition	USD/gal
Lifetime Mileage	Lifetime mileage of vehicle as defined by competition	mi
MotPower	Combined 10 second peak power of an electric motors	kW
NoCyl	Number of engine cylinders	Integer
ResalePrice	Defined as 75% of PurchasePrice	USD

The EMC also attempts to reduce the scope of powertrain electrification as compared to the EcoCAR 3 competition. This is to both make the project more feasible for teams in general, and to increase the focus on CAV technologies. This scope reduction comes with certain limitations on architecture selection, enforced through both rules and incentives. The first of these is a ban on student designed and built Energy Storage Systems (ESSs). This is justified as a large reduction in complexity for teams, allowing a shorter integration timeline, and a reduction in safety concerns for the competition as a whole. This means only black box solutions can be used. As a response there is a GM sponsored battery option, which will be explored further in Chapter 3.

The next scope reduction is a move away from PHEVs towards HEVs. This decreases the size of any ESS, allowing for easier integration into the vehicle. Charging systems are also eliminated with the same effect. The move is not a rule but is incentivized by the available GM battery option and a change in competition event evaluation. The competition no longer measures GHG emissions, Petroleum Energy Usage (PEU), or Well to Wheel (WTW) metrics, and does not use utility factor weighting, all of which benefit from PHEV designs.

In terms of propulsion, P1 and P2 motors are discouraged through the structure of GM sponsored powertrain components. For this competition GM provides five preselected engine and transmission combinations called "powercubes". These powercubes are combinations currently used in GM vehicles, and GM will provide technical support for working with them. This is specifically to combat problems teams had in EcoCAR 3 pairing engines and transmissions that are not offered in a preexisting vehicle, making the integration of the two together difficult. Breaking apart the engine and transmission with a P1 or P2 motor makes the existing calibration maps no longer applicable, and loses the GM support aspect of these components. Additionally a higher burden of proof during the selection process is required to be allowed to execute a P1 or P2 motor, as well as using one of the provided engines or transmissions outside of their defined pairings. These engine options also only support standard E10 fuel, which together with the lack of GHG, PEU, and WTW factors seeks to move the competition away from alternative fuels such as E85 or B20. Alternative fuels have also been a source of integration difficulties for teams in the past.

The final important aspect of the rules relevant to this thesis are the vehicle body modification rules, which are largely unchanged from EcoCAR 3 in terms of structure. The vehicle body structure is color coded into red, yellow, and green [44]. This indicates which panels in the unibody construction are structural or important for crash safety. Diagrams of these areas exist but are omitted due to confidentiality. Red areas cannot be modified under any circumstance. Yellow areas can be modified through the use of a structural waiver, which will be explained below. The only exceptions for red and yellow areas is the drilling of holes less than 13.1 mm for component mounting, as well as welding components to these red or yellow areas. Welds must be done in a way to minimize stress concentrations via heating to the best of the team's abilities [44]. Finally, green areas can be modified freely without structural waivers. Components of the vehicle not included in the body structure are also sorted into modifiable and unmodifiable groups. Unmodifiable components include but are not limited to safety components such as airbags and safety modules, as well as vehicle suspension geometry. Modifiable components using appropriate waivers include the rear subframe, body components within 200 mm of seat or seatbelt mounts, hood and rear hatch, brake pads, brake rotors, and brake calipers. Some components like suspension springs and dampers are modifiable without waivers, as long as they are passive.

The waiver process is a way for teams to justify designs to the competition and GM, in order to ensure safety critical components are modified properly. At a high level the process consists of justifying that the team's design does not contain any stresses at or above the level of the stock component. This is accomplished through FEA of both the stock and modified components by the teams, which is then reviewed by GM. Considering the large amounts of time put into these analyses by students, teams generally try to minimize the amount of waivers in the vehicle design. Components such as brake calipers may require different forms of justification, which usually makes these waivers less intensive from a time perspective.

This is by no means a comprehensive analysis of the competition rules, but serves as an overview to help guide the reader through architecture and component design decisions later in this thesis. Rules which apply to a specific component design or decision will be called out as they are used through the document.

Chapter 3

McMaster EcoCAR Architecture Selection

3.1 Target Market and Vehicle Technical Specifications

One of the first deliverables in Year 1 of competition was to research and outline a target market segment for the team's vehicle, followed by defining VTS based on that market. The architecture selection that followed would then have a list of requirements in the form of those VTS. Some aspects of the target market were pre-defined by the competition, as discussed in Section 2.4. The vehicle is to be targeted at a car-sharing application. Specifically, a car sharing application with both a fleet owner and customer, therefore no peer-to-peer sharing platforms would be allowed. Past this it up to the team to define their specific fleet owner model in general terms, and a prospective target customer.

The first step in this process was to define a geographic region for the service to operate in. The Greater Toronto Hamilton Area (GTHA) was chosen for the following reasons. Being the area that McMaster University is contained within means familiarity with the region, and the ability to easily conduct our own surveys for research purposes. Additionally, the GTHA is the highest population area in Canada with a total population of 7.63 million people in 2018 [45]. Of the citizens of Toronto, 28% of households do not own a car, with households in the downtown core rising to 55%, all as of 2016 [46]. This leaves a large prospective market for a car-sharing service. Commuting into Toronto from the suburbs is also expensive, with a daily commute from Hamilton to Toronto estimated at $7500 per year using a personally owned vehicle and $4843 using public transportation [47]. Therefore the GTHA is considered a good prospective area for a car-sharing service, as both an alternative for commuters and an option for intra-city trips.

The fleet owner was therefore defined as a car-sharing service operating within the GTHA using a blended model of free-floating and stationary vehicles [48]. Stationary vehicle pick-up and drop-off zones would be located at major transit hubs, such as Go Transit stations. The free-floating models would be limited to downtown core usage in the city of Toronto. The fleet owner would pay for vehicle fuel via gas cards within the vehicle. Booking the vehicles would be coordinated via an app.

To define the customer, more research had to be done on the demographics of the selected area. According to a study by Ryerson University, millennials are the fastest growing population in this region, and will continue to be until at least 2026 [49]. Millennials in this case are defined as people born between 1982 and 2001. Millennials encompass a demographic of students and young professionals, being in the age range of 19 to 38 in 2020. Of those currently in the labor force, 80% of millennials in the

GTHA have a post secondary education [49]. The average starting salaries for post secondary educated employees in Canada ranges from \$40 747 to \$71 730 depending on type of degree and position. The average salary for a person with a bachelors degree is \$54 295. The estimated \$7500 per year in commuting costs from above represent 13.8% of that yearly income. Therefore a car-sharing option that would reduce these costs, while representing increased freedom as compared to using public transport, would be marketable to this group.

The MAC team also conducted a survey of over 220 GTHA residents. Of those surveyed, 19.6% had no preference on the type of vehicle they drove, while 35.1% would prefer a HEV and 28.0% would prefer an EV [48]. This shows the general interest in better fuel economy and environmental awareness among the population. Passenger capacity and cargo space were also important, with 75.5% and 68% of respondents rating them a minimum 3 out of 5 importance respectively. Only 8.9% of respondents said they preferred a performance vehicle.

The archetypal customer is therefore defined as a millennial living in the GTHA. They are a young professional with a bachelors degree making approximately \$54 000 per year, who prefers to drive a vehicle with some level of electrification. They do not have an interest in vehicle performance, preferring a practical vehicle with passenger and cargo capacity.

The MAC team then defined a set of VTS, in order to guide the architecture selection process. Based on the team's EcoCAR 3 experience the VTS were made conservative, using the competition targets wherever possible. This was to reduce unnecesary risks in the final architecture, and reduce overall design and integration time. This aligns with the lack of interest in performance vehicles found above, justifying the competition targets for acceleration and braking performance. The priorities for the vehicle, based on the defined target market, are as follows.

MAC Team Vehicle Priorities

1. Low cost of Ownership as defined by Equations 2.1 to 2.7
2. Stock passenger and cargo capacity
3. High fuel economy as measured by the competition defined drive cycles

Low cost of ownership is the highest priority as it is beneficial to both the fleet owner and customer. The fleet owner will benefit financially from lower cost vehicles, and these lower costs can be passed on to consumers via lower pricing models. High passenger and cargo capacity were extremely important to the target customers, and stock values are as high as possible in the confines of this competition. High fuel economy aids in lowering the overall cost of ownership, as well as being important to the defined customer for environmental reasons.

Table 3.1: MAC Vehicle Technical Specifications

Specification	**Competition Target**	**Performance Requirement**	**Safety Requirement**	**Team Targets**	**Units**
Acceleration IVM-60 mph	7	9	TBD	7	s
Acceleration 50-60 mph	6.5	TBD	TBD	6.5	s
Braking 60–0 mph	Stock	n/a	168	Stock	ft
Cargo Capacity	Stock	16.5	n/a	Stock	ft^3
Passenger Capacity	Stock	Stock	2	Stock	(-)
Curb Mass	n/a	n/a	2542	<2542	kg
Front Axle Mass	n/a	n/a	1350	<1350	kg
Rear Axle Mass	n/a	n/a	1450	<1450	kg
Starting Time	<=2	<=5	n/a	<=2	s
Ground Clearance	n/a	n/a	7 in.	7 in.	in
Total Vehicle Range	250	200	n/a	250	mi
Fuel Economy	15% above Stock	Stock	n/a	30.5	mpg
Emissions	Stock	Stock	n/a	<=Stock	(-)

The final VTS can be seen in Table 3.1. All team targets are matched to competition targets. This sets the performance criteria like Initial Vehicle Motion (IVM) to 60 mph times at the lowest realistic values without risking reduced competition points. Cargo and passenger capacity are set to stock value as explained above. Fuel economy is set to 30.5 mpg, which matches the competition target as well as being achievable based on initial simulation data. Curb mass is set as simply lower than the safety requirement. This is to remove the more performance oriented pressure of defining a specific vehicle mass target. However, as lower vehicle mass effects fuel economy, low mass will be prioritized where convenient to do so in component selection and design.

3.2 Selection Process and Year 1 Summary

3.2.1 Considered Components

This section will briefly outline the EM and ICE options available to the team while developing possible architectures. Starting with the GM provided powercube options, mentioned in Section 2.4. A powercube is a GM selected ICE and transmission pairing, that brings with it GM technical support. For this reason, along with the MAC team's experience using an unsupported ICE option in EcoCAR 3, it was decided that these would be the only ICE options considered. The offered ICEs can be found in Table 3.2, along with the powercube numbers they belong to. The three engines are all I4 layouts. The smaller LYX and LTG engines are turbocharged, making them attractive from power to weight ratio and efficiency perspectives. The LCV engine is naturally aspirated but is offered in the base model Chevrolet Blazer, meaning GM parts exist to easily replace the V6 in the Blazer RS the teams were given.

Table 3.3 contains the corresponding transmission options, again with the pow-

Table 3.2: GM engine options by powercube number.

Option #	RPO Code	Displacement (L)	Intake System	Peak Power (kW)	Peak Torque (Nm)
1	LYX	1.5	Turbocharged	126	282
2, 3 ,4	LTG	2	Turbocharged	191	400
5	LCV	2.5	Naturally Aspirated	148	255

ercube numbers they belong to. All transmission options are automatic, nine speed, transversely mounted units. The main differences across the five options come in the presence or absence of an accumulator, and the use of Electronic Transmission Range Selection (ETRS). An accumulator stores hydraulic pressure within the transmission, in order to enable immediate shifting during start stop applications. ETRS is what the name implies, the transmission is not connected to the PRNDL lever via a cable, instead being connected electronically. The Blazer comes with a traditional cable shift lever, so integrating an ETRS transmission will be more work. Note that if a team is selecting powercubes primarily based off of simulated engine performance, only the LTG gives a choice of which of these transmission features a team desires. If a team selects the LYX or LCV engine, there is only one transmission option available. The M3D transmission is offered with the LCV engine in the base model Blazer, as stated above. This means overall much simpler integration if powercube 5 is selected.

Table 3.3: GM transmission options by powercube number.

Option #	RPO Code	Number of Gears	Accumulator	ETRS
1	M3U	9	Yes	Yes
2	M3D	9	Yes	No
3	M3E	9	No	No
4	M3H	9	Yes	Yes
5	M3D	9	Yes	No

Four EM options were considered in the initial MAC vehicle architectures, listed in Table 3.4. Two are traction motors, and two are BAS units. The YASA P400 HC is an extremely power dense axial flux EM used by the MAC team in EcoCAR 3. It can operate at a wide range of voltages, making a peak 165 kW at 700 V [50]. The listed specifications are gathered by the team from EcoCAR 3, and better reflect the expected performance in the current MAC vehicle. The motor's continuous power is limited electrically in these conditions as opposed to thermally, and so is the same as its peak power. One major advantage of this motor is that the MAC team already has it in hand, and therefore can start testing and controls development immediately. Additionally, the use of the motor in EcoCAR 3 means the team can draw on past experience implementing and using it.

The Plettenberg Nova 30 is a larger version of a motor used in McMaster's previous Formula Hybrid team vehicle. For this reason the team has previous experience using this brand of motor, as well as building a set of planetary gearboxes for them. The experience is farther removed from the current team roster than that of the YASA P400 HC, having no remaining team members that contributed to the design of the Formula Hybrid vehicle. Similar to the YASA, these motors are extremely power dense, increasing packaging options as well as lowering overall system mass. These motors would need to be purchased new, which imposes a financial burden as compared to the YASA motor.

Table 3.4: Electric motors considered in MAC architectures.

Electric Motor	**Peak Power (kW)**	**Continuous Power (kW)**	**Max Torque (Nm)**	**Max RPM**
YASA P400 HC [1]	70	70	250	7500
Plettenberg Nova 30 [51]	30	15	80	7000
Denso HV ISG [52]	30	12	60	21000
Valeo i-StARS Gen. 3	4	3	75	18000

[1] YASA P400 HC specifications are for 300 V, 250 Arms

The Denso High Voltage (HV) ISG is a competition sponsored component. It is a 300 V part, which meshes well with the available battery pack to be discussed below. Contrasting this component is the Valeo i-StARS unit, a 12 V BAS unit which interfaces directly with the existing Low Voltage (LV) system of the vehicle. These two BAS units where compared in the team's simulations to find which resulted in the higher overall system efficiency, as will be discussed in upcoming sections.

Table 3.5: Competition level sponsored electric motors.

Electric Motor	**Sponsor**	**Integrated Gearbox**	**Industry Application**
SMG 180/120	Bosch	No	Fiat 500e [53]
Electric Drive Unit 2	AAM	Yes	
Concentric e-Drive	AAM	Yes	Jaguar i-PACE [54]
eRAD	Magna	Yes	Volvo V60/S60 [55]

The were also several EM options available through competition level sponsorship. These components are briefly outlined in Table 3.5. None of these components were considered in the MAC team architectures for the following reasons. As discussed in Section 2.3, there are timeline concerns when using competition sponsored components. Due to the limited quantities of competition sponsored EMs, the competition puts limits on how many proposed architectures per team can contain them. It follows that a team cannot know if they will receive that EM until after the architecture selection process has been completed, and the architecture is confirmed by the competition. This delays the design portion of the integration process, as well as the timeline for receiving the components. Additionally, the motors considered by the team are considerably more power dense in terms of mass and volume than any of the competition sponsored options. This means that the overall electric propulsion system will likely be lighter and smaller than that of the sponsored options. Finally, the full drive units offered by AAM and Magna lock the team into specific gear ratios, features, and packaging layouts. The MAC team wanted to maintain its ability to tailor the propulsion system to meet overall team goals. An example of this would be using simulation data to choose the desired overall gear ratio between the motor and the wheels.

The final component to be considered by the team is the GM HEV4 battery pack. This is the competition sponsored battery pack, originally from the hybrid Chevrolet Malibu. This was the only ESS option considered by the team. Due to the ban on student designed ESSs, only black box solutions may be considered. A coalition of several teams pursued an option where working with a company a pack was designed for EMC purposes, however the MAC team did not believe the increased financial costs were worth the performance increases of this option. Additionally, initial packaging studies show that the Malibu pack can be effectively packaged underneath the vehicle, while the third party pack is much larger and would require packaging in the trunk. Due to the team's priority of stock trunk space this required the Malibu pack. Lastly, the GM support offered with the Malibu pack was deemed too important to opt for other third party options.

3.2.2 Initial Architectures

First a definition of what constitutes an architecture for the EMC will be outlined. An architecture is defined as a powerflow with specific components assigned to it. A powerflow is defined by the competition as a distinct mechanical and electrical layout for power transfer through a vehicle. An example of a powerflow would be a TTR hybrid, with an ICE powering the front axle and a HV EM powering the rear axle, with a HV battery as the ESS. An architecture would then be created by assigning specific components to be used within this powerflow. Changing a single specific powertrain component constitutes as a different architecture. Components such as gearboxes do not define architectures. An example would be placing a gearbox in between an EM and a differential. This does not create a new architecture, it simply modifies the current architecture with a different gear ratio.

The EMC requires that three distinct architectures be presented at the Year 1 Winter Workshop, in order to have them reviewed by the competition. Teams are then given feedback on these architectures by subject matter experts concerning feasibility and execution. The requirements for these architectures are listed below. Following these guidelines, the MAC team generated an initial three architectures which will be outlined in this section.

Requirements for Proposed Architectures for Winter Workshop [56]

1. At least two unique mechanical/electrical powerflows must be represented between the three architectures
2. At least one architecture must include a GM Powercube
3. At least one architecture must not include the competition-donated Bosch motor system
4. At least one architecture must include an unmodified production black-box ESS (GM Malibu HEV pack or otherwise)

Architecture 1 is the first of two architectures sharing the same P0/P4 parallel TTR powerflow. The front axle is powered by GM Powercube 1 containing the LYX engine. This architecture was developed with fuel efficiency as its defining goal as compared to the other architectures. The LYX is the smallest GM sponsored engine, representing the largest downsizing move from the stock vehicle. This gives the largest opportunity for fuel savings, assuming the engine is not over-stressed by the weight of such a large vehicle. This will be explored in Section 3.2.3.

Both Architecture 1 and 2 contain the same rear axle design. The axle is powered by the YASA P400 HC motor. The motor power flows through a single speed gear reduction, a clutch, and a differential before being put to the wheels. The single speed

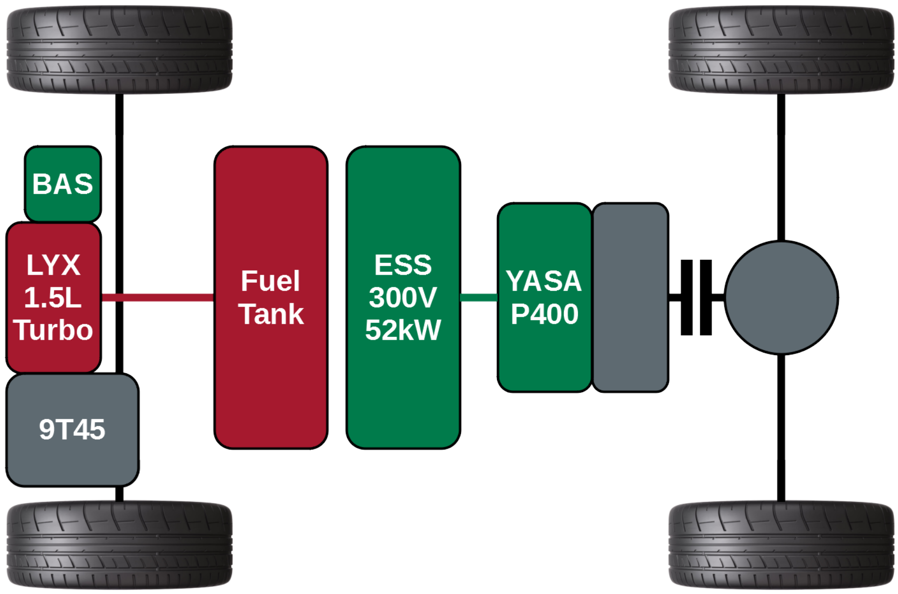

Figure 3.1: Architecture 1 - Efficiency Oriented

gear reduction can be customized by the team in order to maximize fuel economy and electric assist over the specific EMC drive cycles. The clutch allows motor separation when it is not in use, reducing overall system losses. Designing one rear powertrain for both architectures reduced overall project risk, as resources are spread over less total projects during the initial design phase.

Architecture 2 is defined by its goal to be the lowest risk architecture. It uses the GM Powercube 2 option containing the LTG engine. This engine is the most powerful of the GM sponsored options, giving a lower risk of an under powered vehicle as compared to the other turbocharged option. The additional power means that even in an ICE only drive mode, the vehicle would likely be able to meet the stock V6 powered Blazer VTS targets. This gives the architecture some redundancy for an electric powertrain failure scenario. Unlike the Powercube 5 option, which is a stock option for the 2019 Chevrolet Blazer, the turbocharged engine offers more chances for increased fuel economy. The Naturally Aspirated (NA) Powercube 5 would also struggle to meet the stock V6 VTS targets in an ICE only drive mode.

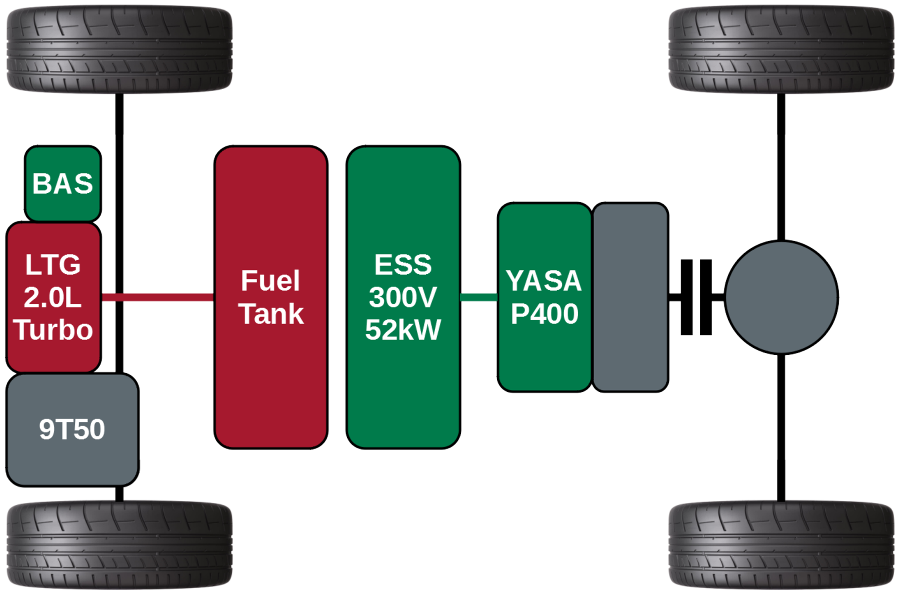

Figure 3.2: Architecture 2 - Low Risk Oriented

Architecture 3 uses a P0 with dual P4 parallel TTR powerflow. This architecture is defined by its innovation potential as compared to the other architectures. The possibility for torque vectoring from the dual rear motors opens up more innovation paths for vehicle control in later competition years. Additionally, the combination of the highest power ICE and torque vectoring potential make this the highest performance of the three architectures.

All architectures include a BAS on the front powertrain. This was chosen to add start stop functionality to all architectures as well as to maximize the efficiency of all ICE choices. The BAS will be used to move the engine operating point towards maximum efficiency by supplying or regenerating torque. At the time these architectures were developed it was not decided whether the HV Denso system or LV Valeo system would be used.

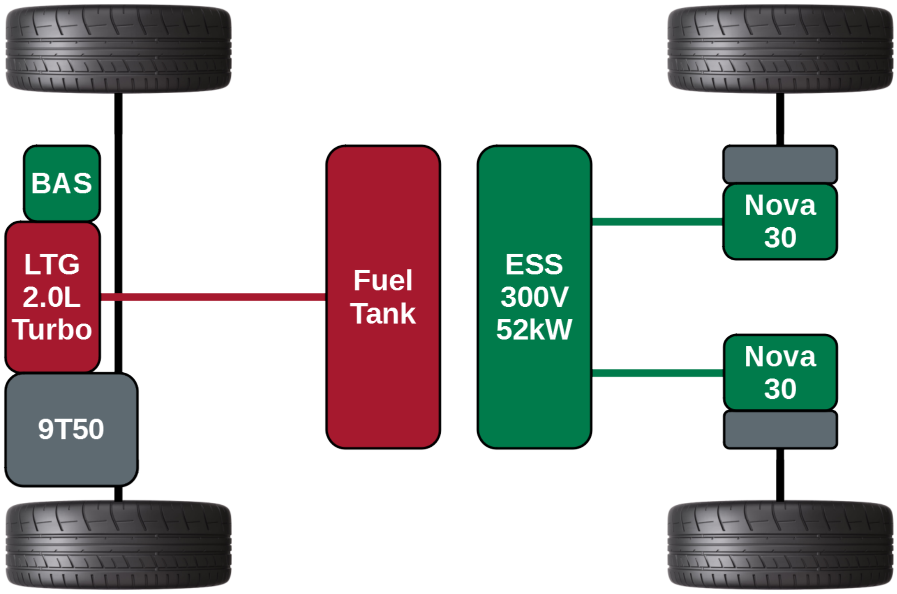

Figure 3.3: Architecture 3 - Innovation Oriented

3.2.3 Selection Process

The selection of the MAC team's preferred architecture was based on a combination of fuel economy, ownership costs, alignment with target market, and overall risk versus reward of each architecture. Vehicle modelling in MATLAB Simulink was used to obtain fuel efficiency values over the competition specified drive cycles. Packaging studies were done in Siemens NX to evaluate the integration difficulty of each architecture. As discussed in Section 3.2.2, three architectures had to be presented at the Year 1 Winter Workshop with certain requirements. Subsequently, two architectures had to be presented in the Architecture Selection Report, adhering to the below requirements. These two architectures need to be ranked as a first and second choice. The competition organizers will then inform the teams if their first choice has been approved. To aid in this process, the competition organizers pre-approved and pre-rejected certain powerflows after Winter Workshop. These powerflows are summarized in Table 3.6. Questionable is a designation given to powerflows that the competition will require a higher burden of proof from teams in order to approve.

Requirements for Proposed Architectures in Architecture Selection Report [56]

1. At least one architecture must include a GM Powercube
2. At least one architecture must include a mechanical/electrical powerflow that is pre-approved by the organizers
3. At least one architecture must not include the following competition-donated motors: Bosch SMG motor system, AAM EDU motor
4. At least one architecture must include an unmodified production black-box ESS (GM Malibu HEV pack or otherwise) NOTE: the HDS battery option does not qualify as an unmodified production black-box ESS

Table 3.6: Pre-approved and rejected powerflows for Architecture Selection Report.

Powerflow	**Designation**
P0	Pre-approved
P4	Pre-approved
P0-P4	Pre-approved
P0-P4 with 300V + 48V systems	Questionable
Dual P4	Questionable
Series	Questionable
P3	Rejected
P2	Rejected

The selection process quickly revealed that architectures 1 and 2 aligned more with team goals than architecture 3. Architecture 3 presents a higher degree of integration difficulty by doubling the amount of electric powertrain components. Its increased potential for innovation does not contribute to specified target market wants and needs, and the smaller Nova 30s are significantly less efficient than the larger YASA P400. This makes its overall risk vs reward proposition unattractive. For these reasons, this architecture was discounted early in the process. It was superficially investigated until winter workshop to comply with the multiple powerflow requirement stated in Section

3.2.2, however internal resources were highly prioritized towards the development of architectures 1 and 2.

Focusing the teams resources towards these two architectures added several additional advantages. As both architectures have identical rear electric powertrains, using an EM already in the team's possession, development of this system could be started early. There was no risk that the final system not be contained in the chosen architecture. This extends to the design and packaging of all components other than the ICE. The vehicle Simulink model was also refined for these architectures, leading to more accurate fuel economy numbers used to compare the two. Using this data it was found that the Valeo BAS unit provided higher overall system efficiencies than the Denso unit on both architectures. This was a result of the increased losses associated with using a high to low DC-DC converter, which would be necessary when using the HV unit to supply 12 V power. Additionally, it was decided that the increased power output of the Denso option made the belt design process more difficult, with a higher risk of crankshaft damage from improper loading.

With both architectures being extremely similar in terms of overall risk, packaging difficulty, and integration timeline, the decision for which architecture was preferred was made on the criteria of fuel efficiency and total ownership cost. These values are shown in Table 3.7. Architecture 1 performs better in all metrics except highway fuel economy, and so is the clear winner. The use of the LYX engine in architecture 2 contributes to the better highway mileage, as the more powerful engine is capable of meeting most drive cycle power requirements without electric assist. The LYX engine requires more electric assist, but as there is less potential for regenerative braking on a highway drive cycle, the charge sustaining control strategy cannot supply as much tractive energy. The LTG engine is also the cause of the large increase to total cost of ownership over the LYX architecture. This is due to the much higher power figure, which is incorporated into the engine cost formula as seen in Equation 2.4. Additionally, the competition specifies the LTG must be run on premium fuel, which is priced at \$3.74 /gal by the competition, as opposed to \$3.19 /gal for standard fuel. This increases the fuel cost disproportionately compared to its fuel economy.

Table 3.7: Architecture comparison using Total Cost of Ownership and Fuel Economy.

Specification	**Architecture 1**	**Architecture 2**
Total Cost of Ownership (USD)	\$3934.45	\$4613.44
Propulsion System Cost (USD)	\$5997.20	\$6400.20
Fuel Cost (USD)	\$3234.20	\$3812.44
EMC Combined Fuel Economy (mpg)	29.59	29.43
EMC City Fuel Economy (mpg)	31.01	29.44
EMC Highway Fuel Economy (mpg)	28.02	29.41

3.3 Final Architecture Decision

The final selection by the MAC team was architecture 1, shown with more detail in Figure 3.4. The architecture is a P0/P4 parallel TTR HEV. The front powertrain consists of the 1.5 L LYX turbocharged engine, with a nine speed automatic transmission and Valeo 12 V BAS system. The rear powertrain consists of the YASA P400 HC EM, with a single speed reduction gearbox, Tilton clutch, and differential. The motor is controlled via the Rinehart PM150 motor controller. The chosen ESS is the Chevrolet Malibu battery pack. The only option for comparison to other universities as of this point in the competition is that of total ownership cost. Table 3.8 contains the total cost of ownership of all teams in the competition. Notable in the table is how all four teams who chose to use the LTG engine have the highest cost of ownership, by a large margin. The MAC team exists as the most expensive non-LTG team in the competition. This is due to the use of the more expensive turbocharged LYX engine in combination with a 70 kW motor system, and a conservative 30.5 mpg fuel economy

Table 3.8: Cost of Ownership comparison of all EMC teams.

School	**Total Ownership Cost (USD)**	**Propsys Cost (USD)**	**Total Fuel Cost (USD)**	**Engine**	**Fuel Economy Target (mpg)**
ERAU	\$ 3190.48	\$ 3995.60	\$ 2990.63	LCV	32.0
GT	\$ 3286.95	\$ 3995.60	\$ 3087.10	LCV	31.0
WVU	\$ 3341.85	\$ 3803.60	\$ 3190.00	LCV	30.0
UA	\$ 3540.88	\$ 5397.20	\$ 2990.63	LYX	32.0
UT	\$ 3607.05	\$ 5073.60	\$ 3137.70	LCV	30.5
VT	\$ 3641.85	\$ 5003.60	\$ 3190.00	LCV	30.0
UWAFT	\$ 3663.99	\$ 5423.60	\$ 3107.14	LCV	30.8
MAC	\$ 3717.95	\$ 5517.20	\$ 3137.70	LYX	30.5
CSU	\$ 4157.25	\$ 5800.20	\$ 3506.25	LTG	32.0
UW	\$ 4329.69	\$ 5800.20	\$ 3678.69	LTG	30.5
MSU	\$ 4427.25	\$ 6880.20	\$ 3506.25	LTG	32.0
OSU	\$ 4666.35	\$ 7384.20	\$ 3619.35	LTG	31.0

target. The cost of ownership could be reduced dramatically by outperforming our fuel economy targets. If we set the MAC fuel economy to 32 mpg, the highest target of any other team, our overall cost drops to 5$^{\text{th}}$ overall as opposed to the current 8$^{\text{th}}$.

During the design process of the rear powertrain, it was proposed that the battery be packaged underneath the vehicle in order to maximise trunk space. This use case was approved by the competition, and the MAC team is now the only team not packaging the battery within the trunk of the vehicle. The battery will be packaged within a carbon fiber enclosure, in the space originally occupied by the stock fuel tank, directly beneath the rear seats. The design of this enclosure is headed by an undergraduate student, and therefore will not be discussed in detail as a part of this thesis. However the integration status and future plans will be discussed in Chapter 6.

The rear differential of the vehicle has been flipped 180° from what would be considered a normal position. This means its input faces the rear of the vehicle. This was done for the following reasons. Mainly, it allows the packaging of the battery

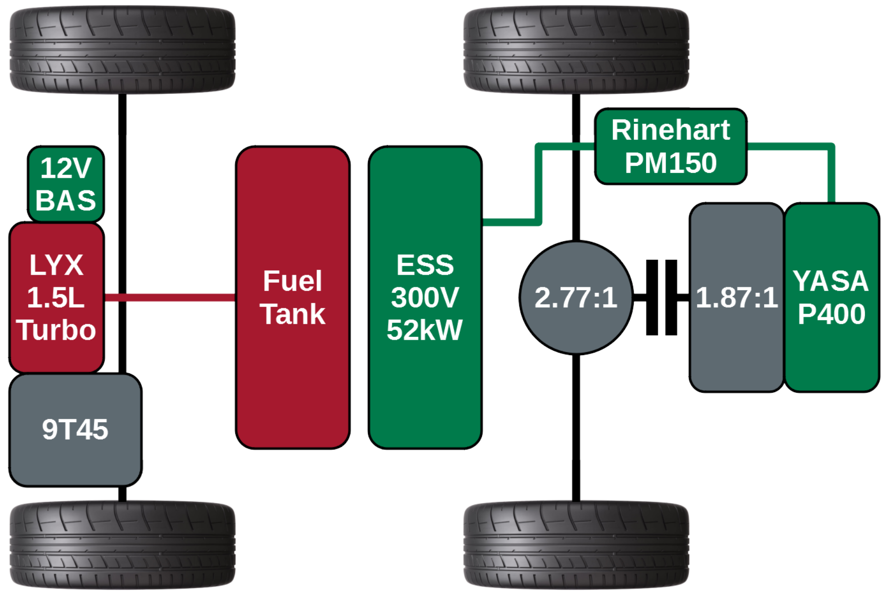

Figure 3.4: McMaster Final Architecture

as discussed above. Additionally, if the differential were to face forward, the motor would need to be packaged beneath the rear seats of the vehicle. A packaging study done on this option made it clear that to maintain competition required ground clearance, the floor underneath the rear seats would need to be modified. Alternatively, turning the differential requires the rear cradle of the vehicle to be modified. The rear cradle modification was deemed as the easier to accomplish, as although it requires a competition waiver, that waiver is a lower burden of proof as compared to seat mounting hardware. The in depth modification of the cradle is headed by another undergraduate student, and therefore will not be discussed in detail as a part of this thesis. As with the battery enclosure the integration status and future plans will be discussed in Chapter 6, as will any interfaces with the rear powertrain in Chapter 5.

Chapter 4

Front Powertrain Design

4.1 Mounting and Integration Stratgey

The overall integration strategy for the front powertrain involved prioritizing GM Original Equipment Manufacturer (OEM) parts in order to reduce design complexity and increase system reliability. This allowed the team to focus on the rear powertrain design, in which more student designed parts were necessary to meet the architecture specifications. This strategy was effective as GM often uses components interchangeably across vehicle models, allowing many Blazer components to be reused for the new powercube. Where this was not possible, GM components from a GMC Terrain were used, as this vehicle comes standard with the team's chosen LYX powercube. These components were purchased using the team's Blue Dollars, a credit given to teams each year which can be used for the purchase of GM parts as part of the competition. This allowed the team to focus financial investment on the rear powertrain.

Starting with the engine and transmission cooling system, the radiator stack and stock piping from the GMC Terrain were used. This means the powercube will be operating with its stock cooling capacity, which eliminates any thermal issues from the front powertrain. The FEAD water pump was bypassed, using a Davies Craig EWP80 electric water pump [57]. The HVAC system will be a combination of Blazer and Terrain components. The condenser from the Terrain is used, as it is integrated into the stock radiator stack as half of a split radiator. The other half of the radiator is the transmission oil cooler, and therefore cannot be removed from the system. Additionally, the Terrain's internal passenger volume is almost identical to that of the Blazer, meaning cooling load will also be similar. The compressor from the stock V6 Blazer engine will be used. These will then be integrated into the normal Blazer cabin side HVAC system and controls.

4.1.1 Engine Mounts

The stock V6 engine in the Blazer RS and the LYX engine in the Terrain are mounted as a unit with their accompanying transmissions. The V6 has four mounts, one on each side of the powercube as shown in Figure 4.1 labelled M1 through M4. The LYX powercube only uses three mounts when installed in the Terrain, due to its significantly lower weight. Specifically mount 4 is not used, and therefore will not be used in the conversion. Both nine speed transmissions are part of the same GM transmission family, therefore their designs and mounting points are similar. Mount 3 uses identical mounting points across the two transmissions, and so will be re-used for the M3U transmission. Mount 2 connects to the Power Transfer Unit (PTU) in the AWD version of the Blazer, however there is an equivalent mount for the I4 FWD version of the car, normally equipped with powercube option 5 as described by the competition. This mount was purchased using Blue Dollars and used for mounting position 2.

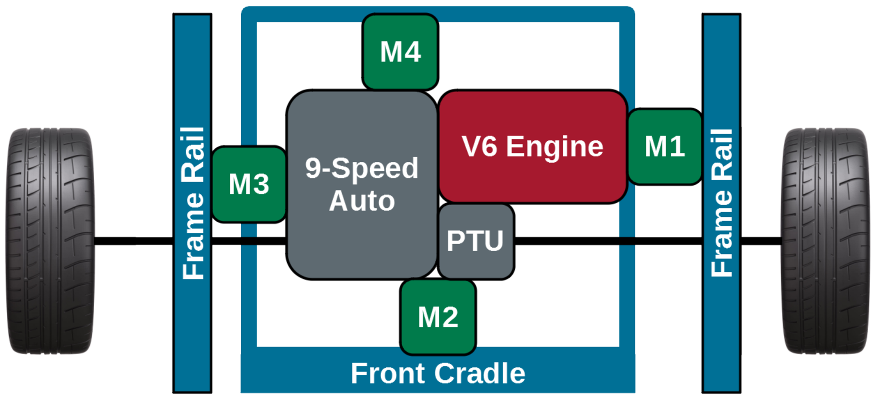

Figure 4.1: Stock Blazer RS engine and transmission mounting configuration.

This leaves mount 1, which due to the smaller LYX engine cannot be re-used. As such a front engine mount had to be custom designed. As part of the technical support received from Valeo, the company provided the team with basic designs for a front engine mount which incorporated mounts for idler pulleys. This design was adapted to create an easily manufactured version, which aided in accelerating the ICE installation timeline. Figure 4.2 shows the design, with Figures A.1 and A.2 showing the technical drawings. The mount is made from welded 4140 steel, with triangular gussets to improve rigidity. The mount attaches to the engine via three M10 bolts, which pass through cylindrical stand offs. The top two bolts attach to original engine mounting points, with the bottom going to where the stock LYX idler pulley originally attached. The two holes in the main face of the mount are for two bosses to be located and then welded. These will be the mounting locations of the new idler pulleys. The belt for the FEAD passes between this mount and then engine. The M12 threaded holes match to the chassis side of the stock engine mounting solution.

The main goal of this design was to reduce overall timeline by overbuilding the mount with a large safety factor. As the ICE installation was the first major component in the

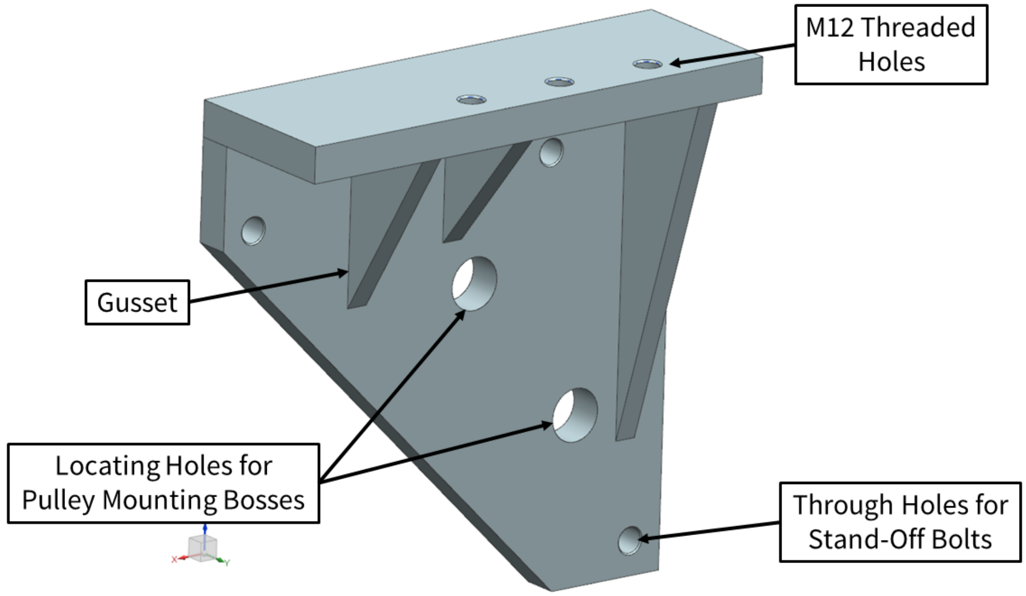

Figure 4.2: CAD model for front engine mount with feature labels.

integration timeline, further design optimization was forgone to meet the manufacturing schedule. This resulted in a high component mass of 6.87 kg. It is suggested that a revision of this mount be designed in future competition years, to reduce the mass and integrate the idler pulley mounts. The current mounting solution is functional but inelegant, and a re-design would pose as an excellent learning opportunity for a younger student.

4.1.2 Front Half Shafts

The stock half shafts in the Blazer RS do not fit the new M3U transmission for two reasons. The passenger side half shaft is too short, as it is intended to interface with the PTU. Additionally the splines used on the higher torque V6 application are larger than those on the M3U, making the driver side shaft also not usable. The half shafts from the GMC Terrain are also not suitable, as the Terrain and Blazer have different track widths. After some investigation, it was found that the M3D transmission from the base model Blazer used the same output spline as the M3U. Therefore the FWD Blazer half shafts were ordered. The longer passenger side half shaft is a two piece design, with an additional bearing and Constant Velocity (CV) joint in the center which mounts to the engine block. An adapter plate was designed to interface the mounting pattern expected on the LCV engine with the new LYX engine. Technical drawings for this adapter plate can be found in Figures A.3 and A.4.

4.2 VALEO BAS System

The Valeo i-StARS BAS system is integral to the fuel economy improvements needed to meet the MAC team's VTS. As discussed in Section 3.2.3, this system was chosen over the HV Denso option for two reasons. The first is that the LV option was simulated to have higher system efficiencies, due to not requiring a high to low DC-DC converter. The HV and LV systems of the vehicle do not interact with each other, meaning energy cannot be transferred from the HV to the LV battery and vice versa. The BAS controls the charge of the 12 V battery, using excess energy to provide torque assist to the engine.

The second reason for choosing the Valeo system was the large amount of technical support offered in the design and integration of the system by Valeo. The team was concerned with the design of a new belt path for the FEAD, with teams in past EcoCAR competitions struggling with these designs. Some teams induced crankshaft failures from improper loading, due to increased belt tension as well as the increased torque transfer. To combat these possible problems, a Valeo engineer designed the belt path for the MAC team. The layout of the system can be seen in Figure 4.3.

The main crankshaft pulley is a six rib stock GM part, adapted to be used in this

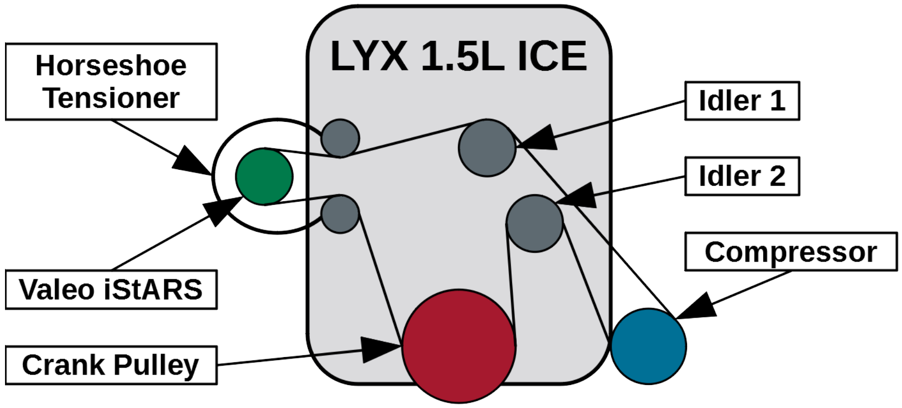

Figure 4.3: Belt path for MAC LYX engine with Valeo i-StARS BAS

application in order to replace the five rib LYX crank pulley. This matches the BAS pulley, as well as allowing a higher torque transfer through the system without belt slip. The compressor is from the V6 engine, again to comply with the increase to a six rib belt. The belt driven water pump originally on the engine has been removed from the system, as its position over complicated the belt route. A blanking plate is used to replace the pulley and pump wheel assembly from the pump housing. The engine will then be cooled by an electric water pump, as discussed in Section 4.1.

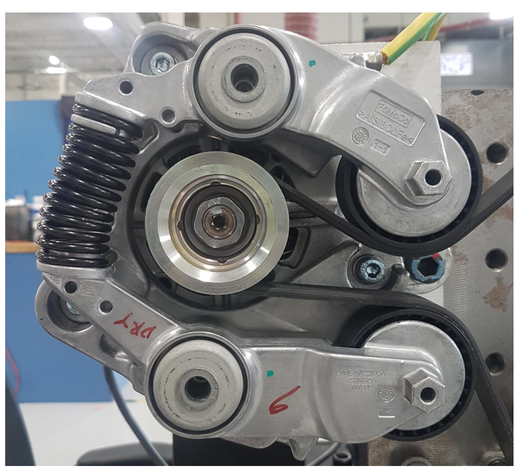

Figure 4.4: Valeo iStARS BAS with horseshoe style belt tensioner on test bench.

The system is driven by the crankshaft pulley as standard, with the addition of the BAS. Based on the control strategy, the BAS will act as a second driver adding torque to the system, or as an additional load subtracting torque from the system. Due to this bi-directional loading, a horseshoe style belt tensioner is needed as seen in Figure 4.4. This absorbs the bi-directional belt tension loads caused by the BAS, protecting the other components.

Designs of the mounts for both the BAS and the V6 compressor were provided by Valeo. These will serve as a first revision for the MAC team, and will be modified to facilitate manufacturing as needed. The initial design of the engine mount in Section 4.1 was also provided, specifically to incorporate mounting for the two idler pulleys in the belt path. Due to Non Disclosure Agreements (NDAs) from both Valeo and GM, no further depth to the design of this system can be provided.

Chapter 5

Rear Powertrain Design

5.1 Design Requirements & Goals

The rear electric powertrain is the main student designed element of the vehicle, and the system which was personally designed by the author. Due to the separate nature of the two powertrains, the system had a high degree of flexibility in its design and packaging. This lead to the rotated differential approach introduced in Section 3.3, which will be expanded upon in Section 5.2. This unique packaging strategy lead to a number of specific requirements in the design of the drivetrain. This section will outline these requirements and limitations, as well as the overall goals for the system.

Rear Powertrain Design Requirements and Limitations

1. Must maintain competition ground clearance requirement of 7 in
2. Must comply with competition minimum loading requirements for powertrain mounting hardware (20g lateral, 8g vertical, SF = 1.5)
3. Must limit axial length of system to be be within rear bumper and rear trailer hitch (512 mm)

4. Must contain a clutch which disconnects the motor from the wheels
5. Gearbox must be rated for 250 N m input torque
6. Gearbox must be rated for a 7000 rpm input speed
7. Gearbox must be rated for a 6970 km lifetime

The first two requirements are the most relevant competition rules to the design of this system. Due to the placement of the rear powertrain under the vehicle, ground clearance is directly effected by the design and placement of the motor and gearbox. The rules around the design of powertrain mounts are also directly applicable, with all mounting hardware having to meet a loading requirement of 20 g in the four lateral directions, and 8 g in the two vertical directions, with a safety factor of 1.5. This was evaluated using FEA, and will be discussed in Section 5.6.

Requirement 3 again pertains to the specific placement of this system. As the differential placement is dictated by the rear wheels and rear cradle design, the rest of the system must maintain an axial length of less than 512 mm to not contact the rear trailer hitch. Requirement 4 exists for two reasons. Firstly, so the motor can be disconnected when not in use, such as high speed highway operation where torque demands are met by the ICE, to protect the system from unnecessary high speed operation. Secondly, in the event of a failure somewhere in the system, the clutch will disconnect the motor from the wheels, protecting the motor from further damage, while allowing the vehicle to continue to operate and enter a reduced function ICE only mode. The MAC team has experience with the YASA P400 being damaged in the previous Camaro project. One suspected source of the damage was from excessive vibrations transferred via the motor output shaft. The disconnection of the motor when not in use or during suspected system failure is in response to these observations.

Requirements 5 and 6 pertain to the gearbox matching the torque and speed capabilities of the YASA P400 EM. Finally requirement 7 relates to the minimum lifecycle distance of the gearbox. The estimated vehicle lifetime is 6970 km, using the competition provided testing glide path. This glide path gives the teams a goal distance to reach with vehicle testing for each year of the competition. The sum of these distances and the 145 km Emissions and Energy Consumption (E&EC) event at Year 3 and Year 4 competitions gives the overall life cycle. This serves as a useful estimate of a minimum distance the gearbox must travel without major repairs.

Rear Powertrain Design Goals

1. Minimise vibrations transferred to YASA P400
2. Minimise axial length of system
3. Maximise safety factors associated with system wear over time
4. Maximise safety factors associated with instantaneous system loading
5. Minimise overall system mass

The design goals encompass aspects of the of the system that the team wished to maximise or minimise. The goals serve as decision making criteria, and therefore are ranked in order of importance. When two goals contradict each other in their influence on a part or system, the ranking shows which will dictate the design.

Ranked as most important is minimising the vibrations transferred to the YASA P400. This includes vibrations from the rest of the powertrain, as well as vehicle and road loads. This is ranked first due to the team's previous experience with these motors, as mentioned above. The MAC team's EcoCAR 3 Camaro damaged the two YASA P400 motors installed in it, likely due to a combination of misalignment and vibrational issues. Therefore to maximise the life of the system, it was the team's goal to minimise these vibrations wherever possible.

Goal 2 is to minimise the axial length of the system. Requirement 3 gives the maximum allowable value, however the shorter the system the better the rear departure angle of the vehicle. As the EM will be the first object to scrape the ground in a high departure angle scenario, reducing the possibility this happens is highly important. A skid plate has also been designed to protect the motor.

Goals 3 and 4 relate to the longevity and durability of the system. As a prototype student vehicle, overbuilt systems are a prudent preventative solution to the myriad of unforeseen load cases the system may encounter over its lifetime. As shown in Section 2.3, past EcoCAR vehicles have failed as a result of excessive NVH loads not included in vehicle analysis, especially in areas of torque transfer. These loads are often impossible to account or test for with the resources available to student teams. Therefore for this system the team has decided to maximise the safety factors of the analyses, to ensure success in the competition irrespective of any unforeseen circumstances. For this vehicle, long term durability was prioritised over instantaneous loading. This is because the team has a lower confidence in the analyses used for long term durability than that for the FEA used for instantaneous loading. This can be seen during the gear analysis in Section 5.3, where no data is available for some of the factors used in the International Organization for Standardization (ISO) 6336 analysis. Additionally, this vehicle is not performance oriented, being used predominantly on standard drive cycles with consistent and slow ramping loads. This is contrasted to a performance vehicle, such as the EcoCAR 3 Camaro, in which performance driving was emphasized in Wide Open Throttle (WOT) events and the shock loading of the drivetrain.

Finally goal 5 is to minimize the overall system mass. This is ranked last in terms of priority to match with the team's overall goals stated in Section 3.1, in which fuel efficiency is ranked third and vehicle performance is absent. Lightweight components make the vehicle more efficient, as well as reduce the loads on the mounting hardware to meet requirement 2. However, this does not take priority over the durability concerns which will be a larger factor in the success of the team overall. The vehicles that historically score the most points at competitions are those that run reliably.

5.2 Rotated Differential and Modified Rear Cradle

As discussed in Section 3.3, the rear cradle of the vehicle is being modified to accept a rotated rear differential. This was done as the alternative packaging solution caused problems for ESS placement, as well as requiring a more complicated waiver process involving seat mounting modifications. The design and modification of the rear cradle is headed by an undergraduate student on the team, and therefore the design decisions will not be discussed in detail. However the relevant changes as they relate to the rear powertrain will be summarized here.

The differential being used is the stock unit from the EcoCAR 3 Camaro. The Rear Drive Unit (RDU) from the Blazer is designed for AWD applications, with a built in clutch to engage and disengage the rear wheels. On its face this seems advantageous, meeting design requirement 4 with an all-in-one solution. However, the clutch controller located on the RDU cannot be controlled by the team's vehicle controller. The RDU controller takes in numerous vehicle dynamic signals and determines when to activate the rear wheels, as opposed to taking in a simple binary comand. GM advised all teams that it would be difficult to repurpose the RDU, and that technical support would be unavailable as the controller was made by an outside contractor, not GM itself. The Camaro unit is a Limited Slip Differential (LSD) with a ratio of 2.77:1.

The modifications to the rear cradle involve cutting a large segment from the rear cross member to allow for the differential input to pass through. Two differential mounts have also been incorporated into the modified design. Unfortunately, NDA restrictions do not allow Computer Aided Design (CAD) images of the modifications to be presented in this forum.

5.3 Gear Sizing and Design

This section will outline the design of the gear pair used in the rear powertrain. To determine the optimal gear ratio, the vehicle Simulink model was used. Simulations were performed with overall vehicle gear ratios ranging from 2.8:1 to 8.4:1 in increments of 0.1. The lower limit is simply the ratio of the chosen differential, rounded to one decimal place for simplicity. The upper limit is the maximum gear ratio that allows the rear axle to reach 130 km/h at the maximum EM speed of 7500 rpm. This speed is chosen as it is the maximum speed of the US06 drive cycle, and the maximum speed the vehicle would need to reach in the competition. These were then evaluated to find the gear ratio that yielded the highest fuel efficiency over the competition drive cycles, which was 5.2:1. Given the differential's ratio of 2.77:1, the gearbox ratio must be 1.877:1. An excel spreadsheet incorporating all gear calculations was made in order to iterate through different combinations of module, helix angle, number of pinion teeth and face width. The final gear ratio achieved with feasible gear tooth numbers was 1.87:1, giving an overall ratio of 5.18:1. The final gear specifications can be found in Table 5.1, with technical drawings in Figures A.5 and A.6.

The decision to design gears as opposed to purchase them was made to better tailor the system to the team's needs. All five of the team's design goals could be better optimized for using custom designed components. Helical gears were chosen to reduce NVH in the vehicle overall, and specifically around the EM. The face width was minimised to 35 mm to reduce axial length, while maintaining suitable strength

Table 5.1: Gear specifications summary.

Specification	**Pinion**	**Wheel**	**Units**
Teeth	23	43	(-)
Module	3	3	mm
Outside Diameter	77.43	139.55	mm
Pitch Diameter	71.43	133.55	mm
Root Diameter	63.93	126.05	mm
Pressure Angle	20	20	°
Helix Angle	15	15	°
Face Width	35	35	mm

and wear characteristics. The wheel gear contains a cutout channel to reduce mass by 31.7%, to a final mass of 2.37 kg. The final gears can be seen in Figure 5.1.

Figure 5.1: Wheel gear (left), pinion gear (right), and shafts as received from Rapid Precision Machining & Gearing Ltd

The team sponsor who manufactured the gears, Rapid Precision Machining & Gearing Ltd, was consulted for material and heat treatment choice. The material choice was 4340 Heat Treated Stress Relieved (HTSR) steel, with the material properties listed in Table 5.2. The gears were then surface nitrided to a hardness range of 58 HRC to

62 HRC. Nitriding was chosen over carborizing in order to minimize warping from the heat treatment process. This was important as post processing on the gear teeth was not possible, since the manufacturer typically works with larger gears, and therefore the grinding and polishing machines were too large for the team's gears.

Table 5.2: Material properties of steel used in gear and shaft production.

Heat Treatment	Yield Str. (MPa)	U.T. Str. (MPa)	Elong. % in 2"	Red. of Area %	BHN Surface	BHN Mid-Radius
H.T.S.R.	1103	1194	13.1	54	337	331

5.3.1 ISO 6336 Calculations

The ISO 6336 standard uses a number of factors to calculate two independent failure mechanics, surface pitting and tooth bending. The entire standard was codified into an excel spreadsheet so as to allow iteration through different gear designs. As it was not possible to test sample gears, due to the time and budget constraints of the competition, this analysis was critical to the success of the rear powertrain. As such, whenever a derating factor present in the standard was not known for certain, or required testing to thoroughly evaluate, a worst case scenario was assumed.

Equations 5.1 to 5.6 were used to calculate the safety factor against surface pitting [58], and equations 5.7 to 5.11 were used to calculate the safety factor against tooth bending [59]. Subscripts 1 and 2 correspond to the pinion and wheel gears respectively. Definitions of the main terms can be found in Table 5.3, however a reading of the official ISO standard is necessary for an in depth understanding. A full list of all values used in these calculations can be found in Table B.1, with a summary of the results found in Table 5.4.

Table 5.3: ISO 6336 term definitions for contact stress and tooth bending.

Term	Definition
$S_{H1,2}$	Contact stress safety factor
$S_{F1,2}$	Tooth bending safety factor
σ_{H0}	Nominal contact stress of error free gear pair under static torque
$\sigma_{H1,2}$	Contact stress accounting for gear error (K factors)
σ_{HG}	Pitting stress limit of gear material
σ_{F0}	Nominal tooth root stress of error free gear pair under static torque
$\sigma_{F1,2}$	Tooth root stress accounting for gear error (K factors)
σ_{FG}	Tooth root stress limit of gear material

$$S_{H1} = \frac{\sigma_{HG}}{\sigma_{H1}} \tag{5.1}$$

$$S_{H2} = \frac{\sigma_{HG}}{\sigma_{H1}} \tag{5.2}$$

$$\sigma_{H0} = Z_H Z_E Z_\eta Z_\beta \sqrt{\frac{F_t}{d_1 b}\frac{u+1}{u}} \tag{5.3}$$

$$\sigma_{H1} = Z_B \sigma_{H0} \sqrt{K_A K_v K_{H\beta} K_{H\alpha}} \tag{5.4}$$

$$\sigma_{H2} = Z_D \sigma_{H0} \sqrt{K_A K_v K_{H\beta} K_{H\alpha}} \tag{5.5}$$

$$\sigma_{HG} = \sigma_{Hlim} Z_{NT} Z_L Z_v Z_R Z_W Z_X \tag{5.6}$$

$$S_{F1} = \frac{\sigma_{FG}}{\sigma_{F1}} \tag{5.7}$$

$$S_{F2} = \frac{\sigma_{FG}}{\sigma_{F2}} \tag{5.8}$$

$$\sigma_{F1,2} = \sigma_{F0} K_A K_v K_{F\beta} K_{F\alpha} \tag{5.9}$$

$$\sigma_{F0} = \frac{F_t}{b m_n} Y_F Y_S Y_\beta Y_B Y_{DT} \tag{5.10}$$

$$\sigma_{FG} = \sigma_{Flim} Y_{ST} Y_{NT} Y_{\delta relT} Y_X \tag{5.11}$$

Table 5.4 shows that contact stress is the limiting factor for this gear pair, with a safety factor of 1.25. This is acceptable for this application, where the gears are only required to last 6970 km. Using the Simulink models of the vehicle, it was found that the electric motor spins an average of 1215.6 rev/km. This takes into account vehicle motion when the motor is not being used with the clutch open. This figure is a weighted average of the two EMC drive cycles, 55% city and 45% highway, which is the ratio set out by the competition rules for all vehicle testing. This would give a total 8.47×10^6 cycles on the pinion gear, and 4.53×10^6 cycles for the wheel gear over the required distance. The calculations where done assuming long life characteristics of the material, meaning cycle life in the range of 1.0×10^8. Therefore the gears are anticipated to complete all competition testing and events without substantial surface wear or pitting.

Table 5.4: ISO 6336 analysis summary, safety factors and calculated stresses.

Term	**Pinion**	**Wheel**	**Unit**
S_H	1.25	1.25	(-)
S_F	2.45	2.53	(-)
σ_{H0}	783.4	783.4	MPa
σ_H	964.3	964.3	MPa
σ_{HG}	1209.0	1209.0	MPa
σ_{F0}	158.0	153.6	MPa
σ_F	226.3	220.1	MPa
σ_{FG}	554.5	556.2	MPa

Preventative maintenance can be done to reduce the likelihood and predict the occurrence of such a failure. Regular oil changes will maintain the lubrication film, protecting the tooth flanks from pitting. Regular inspections can inform on the current surface quality of the tooth flanks. As surface pitting is not an abrupt failure mode, changes to the lubrication strategy could be implemented if signs of surface wear emerge. In the worst case event of large amounts of pitting, the gears would survive a week of competition loading, allowing the team to plan a re-machining of the gears with different surface properties for the following year.

An initial oil choice was made through iterations of different options in the calculations. The goal was to reduce power losses by minimizing oil viscosity, while maintaining a high surface wear safety factor. The gear oil chosen during the surface pitting analysis was Mobil 1 SHC Gear ISO 220. An Exxon Mobil representative was then consulted to verify the choice. It was confirmed that for the given gear setup the 220 oil was optimal. However, if the temperature at the gear contact was raised above 54 °C, the higher viscosity 320 oil of the same brand would be advised. This is due to the breakdown of the lubrication film at these temperatures. Some testing of the system was done to confirm temperatures, which will be discussed in Section 6.2.1. However due to the nature of the testing, temperatures cannot yet be confirmed. If the oil temperature does raise beyond desirable limits during full vehicle testing, it is advised to switch to the more viscous Mobil 1 SHC Gear 320. Additionally, an actively pumped oil cooling system could be added, which the system has been designed to accept if necessary.

The tooth root stress limit is 54% lower than the pitting stress limit, however the actual applied bending stress is low enough to approximately double the safety factors for this failure mechanic to 2.45 and 2.53. This indicates that tooth root fractures are unlikely over the vehicle lifetime. This is good as a fatigue fracture of this nature would be difficult to predict with the team's resources and inspection capabilities. A crack at the tooth root would most likely not be found until fracture occurred. This instantaneous failure would cripple the rear powertrain, and unlike the surface pitting discussed above would be unrecoverable during competition testing. These results will be verified through the FEA in Section 5.3.2.

5.3.2 Individual Gear FEA

Each gear was analysed in NX Nastran to evaluate tooth strength, and validate overall design. During the ISO calculations, the forces at the tooth were calculated based on the maximum input torque of 250 N m. The tooth load normal to the tooth face was calculated to be 7711 N. The total contact ratio was also calculated as $\varepsilon_\gamma = 2.54$, meaning there would be a minimum of two teeth in mesh at all times. Using this information the constraints and loads for this analyses were defined.

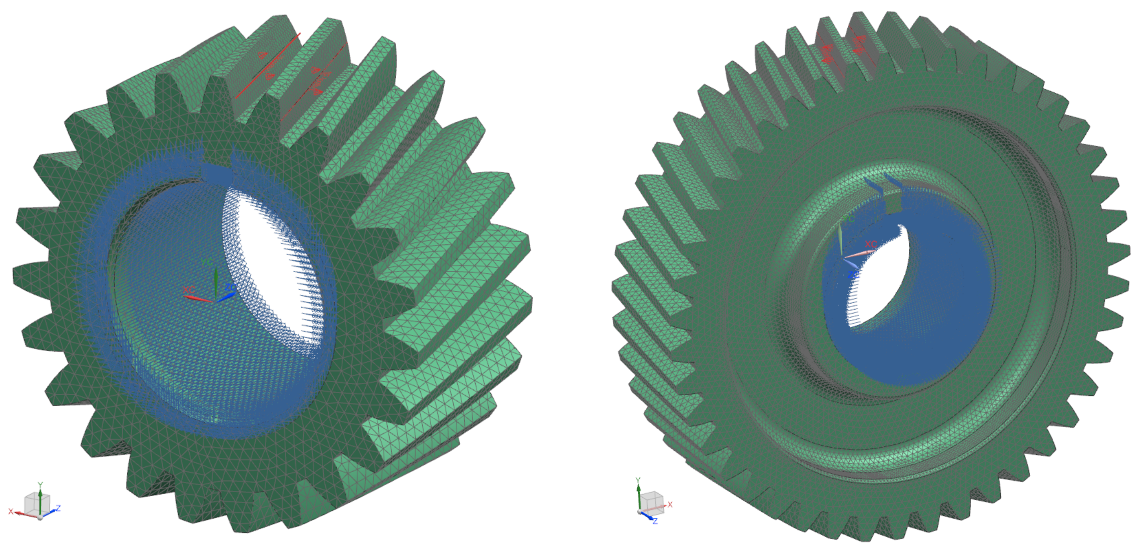

(a) Pinion Gear (b) Wheel Gear

Figure 5.2: Gear FEA constraints (blue) and loads (red) on mesh

Three constraints were used to fully constrain both gears as realistically as possible, seen in Figure 5.2. Both models use the Z axis as the axial direction, with X and Y being in the radial direction, with the Y axis intersecting the keyway. A cylindrical constraint was put on the inner bore, fixing radial growth only. This simulates the surface of the shaft in contact with the gear bore. The side faces of the keyway are then constrained, fixing translation in the X direction and rotation about the Y and Z axes. This simulates the key, effectively restricting rotation about the first cylindrical constraint. Finally, one face of the gear was constrained, fixing translation in the Z direction and rotation about the X and Y axes. This constraint was applied to a 46 mm diameter circle, simulating the snap rings which restrict axial movement on the gear shafts. The load was applied across two gear teeth, with 3855.5 N applied to each tooth. The load was specifically applied to a line across the tooth flank, representing contact with the other gear.

Table 5.5: FEA results for gears

Gear	MAX. Displacement (mm)	MAX. Stress (MPa)	Yield Strength (MPa)	Safety Factor
Pinion	0.0066	359.8	1103	3.07
Wheel	0.0274	305.6	1103	3.61

The results from the FEA are shown in Table 5.5. Both gears have safety factors for yield strength above 3, and therefore are not at risk of failure under the maximum torque output of the motor. The stress distribution for each gear can be seen in Figures 5.3 and 5.4. Stress is concentrated on the application line, and near the surface, for both gears. There is very little stress at the tooth root, as well as little to no stress on the rest of the gear body. This agrees with the ISO 6336 analysis, showing that tooth bending is of less concern as compared to surface pitting over time. The keyways also maintain low stress values, staying in the light blue area of the distribution. This indicates the choice of interface is satisfactory for the application.

This analysis assumes perfectly rigid interfaces with the shaft and key, by fixing the radial growth of the bore face and translation of the keyway. This was deemed suitable considering the low stresses in these regions. A system analysis with the gear, shaft, and key will be discussed in Section 5.6 which further justifies these choices.

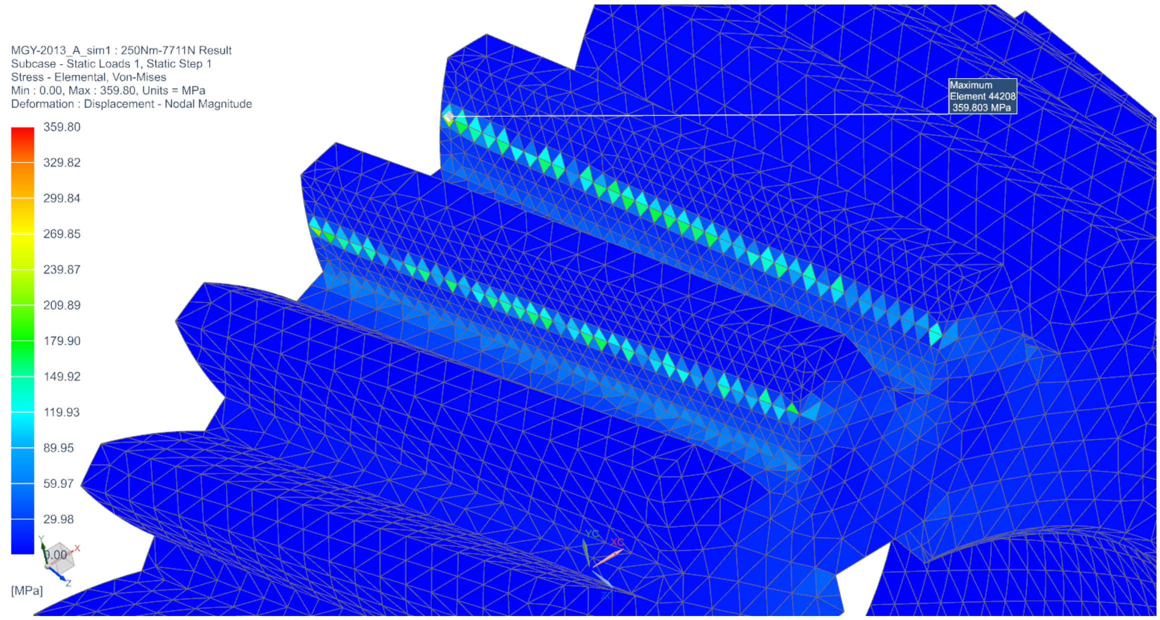

Figure 5.3: Pinion gear FEA, 7711 N (250 N m) loaded over two teeth

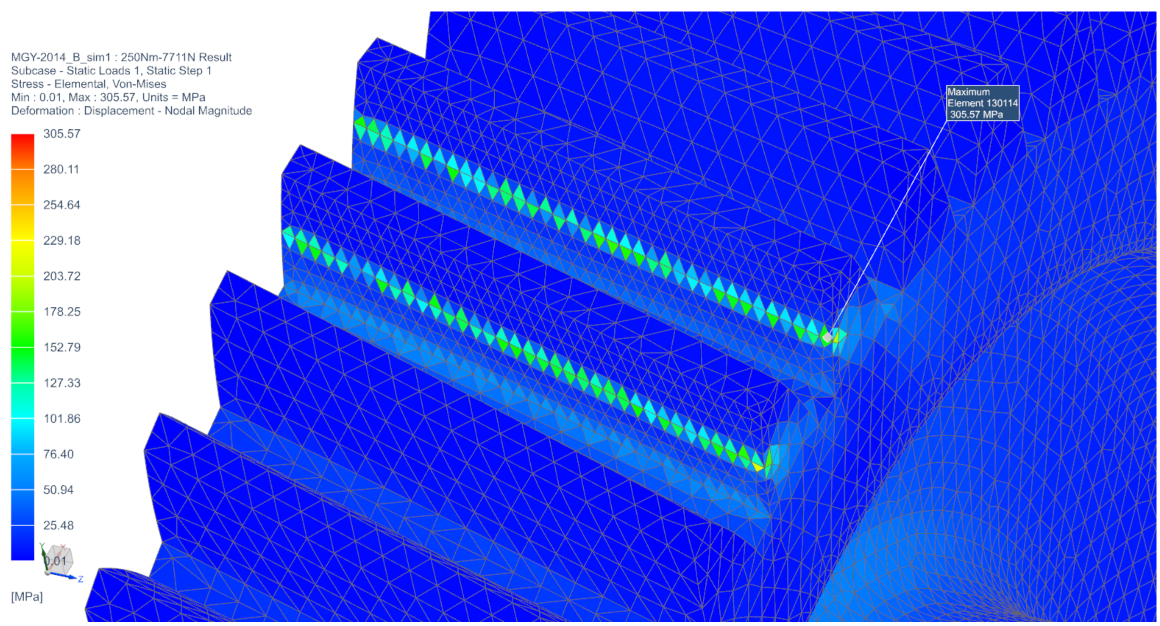

Figure 5.4: Wheel gear FEA, 7711 N (250 N m) loaded over two teeth

5.4 Shaft and Torque Transfer Design

This section will walk through the design of all torque transfer components in the system. These components are broken into four rotating assemblies, shown in Figure 5.5, the pinion gear and shaft, the wheel gear and shaft, the clutch output, and the CV joint assembly. These assemblies are groups of components that rotate at the same speed and on the same axis. Each component is analysed individually, with the assemblies being analysed in Section 5.6. Bearing layouts for the assemblies will also be discussed, in the section of the shaft they interface with. Technical drawings for all of the components can be found in Appendix A.

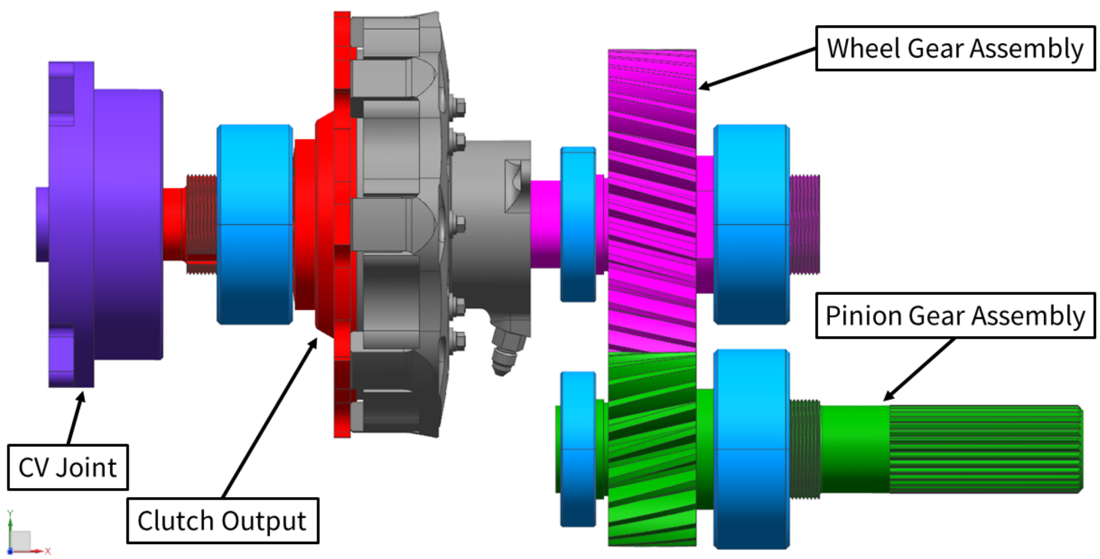

Figure 5.5: Torque transfer assemblies, with bearings shown in blue.

5.4.1 Pinion and Wheel Gear Shafts

The pinion and wheel gear shafts were designed together, as they share numerous design features. Figures 5.6 and 5.7 show the shafts as delivered, with major design features labelled.

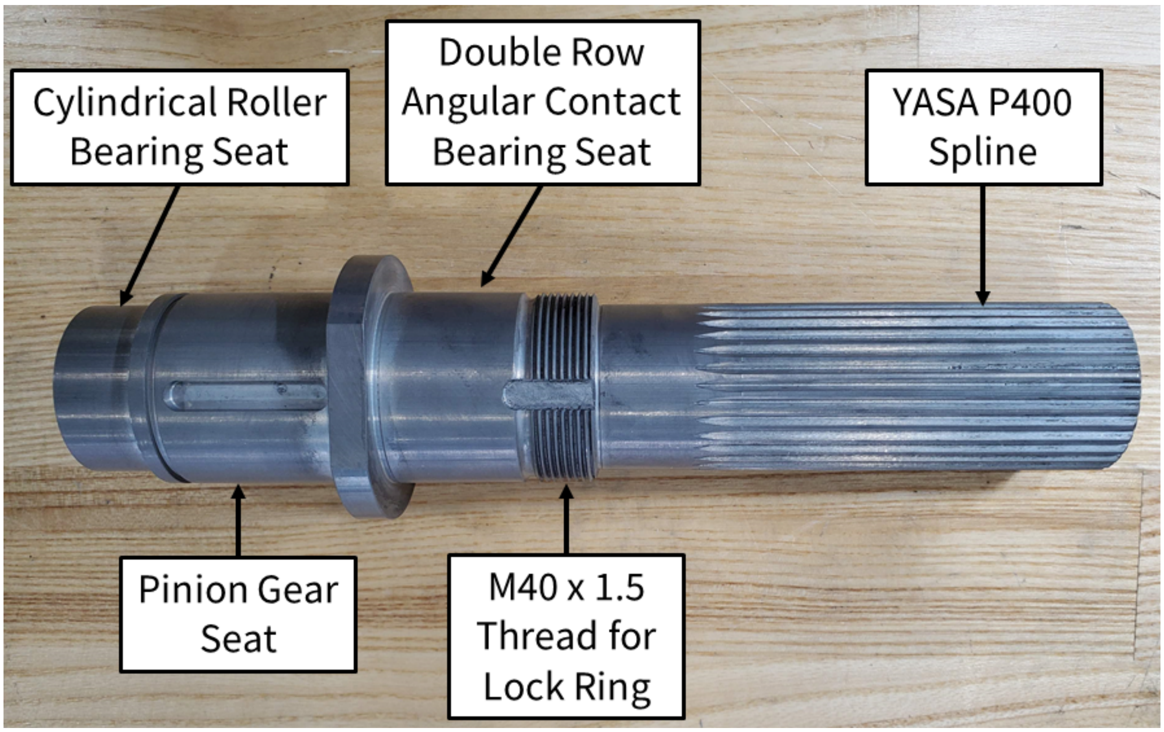

Figure 5.6: Pinion shaft as delivered with labeled features

The most influential design feature is the bearing layout. Design choices for the bearing layout were dominated by design goal 2, to reduce the axial length of the gearbox casing. Two main bearing layouts were investigated and can be seen in Figure 5.8. Ultimately the arrangement using a double row angular contact bearing, seen in Figure 5.8b, was chosen for three main reasons. Firstly, after many revisions of the shaft layouts, the overall axial length of this arrangement was shorter than the opposed angular bearing solution (Figure 5.8a). Secondly, the opposed angular contact bearings required a precise amount of preload to function properly, being provided

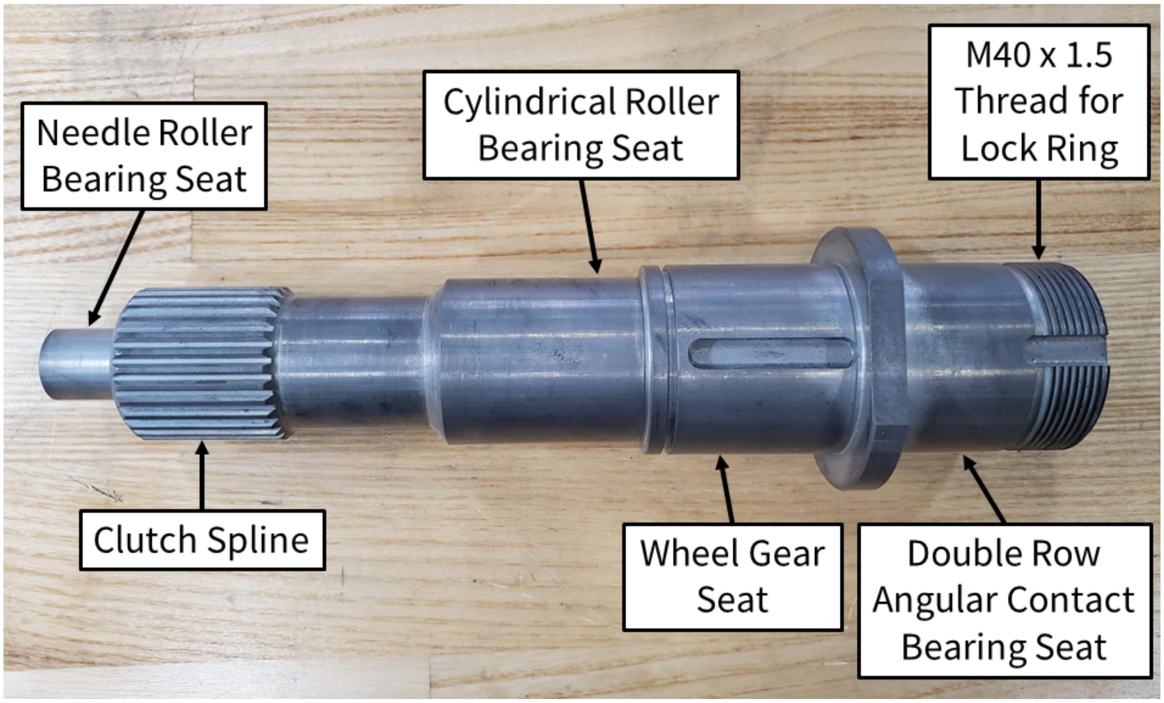

Figure 5.7: Wheel shaft as delivered with labeled features.

in this situation by the gearbox casing. The tolerances required to achieve this were deemed infeasible, due to silicone sealant being used in the lid closure. Lastly, this bearing arrangement offered better overall strength characteristics. To secure the double row angular contact bearings to the shafts, the bearing journal transitions into a threaded section. This accepts a nut and lock washer to retain the bearing on the shaft. The lock washer is keyed to the shaft, and has a tab hammered into the nut, to prevent loosening through vibrations.

The specific bearings selected for the shafts were chosen primarily by sizing requirements, with a basic rating life calculation done to ensure they met loading requirements. The calculation was done following all guidelines provided in the SKF rolling bearing catalogue [60]. A summary of the bearing specifications can be seen in Table 5.6. The L_{10} term is basic rating life at 90% reliability, measured in millions of revolutions. This was converted into an estimated life in kilometers using the average cycles per

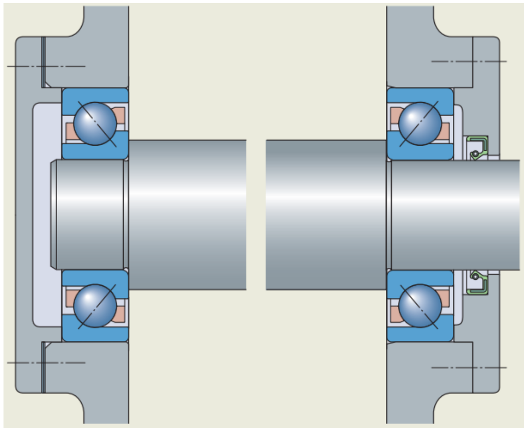

(a) Angular contact ball bearings arranged face-to-face.

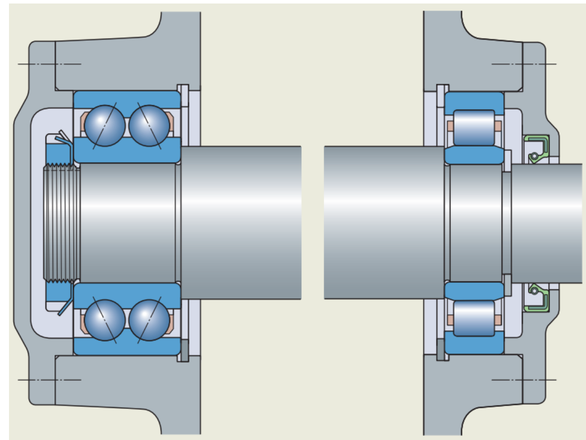

(b) Double row angular contact ball bearing with NU design cylindrical roller bearing.

Figure 5.8: Bearing arrangements considered for gear shaft design, figures from SKF rolling bearing catalogue [60].

kilometer discussed in Section 5.3.1, which is 1215.6 rev/km. The wheel gear shaft sees lower cycles due to its lower speed, however since the bearings are identical between the shafts, the higher cycle number will be the limiting factor. The calculated life term for all bearings is well beyond the expected life of the prototype vehicle. This provides substantial safety factors for these components, which outweigh any uncertainties brought by the relatively simple basic life rating analysis. The fits used between the bearings, shafts, and casing were also taken from SKF recommendations, to maximise bearing life.

Table 5.6: Summary of bearings used on gear shafts, bearings provided by SKF.

Part #	**ID (mm)**	**OD (mm)**	**T (mm)**	**Limit Speed (rpm)**	L_{10} **(mil. rev)**	**Calculated Life (km)**
3208 A	40	80	30.2	8000	651.9	536,259
NU 1007 ECP	35	62	14	13000	647.0	1,092,534
NA 4902.2RS	15	28	14	9500	N/A	N/A

Table 5.6 also contains a small needle roller bearing, used as a clutch pilot bearing.

The only radial loads in this section of the shaft will be from clutch vibrations, and are therefore difficult to estimate without thorough testing, which is outside the timeline of this project. For this reason, a meaningful L_{10} cannot be calculated for this bearing. However, it is expected that any loading this bearing receives will be low, and therefore its life will not be the limiting factor in terms of system longevity.

The next major design feature on the two shafts are the spline interfaces. The pinion gear shaft has a spline matching the YASA P400, as it is the input shaft for the gearbox. The wheel gear shaft has a spline matching the Tilton metallic clutch plates, as it is the output of the gearbox. These were areas of concern as in the past EcoCAR 3 competition the team had several shaft failures, specifically around spline interfaces with the YASA P400. A coupling shaft between the EM and engine crankshaft of this vehicle failed early in the testing process. The fracture was analysed by the mechanical team lead at the time. Findings include a starburst pattern indicating fracture by reversed torsional fatigue failure, likely caused by torsional vibration from the ICE [61]. It was recommended that relief cuts at the tool lead out of the spline teeth be used on later shaft designs. These concerns and recommendations were brought to the attention of Rapid Precision Machining & Gearing Ltd., the manufacturer of the gears and gear shafts, for consultation. The company recommended not adding a relief cut on the constant diameter YASA spline section of the pinion gear shaft. It was advised that in the experience of this manufacturer, smooth tool exit of a hobbed spline provided minimal stress concentration, and that the material removal for a relief would make fracture more likely. It was decided that no relief would be made, trusting the expert opinion of the manufacturer. Additionally, the loading conditions for this shaft would involve considerably less torsional vibration than that of the EcoCAR 3 shaft, as it would be driven by an EM only, giving much smoother torque delivery than the periodic nature of an ICE.

The spline on the wheel gear shaft does have a spline relief, however the its purpose is to aid with shaft clearances. The shaft passes through the release bearing and clutch diaphragm, which have identical internal diameters of 32 mm. The outer diameter of the clutch interface spline is 31.75 mm, so the shaft has been narrowed to 28 mm in order to give more clearance for shaft deflections and diaphragm movement, as shown in Figure 5.9. The shaft ends in a 15 mm journal for the needle roller bearing, acting as a pilot bearing to stabilize this portion of the shaft.

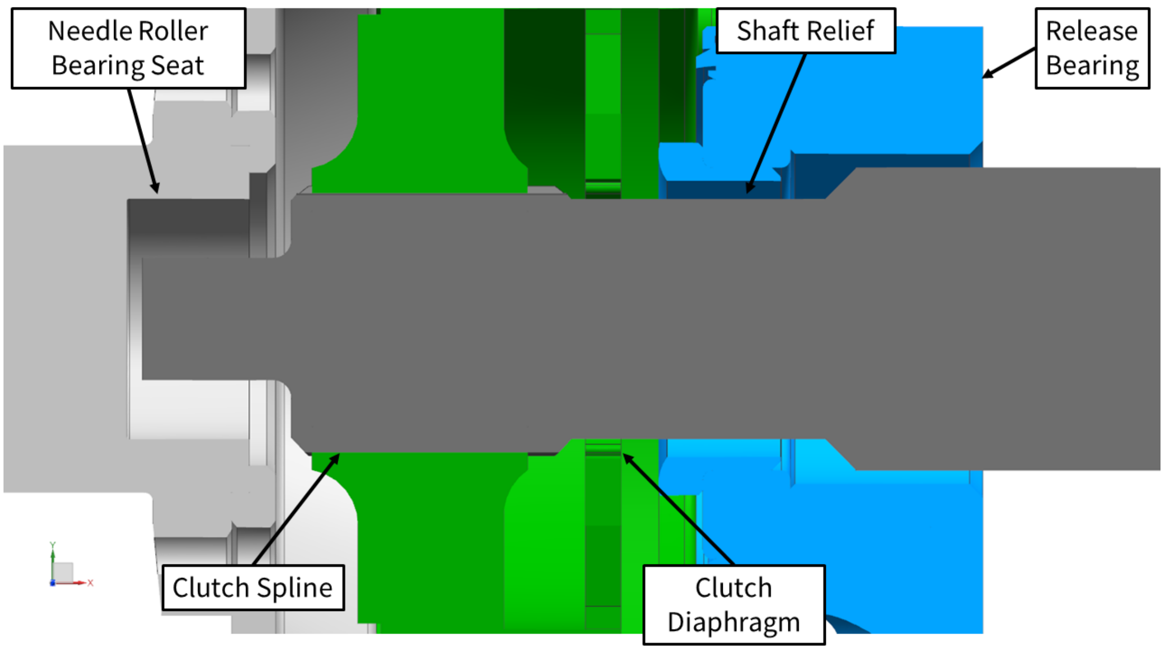

Figure 5.9: Wheel gear shaft, clutch, and release bearing.

A simple key design was chosen for the gear interface on both shafts. A spline was considered, but was unnecessary for the force transmitted by the shafts. Additionally, the key provides a relatively non-destructive point of failure for the shafts. As mentioned in previous sections, student competitions such as EcoCAR frequently feature component failures from unforeseen or unintentional load cases. In the event of an excessive torque being put through the system, the key on the wheel gear shaft will crush or shear before the failure of any other torque transfer components. This in effect acts as a mechanical fuse, protecting other components from overloading. The key can then be replaced with relative ease and little to no cost as compared to the other components of the system. Due to the budgetary limitations of a student team, no spare components were ordered for the complex machined parts such as the gears and shafts.

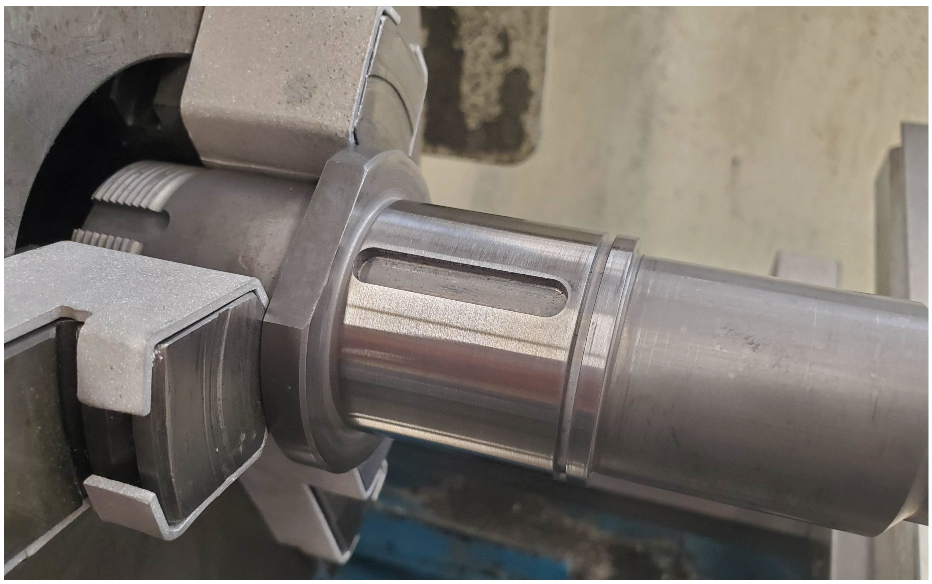

Figure 5.10: Post processing of the wheel gear shaft, lathe with aluminum soft jaws.

When the shafts were received, a test fit revealed that the gears were not a sliding fit with the shafts as intended. After consulting with the manufacturer, it was determined that the nitriding process added approximately 0.0076 mm (0.0003 in) to the surfaces of both the shafts and gears. As a sliding fit was desirable to maintain the function of the key design as described above, some post processing of the shafts was conducted. The shafts were gripped in a lathe with soft aluminum jaws so as not to mark the surfaces, then the gear interface surfaces were sanded down. Fine sandpaper was used so as not to remove excess material and to maintain a suitable surface finish. The sandpaper was applied over a file to maintain even pressure and remove material uniformly. The process was interrupted by regular test fits, and stopped when a suitable tight sliding fit was achieved with the gears. The finished product can be seen in Figure 5.10, with the brighter surface on the keyed journal being where material was removed.

5.4.2 Flywheel

The system required a custom flywheel to interface with the Tilton 5.5 in metallic two plate clutch, and provide a suitable output towards the differential. The choice to have the flywheel on the wheel side of the clutch, as opposed to the torque producing side as would be standard on an ICE, was made to aid the assembly process. Due to the geometry of the wheel gear shaft, it would have been extremely difficult to have a suitable flange on the clutch side of the system, without reversing the bearing layout as compared to the pinion gear shaft. This would significantly increase the axial length of the system. Additionally, the EM does not benefit from the increased rotational inertia that a flywheel provides in the same way an ICE would. It is beneficial for the EM to have a low rotational inertia, to quickly spin up from a stop in order to speed match the clutch when closing it, or spin down after opening it.

The main design features of the flywheel can be seen in Figure 5.11. The design is made to match the Tilton clutch, and therefore dimensions of the friction surface and threaded bolt circle were pre-determined. The inner recess was made as minimal as possible to decrease axial length, and fits eight M8 bolts with enough clearance to clear the clutch disks. The back of the flywheel is cut out around the friction surface to decrease overall mass. The back also contains a small step cut to locate the output shaft concentrically.

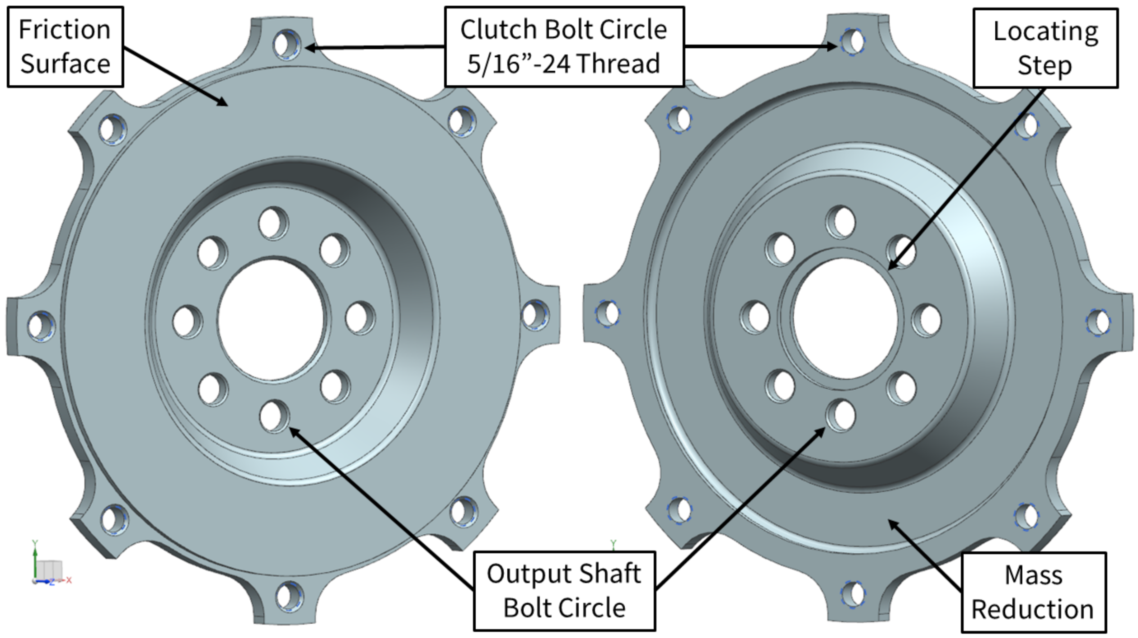

Figure 5.11: Flywheel CAD with labeled features.

5.4.3 Clutch Output Shaft

The clutch output shaft transfers torque from the flywheel to the CV joint on the differential input. It has a matching bolt circle of M8 threaded holes, and a protruding circular lip which locates on the flywheel. This transitions to a bearing seat identical to that found on the pinion and wheel shafts, in order to fit a sealed version of the SKF 3208 bearing. This is then locked into place identically to the previous shafts. The front of the shaft also contains a bore to accept the needle roller pilot bearing from the wheel gear shaft. These design features can be seen in Figure 5.12.

The spline on this shaft is to match the CV joint discussed in Section 5.4.4. The joint is one the team has in hand, but does not have a CAD model or specifications for. The team therefore partnered with Avion Technologies Inc. to have the shaft manufactured. The team gave Avion a sample of the female spline, for which they generated the corresponding male spline. The shaft contains a groove in the spline to

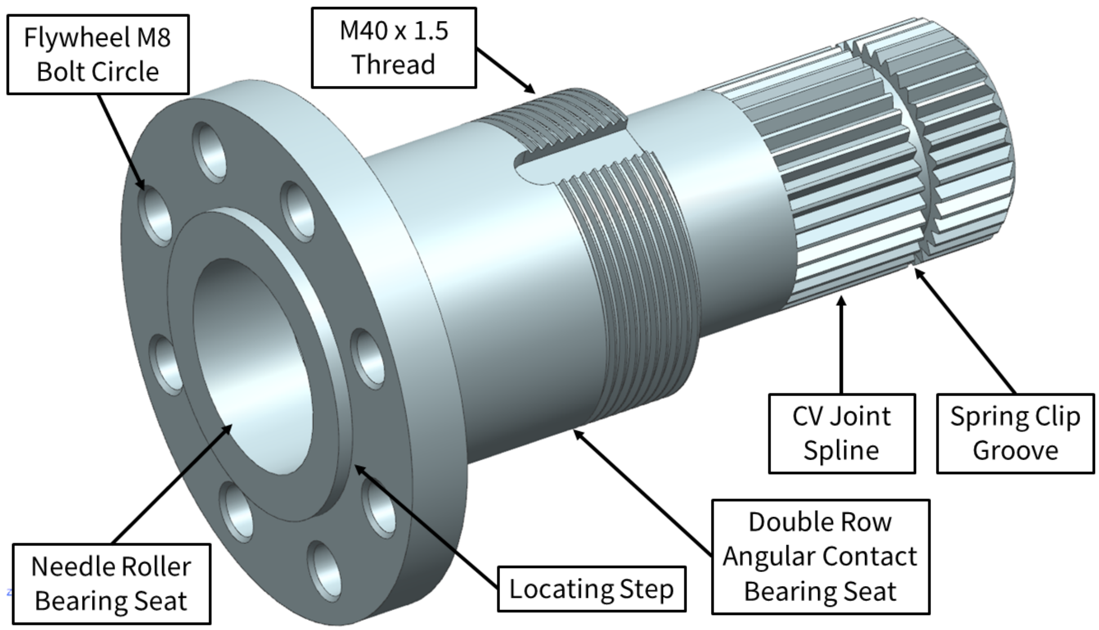

Figure 5.12: Clutch output shaft CAD with labeled features

hold a spring clip retaining ring, matching the OEM implementation on the original CV joint.

5.4.4 CV Joint Adapter

In order to improve vibration isolation, and to account for possible mounting misalignment, it was decided to separate the differential from the gearbox assembly with a CV joint. The chosen joint is from the Camaro half shafts the team had in hand, which normally attach to the output of the chosen differential. This joint was chosen as having it in hand allowed for a more in depth design process to ensure proper packaging in the system. Additionally, the joint uses bolts to attach to the differential, meaning it can be easily adapted to the input with a plate design.

After removing the rubber boot and thin steel backing plate, the main structure of the joint can be seen in Figure 5.13a. The joint uses a six bolt pattern, and the

(a) CV joint top view.

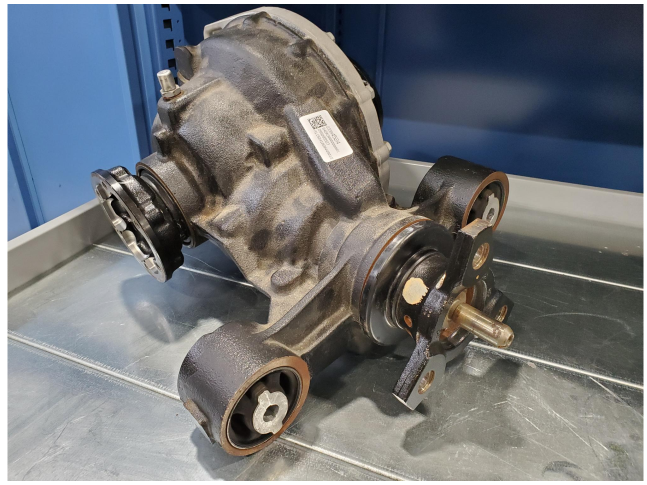

(b) Camaro differential to be used in rear powertrain.

Figure 5.13: CV Joint and chosen differential.

differential input yolk seen in Figure 5.13b uses a 3 bolt pattern. Therefore a simple adapter was designed, which also encloses the rear of the joint to seal in the grease, as the old backing plate did. The differential also has a locating pin in the center of the input yolk, that the adapter will interface with to ensure concentricity. The locating pin will be cut short to reduce overall axial length.

The simple initial design was used by the author in the Mechanical Engineering 759 course, in which an object had to be optimized, including using an FEA topology study. This resulted in a 77.3% reduction in mass. This was achieved by first performing the topology study in Fusion 360, the chosen software by the course administrator for this task. The results, which can be seen in Figure 5.14a, show that very little of the material is load bearing. As this adapter still needed to be a sealing end cap for the CV joint grease, not all material could be removed. However a significant reduction in cross section was made, as can be seen in Figure 5.15. This reduced the axial length from the CV mating surface to the differential input from 18 mm to 13 mm. This final design was then validated in NX Nastran as can be seen in Figure 5.14b. Loaded

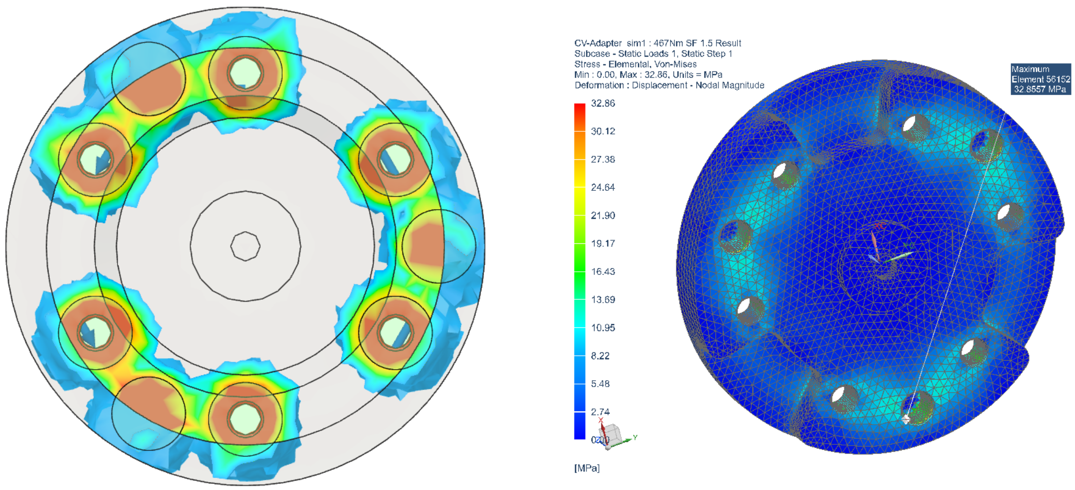

(a) CV adapter topology optimization in Fusion 360.

(b) Optimized CV adapter FEA in NX Nastran, max stress 32.86 MPa.

Figure 5.14: CV adapter topology optimization and NX Nastran FEA.

at 1.5 times the maximum gearbox output torque, the maximum stress rises to only 32.86 MPa. The component will be manufactured from a steel alloy, most likely 4340, and therefore this stress is acceptable. With such a low stress value aluminum was considered, however the threaded holes for the differential yolk have only a single bolt diameter of thread engagement, making thread pull out a concern. Future component optimization by the team may involve a two piece component, utilizing a steel structure as the adapter and thin aluminum sheet as a sealing plate.

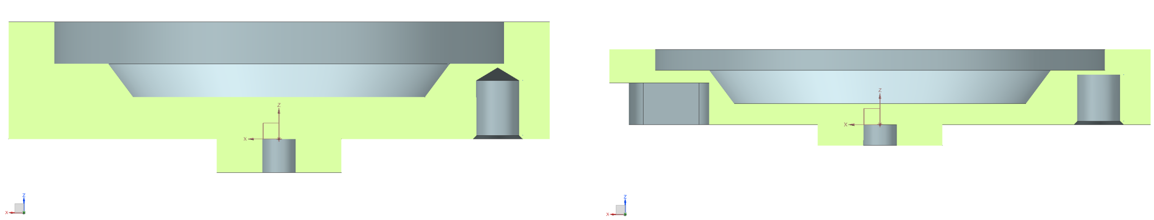

(a) Cross section before optimization.

(b) Cross section after optimization.

Figure 5.15: CV adapter cross sections, before and after optimization.

5.4.5 Rear Half Shafts

The rear half shafts present more design challenges than the front half shafts. The rear half shafts must connect the output of the Camaro differential to the stock Blazer wheels, while also accounting for the different position of the differential outputs as compared to stock. It was decided early on to utilize OEM components for the CV joints at either end of the shafts, which leaves two possible designs for the intermediate shafts. The first involves taking the stock rear Blazer half shafts and the stock Camaro half shafts, cutting them, and welding the two together. This achieves all of the requirements for the shafts, but does lead to concerns about fracture during torque transfer. The second option is to have new intermediary shafts made to the appropriate lengths, with the corresponding splines machined into each end. This removes the torque transfer risks, however introduces some manufacturing concerns. Similar to the CV joint used on the differential input, the joints on either end of the half shafts are ones the team has in hand with no specifications. Therefore a manufacturer would need to measure and recreate these splines for the team. To aide in the process, a half shaft design guide was released by American Axle & Manufacturing (AAM), a competition level sponsor. This guide has recommendations for both the design options, and estimates the welded design presented therein can transmit 75% the torque of a similar OEM shaft.

The welded design was chosen in order to meet the aggressive timeline of the competition. This involved the design of a sleeve to be welded at the intersection of the two shafts, as per the AAM guide. This welded solution was to be used for vehicle testing and Year 2 competition. At that point, the team could evaluate the effectiveness of the solution, and have single piece shafts manufactured on the more open Year 3 timeline if necessary.

5.5 Housing and Mounting Design

The design of the gearbox housing and mounting was done in tandem with the torque transfer component. Its purpose is simply to provide mounting locations for all components. As such the relevant design goals from Section 5.1 are numbers one, two, and five. Vibrations transferred to the EM from the vehicle can be reduced via the mounting strategy. Minimising the axial length of the system began with the shaft designs, but follows into the housing design by selecting appropriate wall thicknesses. Finally, overall system mass is highly influenced by the housing design, as it represents the largest volume of material in the rear powertrain.

5.5.1 Gear and Clutch Housing

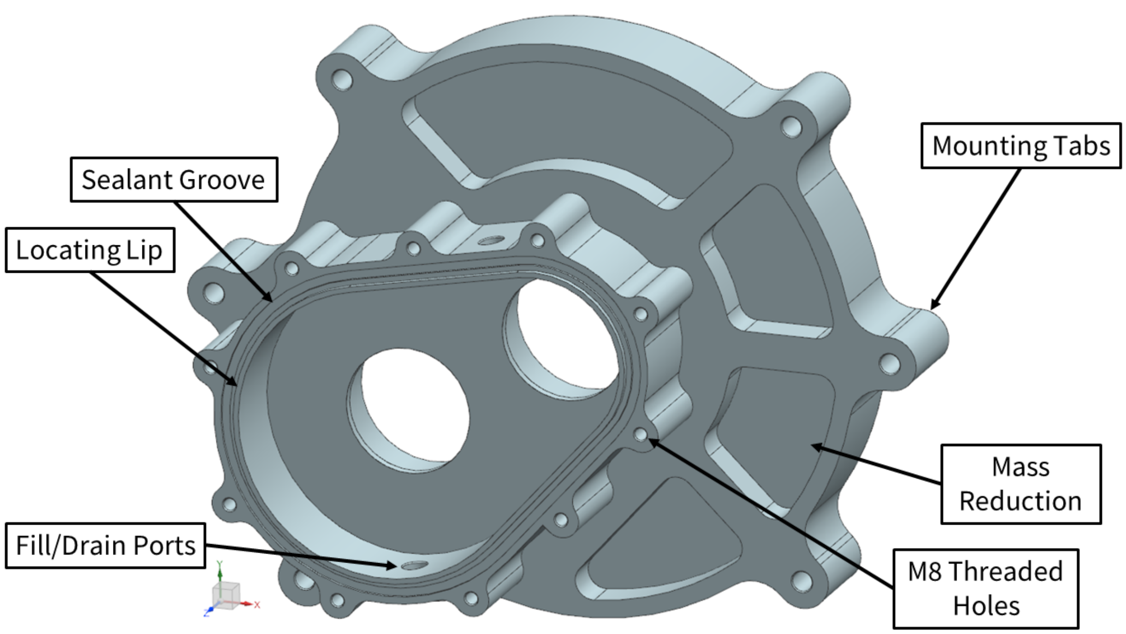

Figure 5.16: Main gear housing CAD front view with labelled design features.

The main housing, as shown in Figures 5.16 and 5.17, is geometrically made up of two circles. The larger circle matches with the EM and has has space for the pinion gear, while the smaller circle gives space for the wheel gear. The angle at which the gears are placed relative to each other allows the EM to sit higher in the vehicle, maintaining competition mandated ground clearance. The main wall thickness on the larger motor mounting circle is 48 mm, which matches the spacing of the rubber isolators discussed in Section 5.5.2. However, this thickness is not necessary throughout for strength and is pocketed to lower the mass of the component by 26%. The gear chamber protrudes from the main structure, and ends in a lip used to locate the lid of the enclosure. There is also a groove set into the top to hold the silicone based sealant, in order to ensure a leak proof enclosure. The M8 threaded holes match those on the lid in order to secure it, and the chamber has fill and drain ports machined into the sides. These are threaded to accept plugs or AN fittings, so that an active oil cooling system could be implemented if necessary in the future.

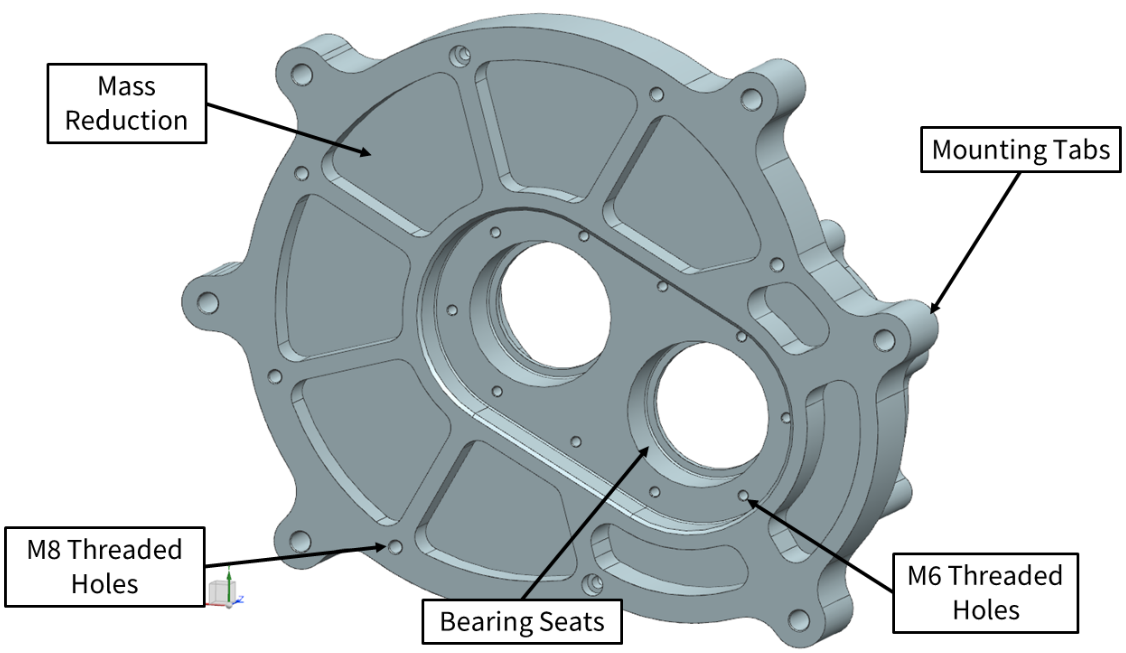

Figure 5.17: Main gear housing CAD rear view with labelled design features.

The double row angular contact bearings sit in the main housing, entering from the rear EM side of the component. They are held into the housing by a rear cover, which secures into the recess shown in Figure 5.17 with ten M6 bolts. The EM then bolts on top of this cover to the eight M8 threaded holes in the casing, two of which are counterbored to accept locating pins.

The rear cover is a simple component. It has counterbored through holes for the M6 mounting bolts, as well as an additional M8 threaded hole to complete the motor bolt pattern. The side facing into the housing has clearance holes to allow the shaft ends to rotate freely. The other side contains a small inset for a rotary shaft seal, which seals against the pinion shaft going to the motor. The sides contain two grooves for o-rings, which seal against the casing.

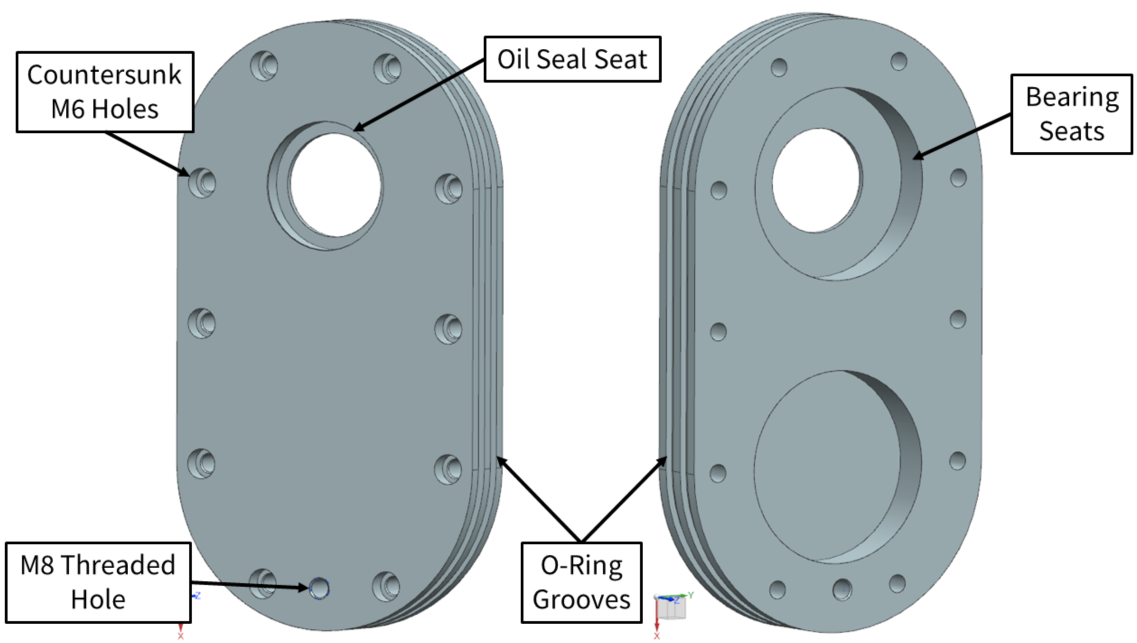

Figure 5.18: Rear cover CAD with labelled design features.

The housing lid contains the cylindrical roller bearings, as well as another rotary shaft seal for the wheel gear shaft. As seen in Figure 5.19, it contains a matching locating lip and sealant groove to the main housing. The combination of the interlocking lip and large amount of silicone sealant ensures a completely leak proof design. The top side of the lid contains eight M8 threaded holes, where the clutch housing will mount to. Additionally it has two M6 threaded holes for the Tilton release bearing to mount to.

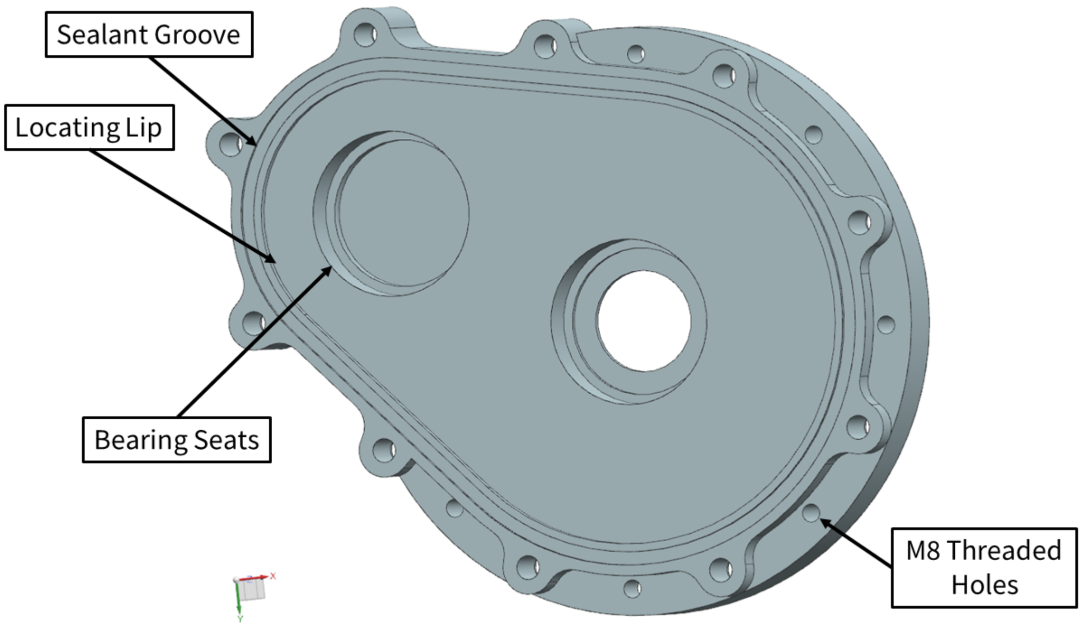

Figure 5.19: Gear housing lid CAD with labelled design features.

The clutch housing is a deep cylinder with eight through holes arranged around the outer edge. The front side contains a bearing seat for the sealed double row angular contact bearing, as well as eight M5 threaded holes for a bearing retention plate. Two of the through holes have bores on the rear side for locating pins, which match to similar bores on the main housing lid. These will ensure concentric alignment of the clutch input and output shafts.

All the above components were Computer Numerical Control (CNC) machined out of 7050 aluminum alloy, donated by Samuel, Son & Co. The 7000 series aluminum alloys have high strength characteristics, as well as excellent fatigue resistance. Due to the donated nature of the material, the components were made from two heat treatments of the 7050 alloy. The gear and clutch housings were Al 7050 T7651, while

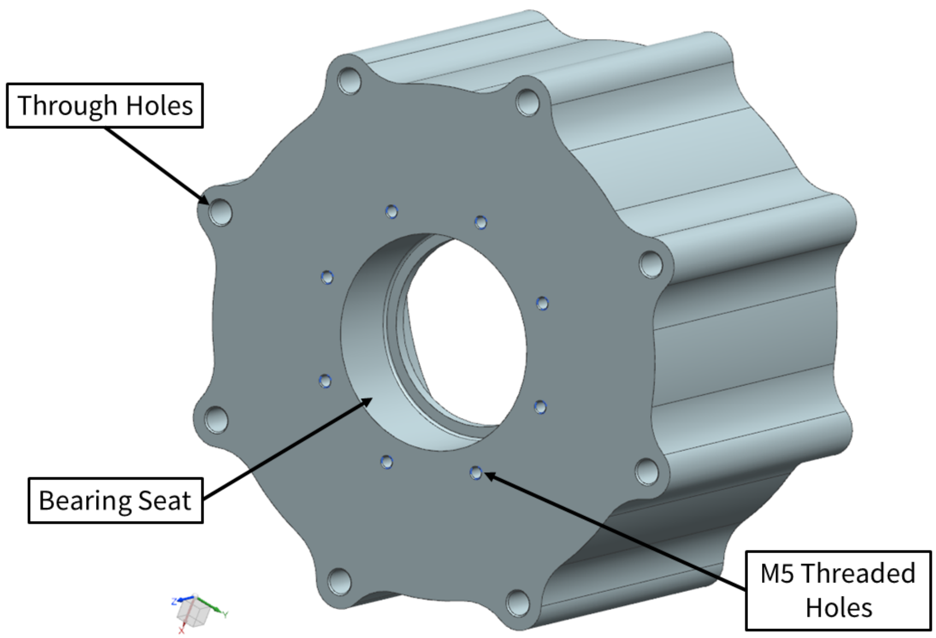

Figure 5.20: Clutch housing CAD with labelled design features.

the lid and rear cover were Al 7050 T7451..

5.5.2 System Mounting

The mounting strategy for the rear powertrain can be seen in Figure 5.21. The system attaches to the driveline in four places, two on the main housing and two at the end of the clutch housing. Each mount has a rubber vibration isolator attached to the vehicle body, which in turn means the driveline has no rigid mounts to the vehicle. This will aid in overall vehicle NVH by reducing vibrations from the driveline to the vehicle. The isolators chosen are used in the mounting of the stock Blazer differential to the rear cradle. They were chosen as the new rear powertrain will see similar speeds and vibrational loads to the stock differential. A full vibration study as well as the design of custom isolators are beyond the timeline of the competition.

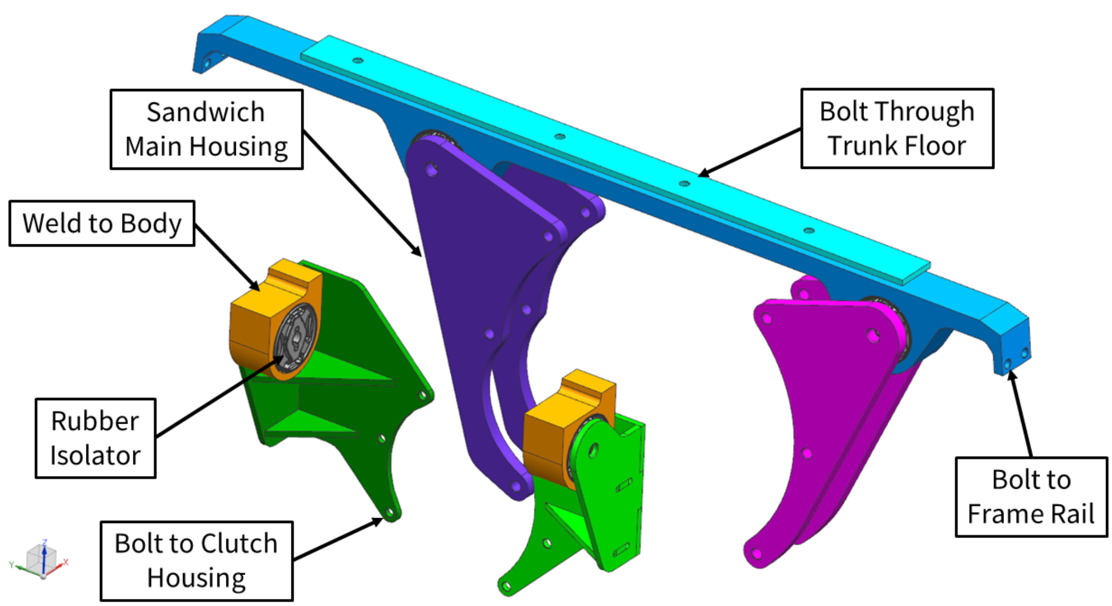

Figure 5.21: Gearbox mounting components CAD model labelled.

The main gear housing is mounted beneath the trunk floor. As such, it does not have a nearby structural point as the trunk floor is a thin steel sheet. Therefore an aluminum cross member was designed, which bolts into the frame rails on either side of the vehicle. The span of the cross member also has bolts which sandwich the trunk floor between it and an additional aluminum plate, for added rigidity and load distribution. The crossmember is made from the same donated aluminum alloy as the housings in Section 5.5.1, Al 7050 T7451. This cross member then holds two vibration isolators. Four 9.525 mm (0.375 in) aluminum 7075 plates then sandwhich both the isolators and the main housing. These rear mounts are larger than the front ones due to most of the system mass being concentrated near the rear. The YASA P400 EM, gears, and shafts are all concentrated around this point.

The front of the system contains another two mounts. These are made from several aluminum 6061 pieces, welded together to form right angle components with gussets. These bolt to the front of the clutch housing, using the through bolts which hold the clutch housing to the gearbox lid. The other side of each mount connects to a rubber isolator, which sits in a small steel enclosure. The steel enclosures are welded onto a body cross member. The rubber isolators at the front are rotated 90 degrees in relation to their rear counterparts, in order for the system to be damped in all directions.

Figures 5.22 and 5.23 show the full CAD model of the rear powertrain. The mounting system is semi-transparent gray, with each of the main housing components colored differently to easily differentiate them.

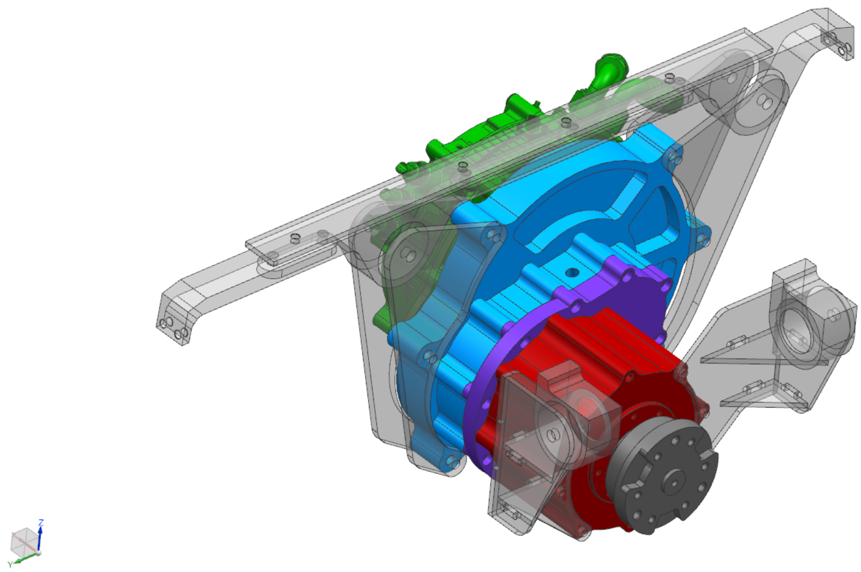

Figure 5.22: Full gearbox system, CAD model with mounts semi-transparent, reverse isometric view.

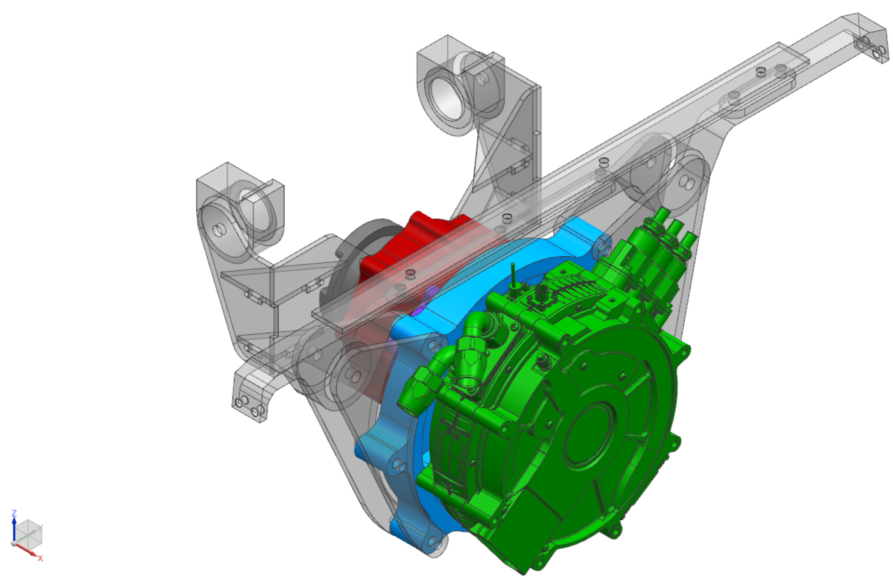

Figure 5.23: Full gearbox system, CAD model with mounts semi-transparent, isometric view.

5.6 System FEA

This section will overview the results from four system level FEAs on the pinion gear, wheel gear, clutch output, and housing assemblies to validate the rear powertrain design. The CV joint system, studied in Section 5.4.4, contained only a single component to analyse, and so is not included here. All four analyses were conducted in NX Nastran using identical principles and techniques, as described below.

Per competition rules, all powertrain mounting components must withstand 20 g lateral and 8 g vertical loading conditions, with a safety factor of 1.5, without entering into the plastic region of deformation. For ease of simulation, the safety factor and loading conditions are combined to become 30 g lateral and 12 g vertical without exceeding the yield strength of the material. Similar loading conditions have been adopted for the three torque producing systems, using the input torque multiplied by a safety factor of 1.5, and requiring the resulting stress be within the yield strength of the material.

The torque based simulations are all structured in the same manner. One end of the system is chosen as the fixed side, the other as the loaded end. To join the two ends of the system, surface contact is established between the components. Additional radial constraints are placed on bearing surfaces, simulating perfectly rigid bearing interactions. Finally, the system is given a fixed constraint in the axial direction. Testing the components as a system, instead of individually, gives a more accurate account of their strength under load. This accuracy comes at the expense of computational time, as the addition of surface contact to a simulation can increase the time needed from several minutes to several hours.

Most components are modelled using CTETRA10 elements, which are tetrahedral shaped with ten nodes. These are used for the ease in which the meshes can be auto-generated for 3D shapes. Some flat sheet components are modelled with CHEXA8 elements, which are rectangular prisms with eight nodes, as they can reduce computational load and increase accuracy in some situations. However, due to the increased difficulty in generating CHEXA8 meshes for complex 3D shapes, and the adequate accuracy of CTETRA10 elements, CHEXA8 usage is limited in these studies. Any bolted connections were modelled using 1D CBEAM elements with circular cross sections. They are attached to the 3D components using spiders of 1D RBE3 and RBE2 elements. The RBE elements are rigid, while the CBEAM elements act as a 1D beam of specified size. These are given bolt pre-load forces, in order to replicate the tension provided by the fasteners to the system.

The following sections will contain images of the stress distributions of each system, with a short summary of any notable findings. All components pass the requirement of not entering plastic deformation.

5.6.1 Pinion Gear Assembly

The pinion gear assembly was loaded at two of the gear teeth in the same manner as in Section 5.3.2, and fixed at the YASA P400 interface spline. A load of 5785 N was applied to each tooth, simulating a 375 N m input load to the gearbox. The maximum stress recorded was 250.82 MPa on the gear tooth, well under the 1103 MPa yield strength of the gear and shaft. As seen in Figure 5.24 the stress is concentrated around the pitch line of the teeth, as well as the end of the spline. The CAD model has an abrupt end to the spline, while the real shaft has a smooth tool exit, which makes the model a worst case scenario. This stress distribution corroborates that gear tooth pitting and spline exit stress concentrations are the most likely failure modes for this assembly. However the low stress values indicate that this assembly will not be the limiting factor for the rear driveline life.

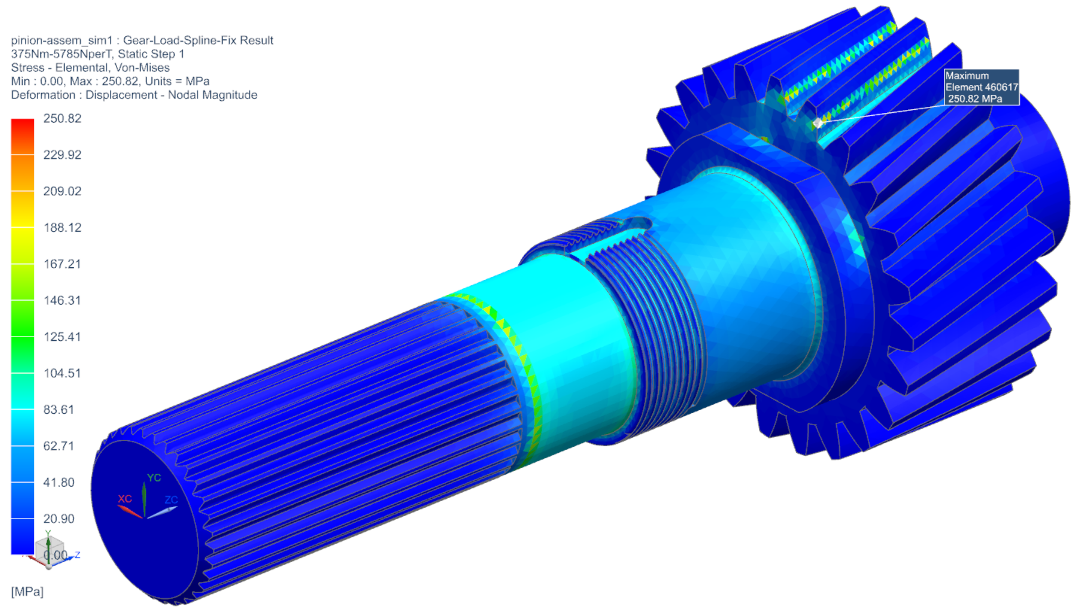

Figure 5.24: Pinion gear assembly FEA, max stress of 250.82 MPa

The maximum stress over the key is 52.74 MPa, with an expected key yield strength of 370 MPa. This validates that the pinion key is a more than adequate interface for the application. The stress distribution of the key can be seen in Figure 5.25.

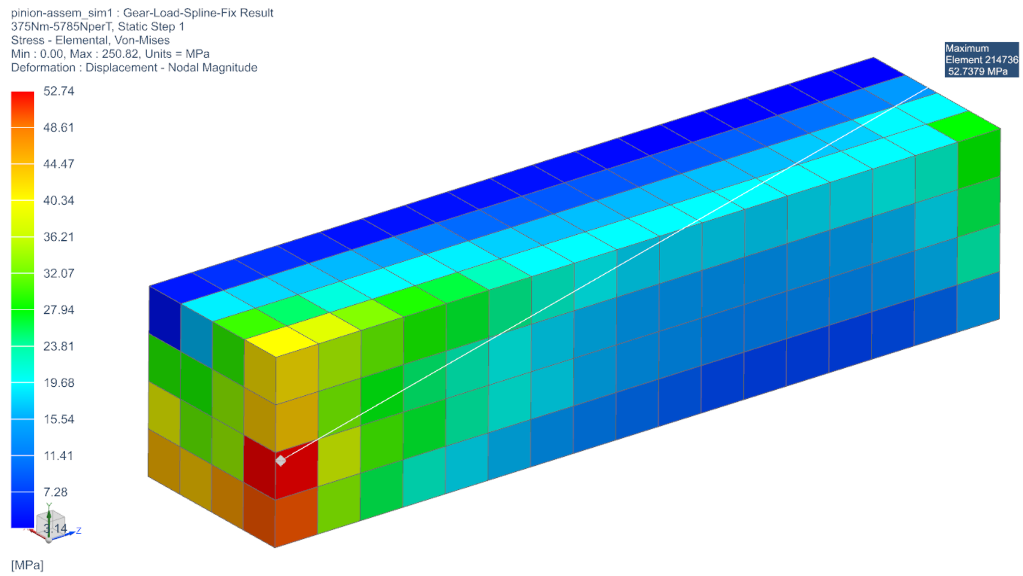

Figure 5.25: Pinion gear assembly FEA, key mesh, max stress of 52.74 MPa

5.6.2 Wheel Gear Assembly

The wheel gear assembly was loaded at two gear teeth in the same manner as the pinion above, as well as the gears in Section 5.3.2. The clutch interface spline was fixed. The system experienced a maximum stress of 865.52 MPa at the edge of the clutch spline. With a yield strength of 1103 MPa for the gear and shaft, this gives a comfortable safety margin, considering the safety factor of 1.5 incorporated into the load. Each tooth was loaded with 5785 N, simulating a 375 N m gearbox input torque, or a 701.3 N m torque on this system. The stress distribution shows that the thinner 28 mm section had the highest stress, as would be expected. Additionally, the stress concentration at the edge of the spline was influenced by the rigid fixing of the spline in the simulation. The real shaft will have flexion throughout the spline as it interfaces with the clutch plates, which should distribute the stress more evenly and lower the peak value.

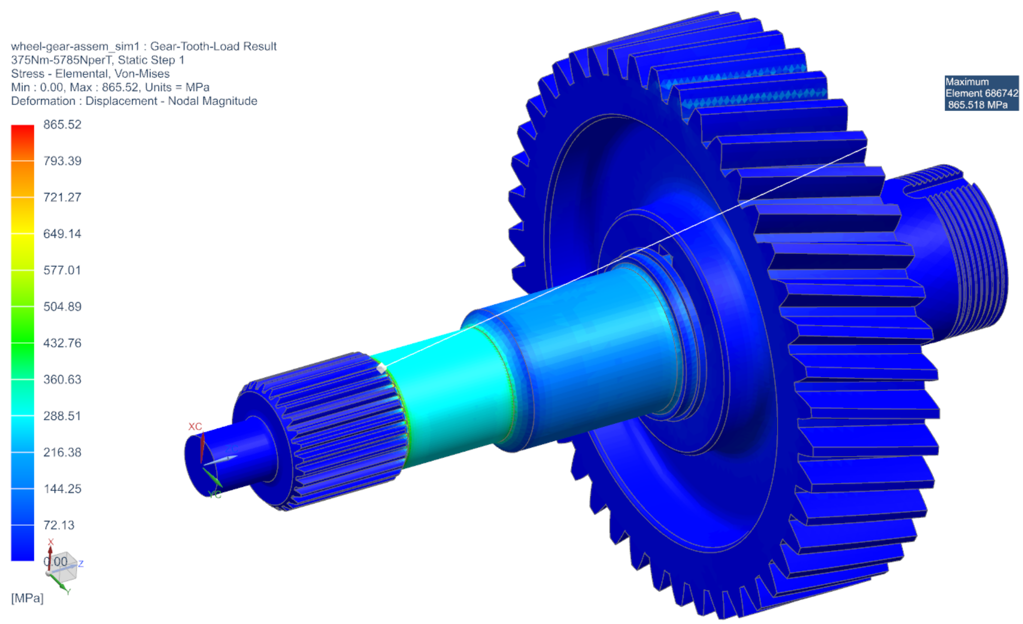

Figure 5.26: Wheel gear assembly FEA, max stress of 865.52 MPa

Isolating the key mesh, a maximum stress of 118.95 MPa is found, as seen in Figure 5.27. With an expected key yield strength of 370 MPa, this validates that this interface is adequate for this application. Due to the higher torque seen by this shaft, the stress of this key is raised as compared to that of the pinion assembly. In the event of an unexpected high torque event, this interface will be the failure point in the system.

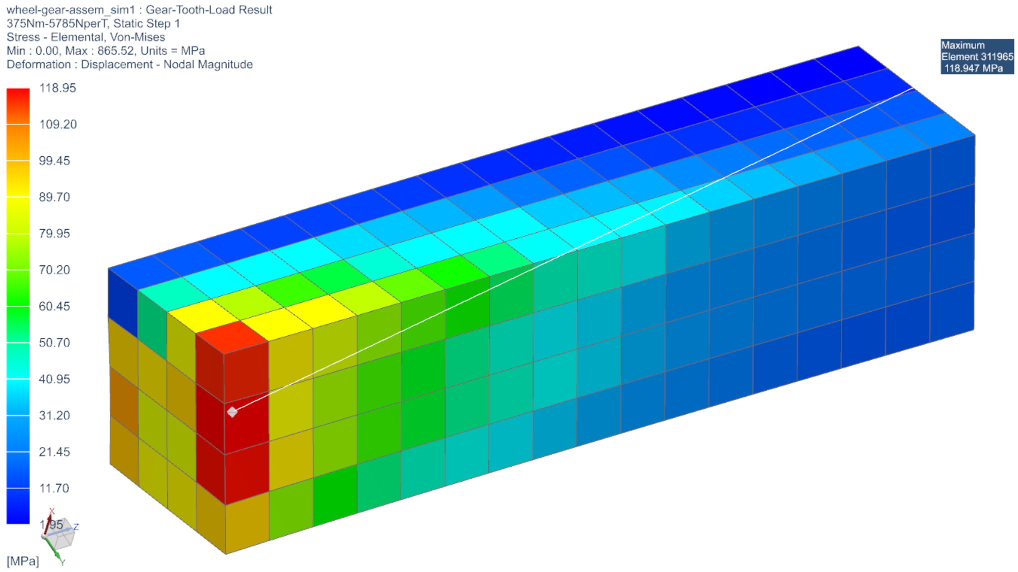

Figure 5.27: Wheel gear assembly FEA, key mesh, max stress of 118.95 MPa

5.6.3 Flywheel and Clutch Output

A 702 N m load was input onto the friction surface of the flywheel, while the CV interface spline was fixed in rotation. The eight 1D bolts were given a preload of 20 kN each, corresponding to a bolt installation torque of 32.5 N m. The system experienced a maximum stress of 714.88 MPa as seen in Figure 5.28a, as compared to a yield strength of 1103 MPa. This maximum stress was on an element below the surface of the threaded holes on the clutch shaft. It is suspected that issues with element shape around these areas is influencing several stress spikes. The sub-surface elements seen in Figure 5.28b are small with extremely acute angles, meaning they are not well conditioned. Poorly conditioned mesh is prone to stress spikes, and as can be seen the stress is concentrated in only a few elements, with those around them quickly dropping back to a lower stress values. Initial simulations saw stress spikes above 1300 MPa. The presented simulation was achieved by removing the chamfers on all of the holes, allowing the mesh to more easily conform to the component shape. The mesh around the holes was shrunk to a 1 mm size as opposed to the 2 mm seen on the rest of the model. It is suspected that the real life stress of these regions will be less. However, even with the suspected unrealistic outlier elements, the simulation remains within the yield strength of the material.

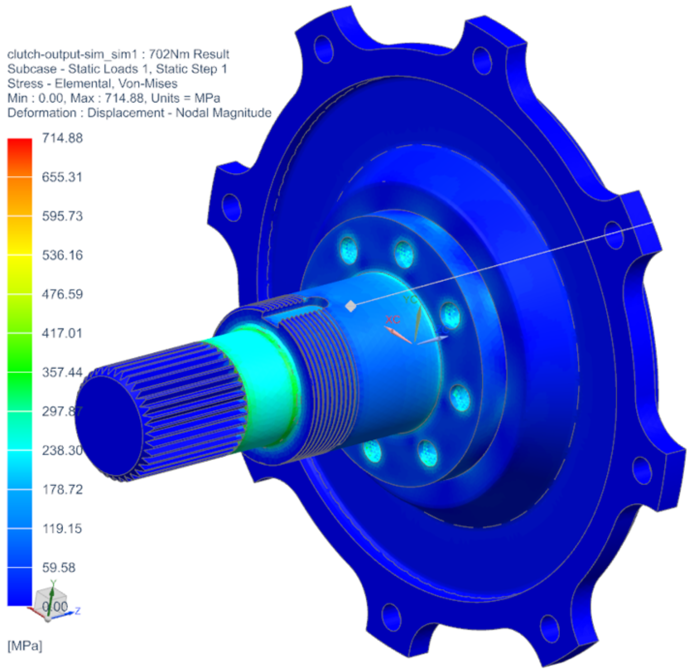

(a) Clutch output assembly stress distribution.

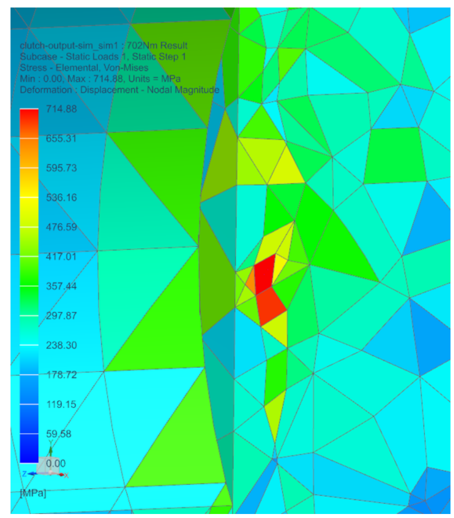

(b) Cross section of bolt interace elements.

Figure 5.28: Clutch output assembly FEA, max stress of 714.88 MPa

The stress distribution indicates that the flywheel experiences little to no stress on its outer portions, being concentrated at the bolt interfaces. The spline diameter portion of the shaft experiences stresses between 250 MPa and 350 MPa. This is the highest stress outside of the bolt regions, but being substantially below yield strength is not of concern.

5.6.4 Housing and Mounting

This system is loaded in a different manner to the torque transfer systems above. A global acceleration matching the 30 g and 12 g loads is used, which accelerates the housing and mounting components according to their mass. The YASA P400, gears, and shafts are then modelled with rigid 1D RBE2 spiders connected to a central node for each component. A force equaling that components load is then put on that node, which transfers to the appropriate bolt points or bearing journals. This simplifies the simulation slightly, but saves a large amount of computational time with minimal losses in accuracy.

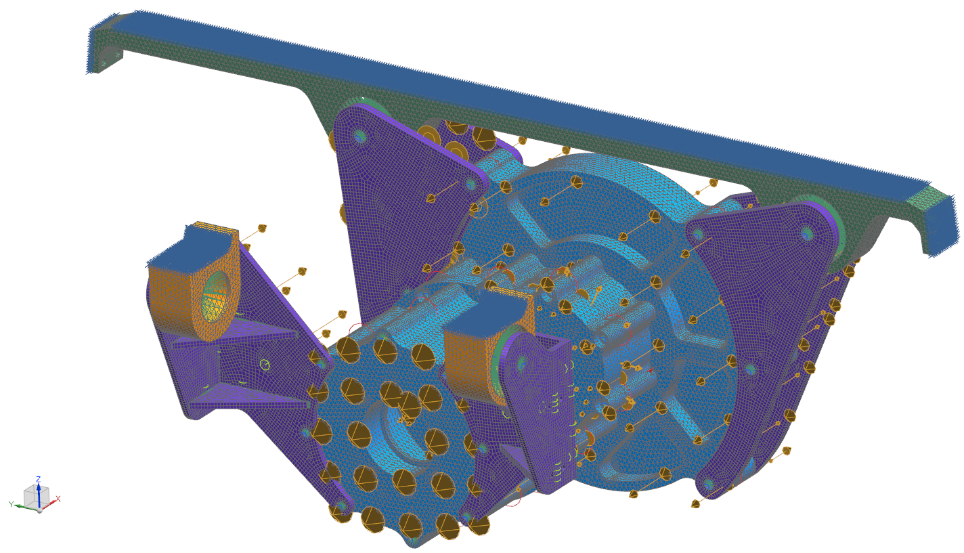

Figure 5.29: Housing and mounting simulation setup.

The results of all six load cases can be seen in Table 5.7. The 30 g load in the negative X axis direction creates the largest overall stress of 235.16 MPa, located in the front welded mounting components. The negative X axis direction is towards the front of the vehicle, which pushes the rest of the components into these mounts, causing compression and bending loads. These components are made from aluminum 6061 alloy with a yield strength of 276 MPa. Therefore no plastic deformation is seen in these components. All other components in the system are made from either aluminum 7075 or 7050 alloys with yield strengths almost double that of the 6061, meaning no other components are at risk of yield. As can be seen in Figure 5.30, the stress concentrates around the connections points between the mounts and the main housings. This is due to both the increased bending loads at these sections, and the bolt preload forces present there. The system has a very low overall stress profile, indicating that mounting failures will not be a concern during normal operation of the vehicle.

Table 5.7: Housing and mounting assembly FEA maximum stress for all load cases.

Load Case	**Max. Stress (MPa)**
+X 30g	211.09
- X 30g	235.16
+Y 30g	162.73
- Y 30g	162.2
+Z 12g	162.28
- Z 12g	162.79

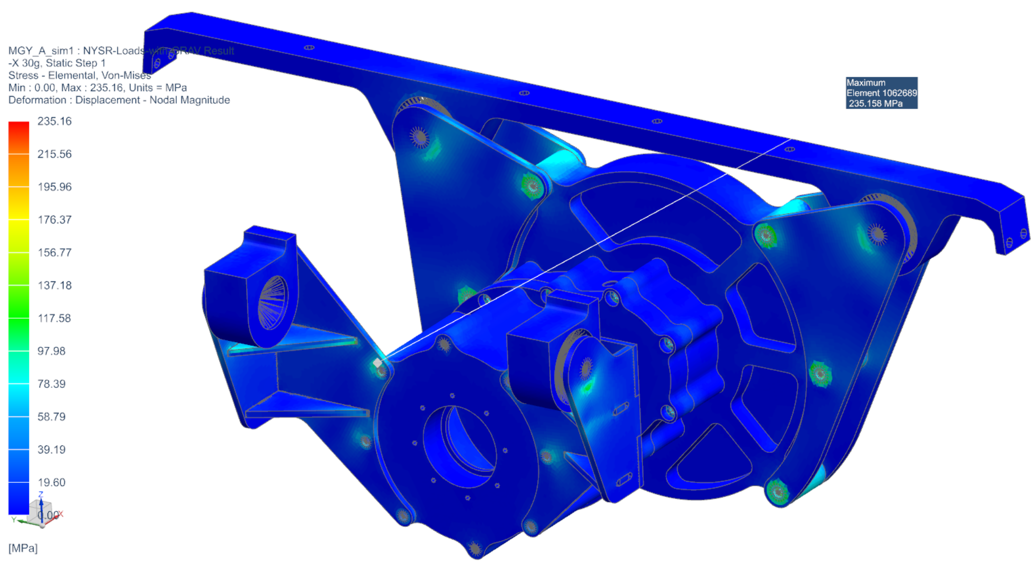

Figure 5.30: Housing and mounting assembly FEA, -X 30g load, max stress of 235.16 MPa

Chapter 6

Vehicle Integration

This chapter will discuss the vehicle integration done up until mid March of 2020. At that point the COVID-19 epidemic caused the MARC building, along with all of McMaster, to be closed due to safety concerns. The original integration timeline ended in mid May of 2020, when the EMC Year 2 competition was to be held. Unfortunately this competition was also cancelled. Therefore, significant changes to the integration strategy and timeline have been made. This chapter will mainly discuss the work already completed, with some recommendations for the MAC team going forward. Concrete plans such as a new integration timeline cannot be presented at this time, as the COVID-19 epidemic continues to effect the team's abilities to function as normal, therefore all plans for the upcoming semesters remain fluid at this time.

During first semester of 2019, the vehicle was completely stripped of interior components as can be seen in Figure 6.1. This was done to facilitate the future work being done on the car, in particular the routing of electrical harnesses. The hood, front fascia, and bumpers were also removed. As of this writing, the vehicle remains in this state.

Figure 6.1: Vehicle interior post strip down.

6.1 Front Powertrain Integration

The front powertrain is the backbone of the vehicle. Being made up of predominantly OEM parts, and producing a significant fraction of the total vehicle power, it is to be used as the main power source of the vehicle as well as a fallback system in case of a rear powertrain failure. For these reasons the integration of this system was started early, in December of 2019. At this time an engine swap was performed, were the old V6 was removed and the new LYX engine and M3U transmission were installed, as seen in Figure 6.2. In January of 2020, some remaining supporting components were installed, and the engine was started for the first time. The Engine Control

Module (ECM) and Transmission Control Module (TCM) used were provided by GM, and are flashed to function in the Blazer vehicle. To note is that the engine has no FEAD at this time. The water pump is now electric as discussed in Section 4.1, and the BAS is not yet installed. This means the vehicle battery needs to be attached to an external charger to function. This is not limiting as at this point the vehicle is disassembled to a point where it is undrivable, and remains on the lift at all times.

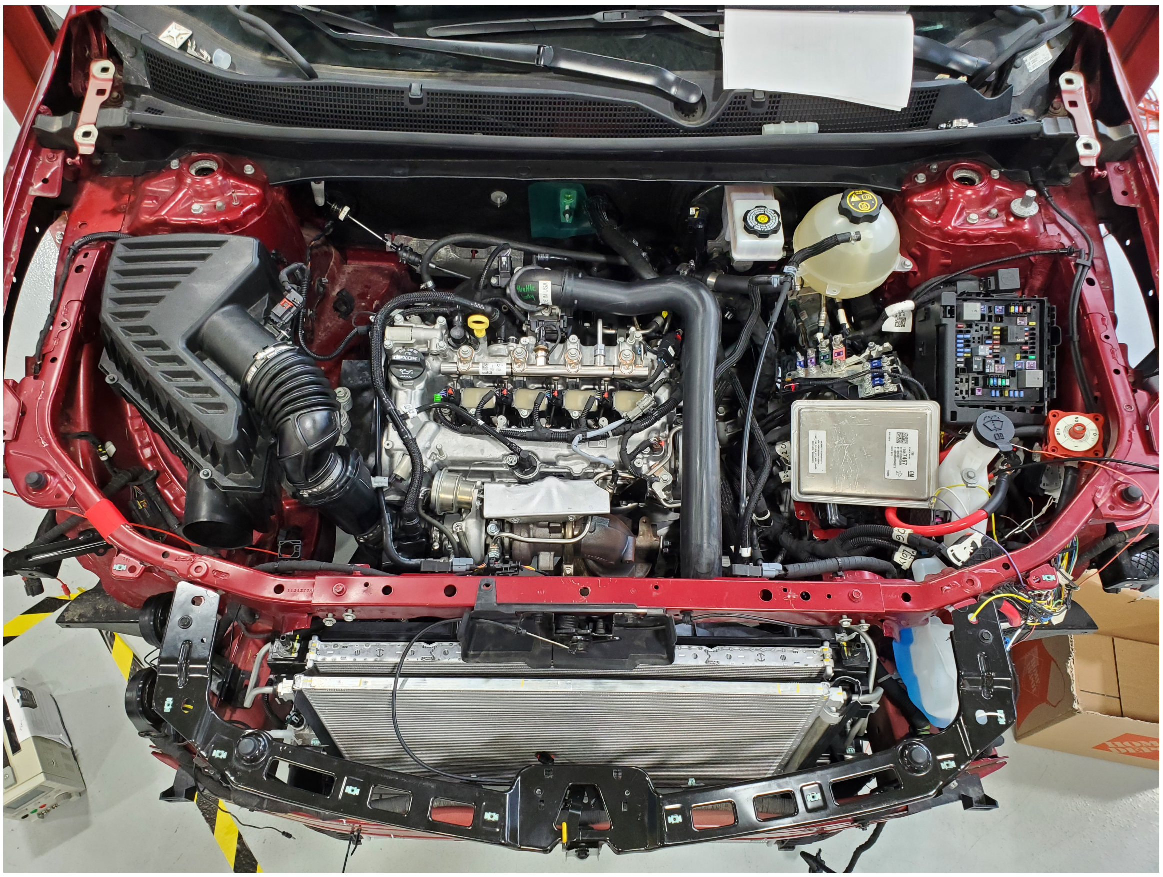

Figure 6.2: Top view of MAC Blazer with new LYX engine and M3U transmission installed.

Having a functioning ICE, work turned to integrating the ETRS of the new transmission with the Blazer. Through the installation of a GMC Terrain ETRS module, control over the park, reverse, neutral and drive states was achieved. This also required the implementation of a serial gateway, where vehicle Controller Area

Network (CAN) messages are passed through the team controller and can be modified if necessary. This allows the team to smooth out the interface between the ECM, TCM, and Body Control Module (BCM). For example, the BCM was sending error codes about a missing transmission shift lever, as it had been removed to make way for the new shift buttons. The vehicle can now shift gears successfully, and spin the front wheels on the lift. However, the internal integration of the ETRS is currently limited to being wired into the car. As can be seen in Figure 6.3, no work to rebuild the dashboard or center console has been done as of yet.

Figure 6.3: Current cockpit view of the MAC Chevrolet Blazer.

A BAS test bench has been constructed, with initial controls development for the motor underway. Moving towards a fully functional front powertrain, it is the author's reccomendation to focus resources towards integrating the BAS onto the ICE. This will allow controls development to move forward at a system level. Additionally, this would allow dynamometer testing of the front powertrain, which will be necessary to fully evaluate the system under load.

The new smaller vehicle fuel tank should be pursued after BAS installation. The aluminum panels for this component have been manufactured, but still need to be welded together. Replacement of the stock fuel tank will make room for battery enclosure to be installed into the vehicle. Both components are necessary for full vehicle testing to take place.

6.2 Rear Powertrain Integration

Rear powertrain integration began in November of 2019 when the main housing components were received from MERQ Inc., and the gears and shafts were received from Rapid Rapid Precision Machining & Gearing Ltd. The post processing of the shafts as discussed in Section 5.4.1 took place in January of 2020, with gearbox assembly beginning in February of 2020. As of this point the flywheel and clutch output shaft have yet to be manufactured. It was difficult to find a manufacturer for the clutch output shaft in particular, as it contains a spline that the team has no specifications for, as discussed in Section 5.4.3. Therefore, the gearbox assembly went ahead without the clutch housing in order to begin testing. A test fit of the shaft components can be seen in Figure 6.4. This was done to ensure that all components had the correct fits, and that they could be disassembled if necessary. Pictures of the gearbox assembly process can be found in Appendix C.

Once the gearbox was fully assembled as seen in Figure 6.5, a measurement of the pinion gear shaft runout was taken. The measurement was done via an imperial dial

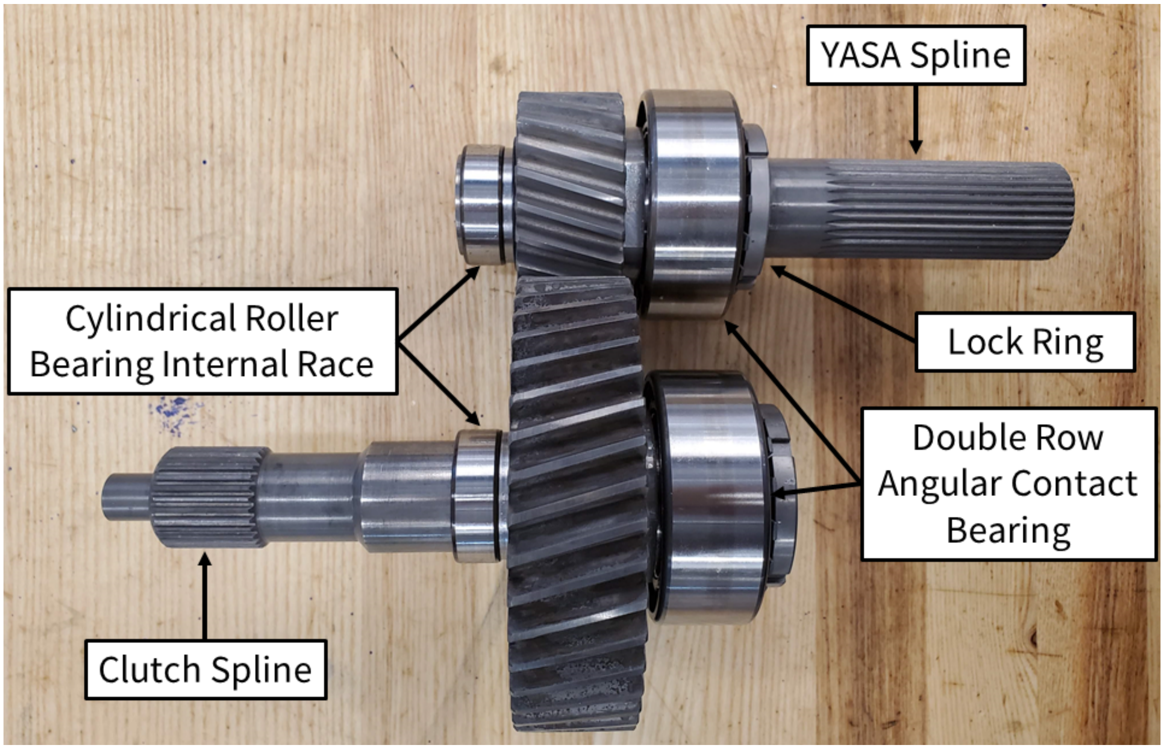

Figure 6.4: Test fit of shaft assemblies with labeled components.

indicator, and was 0.0005 in (0.0127 mm) at the shaft base, and 0.002 in (0.0508 mm) at the end. The end measurement had to be performed using the spline tips as no round section exists there. The YASA P400 has specific tolerances for misalignment between the shaft and hub. It has a $\pm 25\,\mu m$ tolerance for perpendicularity, and a $\pm 50\,\mu m$ tolerance coaxially. The simple shaft runout measurement is not a perfect measure of whether these tolerances were met. Additionally, there are no steps to be taken to remedy misalignment in any substantial way, as the cost of re-manufacturing components for the gearbox is infeasible for the team. The motor is aligned via two locating spring pins in two of the mounting positions. When placed, it formed a tight sliding fit between the male and female splines, with no backlash when rotated. This is the most important feature of the installation, as backlash can create high NVH which can damage the motor. As the YASA P400 will be running at a relatively low power

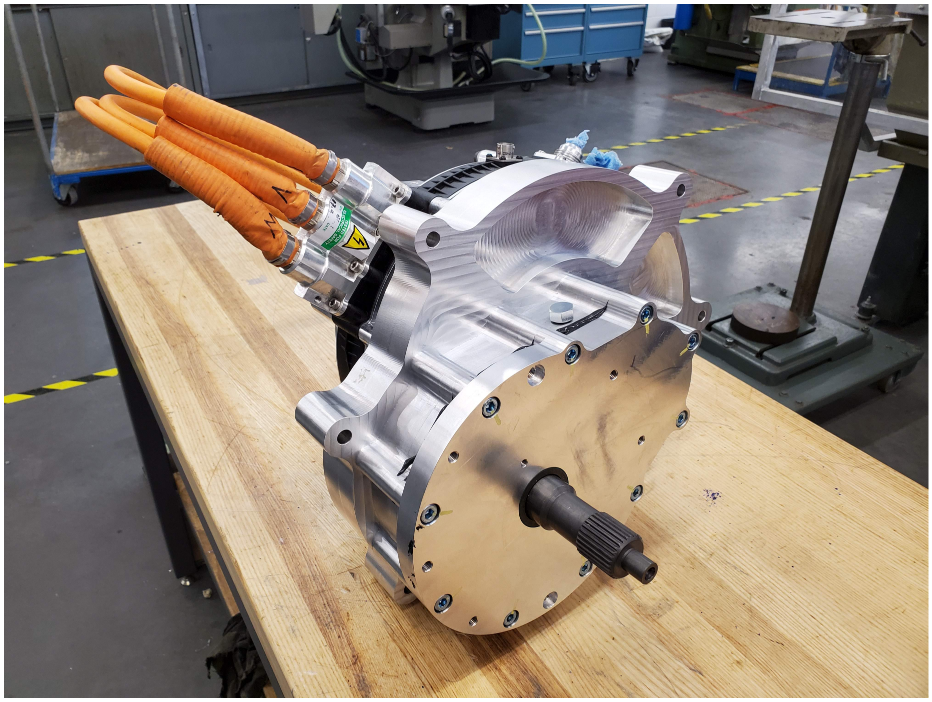

Figure 6.5: Fully assembled gear housing with attached YASA P400.

level as compared to what it is capable of if run at a higher voltage and amperage, shaft misalignment loads should be low if present.

The gearbox mounting hardware has also been manufactured, as seen in Figure 6.6. A test fit of the system into the vehicle, without clutch components, was to be performed in late March of 2020 until the COVID-19 shutdown prevented it. At this point the team is pursuing outside manufacturing for the flywheel and clutch output assembly, so as to be ready to finish gearbox assembly some time in fall of 2020. Once fully assembled the system can be installed into the vehicle. Clutch actuation should be tested at this time, in preparation for connection to the differential.

The rear cradle modification is another large timeline item left to be manufactured for the rear powertrain. The stock cradle has been cut to accept the new strengthening plates as seen in Figure 6.7. All but two of the new pieces to be welded onto the cradle have been manufactured. The current target for finishing the modification is October

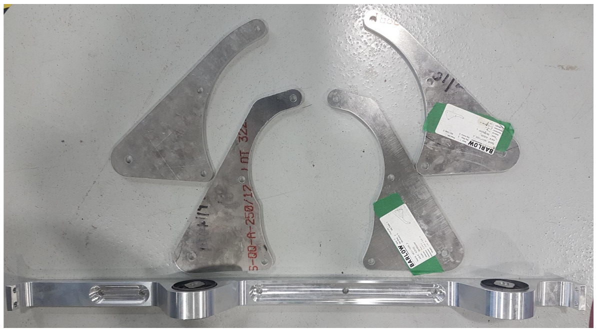

(a) Rear gearbox mounting system.

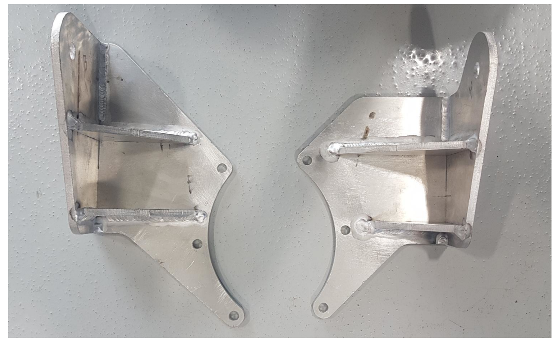

(b) Front gearbox mounting system.

Figure 6.6: Mounting system components current status.

Figure 6.7: Rear cradle with modification cuts.

of 2020. Once installed, the differential can be mounted in the vehicle, and the rear powertrain system can be no load tested on the vehicle lift. With the addition of the rear half shafts, the system will be ready for dynamometer testing.

The carbon fiber battery enclosure is the final item to be integrated before full vehicle testing can take place. Currently the enclosure lid has been successfully infused, as seen in Figure 6.8. Post processing for access panel cut-outs still needs to be done. The mold for the main enclosure is constructed, with the infusion to take place in early September 2020.

Figure 6.8: Battery enclosure carbon fiber lid, post infusion.

6.2.1 Rear Powertrain Testing

With the gearbox and YASA P400 assembled, several no load testing runs were performed to ensure functionality, as well as to run in the gears. The bench testing setup can be seen in Figure 6.9. The gearbox lid is bolted to a fixed plate using the threaded holes where the clutch housing will mount, while some small steel feet are bolted to the main housing to support the motor mass. This was suitable as the testing to be done would not impose any loads on the gearbox itself.

Four testing runs were done at a variety of motor speeds. The testing is by no means comprehensive, and was meant as an initial evaluation only. The testing is summarized in Table 6.1. All tests had the same basic outline. The gearbox was filled with 300 mL of fresh oil before the start of the test. The motor was brought up to speed in steps of 500 RPM. Motor speed was brought down in steps of 50 RPM at higher speeds, and steps of 500 RPM once below 2000 RPM. This was due to limitations of

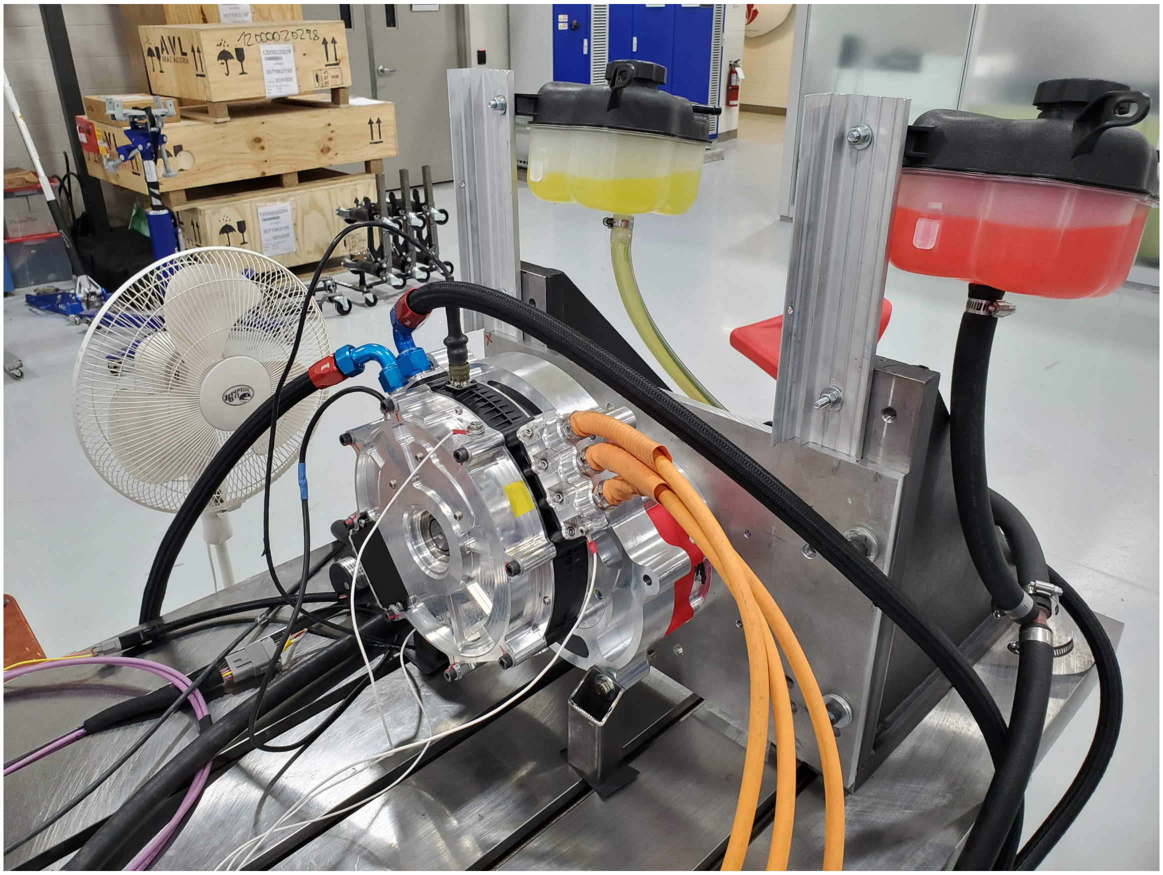

Figure 6.9: YASA P400 and gearbox test bench.

the HV power supply used, where large steps up or down would cause the supply to disconnect itself from the load. Future tests connected to the vehicle battery would solve this issue. During some of the tests, gearbox casing temperature was taken in order to investigate oil temperatures. This was done by reading the outside gear housing temperature via thermal camera. Green masking tape was applied to the housing in order to reduce emissivity effects from the polished surface. Even with this precaution, these temperatures are not considered extremely accurate, and are only used as a reference.

The first test ran the motor at 500 RPM for 30 minutes. This was the first ever running of the gearbox, and as such the low speed was deemed suitable. During the

Table 6.1: Gearbox no load testing data.

Test #	**Motor RPM**	**Time (min)**	**Veh. Speed (km/h)**	**Distance (km)**	**Max. Temp.** °C
1	500	30	14	7.01	
2	1782	30	50	25.00	44.5
3	3565	5	100	8.34	
	4099	3	115	5.75	
	4633	2	130	4.33	49.0
	3565	5	100	8.34	59.0
4	6500		182		39.0*

*Fan pointed at gearbox during test.

test the top oil fill cap was removed to inspect oil splash, and it was found that the gears were adequately coated with good splash to lubricate the bearings. The gear interaction revealed no grinding sounds. Temperature was not taken during this test.

Test 2 ran the motor at 1782 RPM for 30 minutes, the equivalent of a 50 km/h vehicle speed. Gear noise was louder during this test, but still did not contain grinding noises. The casing temperature rose to 39 °C at the 15 minute mark, with the final maximum temperature being 44.5 °C. This indicates a relatively high temperature being produced inside the gearbox, to be discussed below.

Test 3 ran for a total of 15 minutes, using a stepped speed profile that can be seen in Table 6.1. This went to the maximum vehicle speed expected at any point during the competition drive cycles. At peak speed the outside casing temperature climbed to 49 °C, further climbing to 59 °C by the end of the test. This suggests the oil inside the gearbox is overheating, and may need to be switched for a more viscous alternative as discussed in Section 5.3.1. However, the real duty cycle of this system involves the motor spinning up to fill torque requests and then being disconnected. The system will never run for substantial continuous time, as the small battery would run out of energy. Additionally, when the vehicle is at speed the gearbox will have airflow from under the vehicle, and will act as a large aluminum heat sync for the oil. Therefore the team should continue to monitor the temperature during future testing to evaluate if under realistic scenarios the oil is overheating, before making a change.

Test 4 was done only to test the speed limitations of the gearbox, in order to validate the requirement of a 7000 RPM input speed. Unfortunately the test was only able to go to 6500 RPM, again due to power supply limitations. However, this corresponds to a vehicle speed of 182 km/h, much higher than will ever be attempted in this vehicle. The test was conducted over approximately 5 minutes, using the same stepped speed changes as before. The maximum speed was only maintained for a few seconds before coming back down. The gearbox produced no unexpected noises, or indications of strain at that speed. During this test, an office style tower fan, seen in Figure 6.9 was pointed at the gearbox, which resulted in a maximum temperature of only 39 °C. This indicated that the much greater airflow of a moving vehicle would effectively manage the oil temperature overall.

The drain plug of the gearbox was fitted with several neodymium magnets, and then filled with epoxy. This was done in an effort to collect any metal pieces generated in the wearing in process. This was somewhat successful, as can be seen in Figure 6.10. Further experimentation with different magnets could be done to ensure metal particles do not decrease the life of the gearbox.

After each test the used oil was collected, as can be seen in Figure 6.11. This picture shows the oils on the same day as the testing occurred. The oil samples were examined to gain insight into the gear run in process. Test 1 oil was discolored as compared to the fresh sample seen on the left, becoming a darker yellow color. Several small metal pieces were found in the oil, as well as some found on the magnetic drain plug. Tests 2 and 3 oil appeared grey in color at this time, with significantly less metal pieces. This suggests that these small pieces were from initial run in, or possibly just stray metal particles in the gear housing from the assembly process.

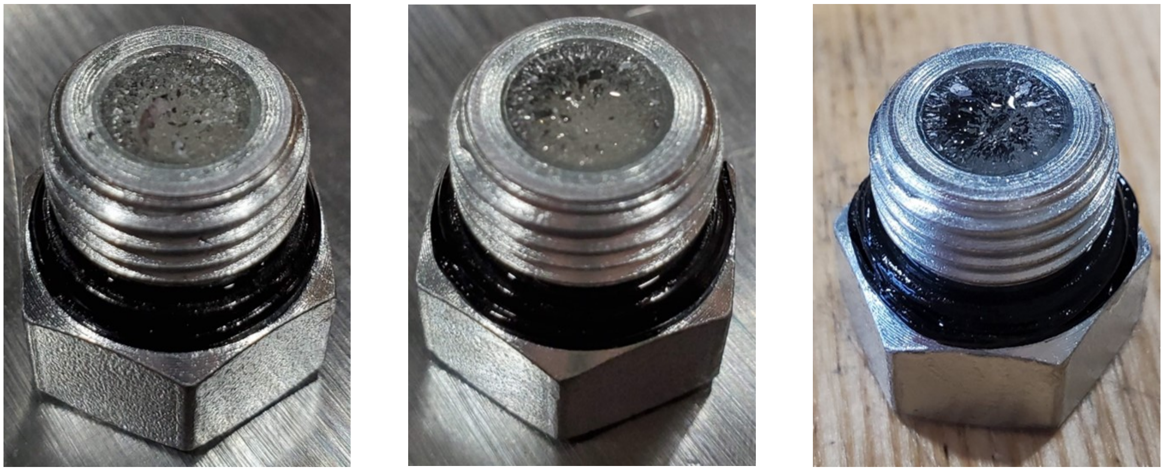

(a) (b) (c)

Figure 6.10: Drain plug with magnet, residue after various testing runs.

Figure 6.12 shows the oil from all four testing runs after several months of sitting in the containers. This allowed all particles in solution to fall to the bottom. As can be seen, test 1 oil contains a small amount of sediment, with a more pronounced color change as compared to the other samples. The lower sediment content is most likely due to the low speed nature of the test, therefore having less run in effect on the gears. Tests 2 and 3 have similar oil colors and sediment amounts. They appear lighter in color than test 1, but still darker than test 4. The increased amount of fine sediment appears to be from a more effective gear wear in, in which fine particles were removed from the gear flanks. Test 4 contains little to no sediment, and has little to no color change. It was not as long of a test as the others, but achieved a significantly higher speed. This suggests that tests 2 and 3 effectively wore the gears in to being a more mated pair, and therefore the initial higher wear period may be over. It is suggested that the gearbox oil be changed frequently throughout future testing to monitor changes in gear wear. Additionally, sending the existing samples for chemistry analysis could reveal the source of the color change, as well as if overheating at the gear interface broke down the oil in any way.

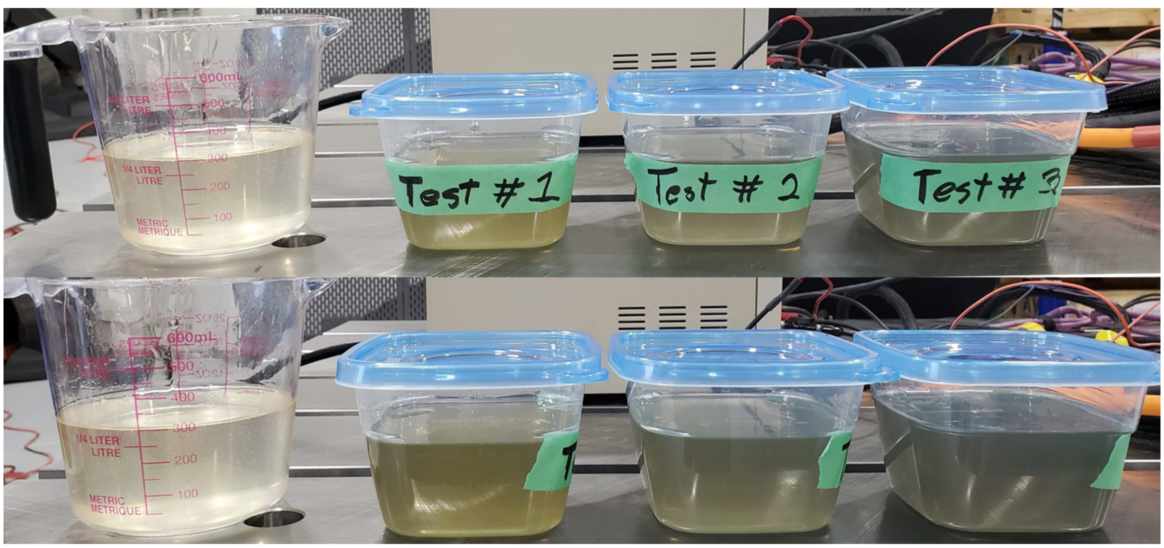

Figure 6.11: Post testing oil comparison, on day of testing.

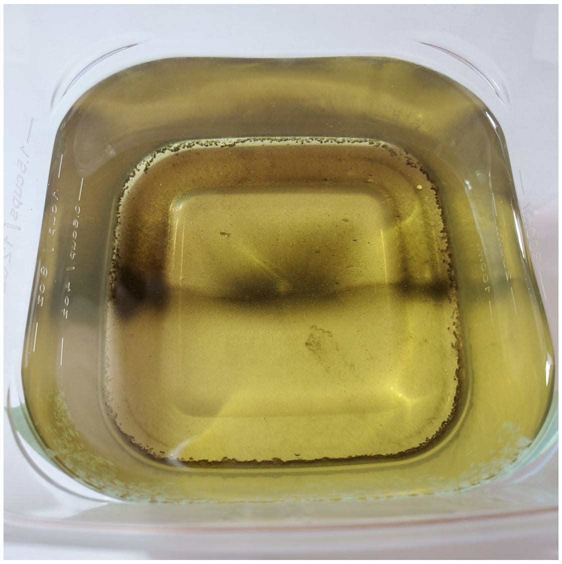

(a) Oil Test 1

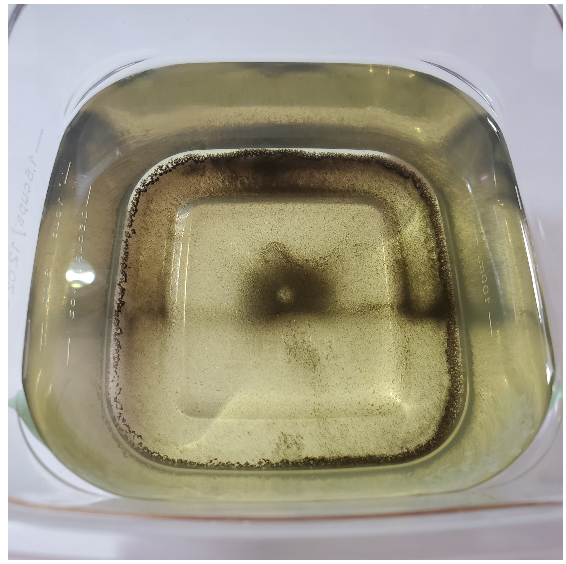

(b) Oil Test 2

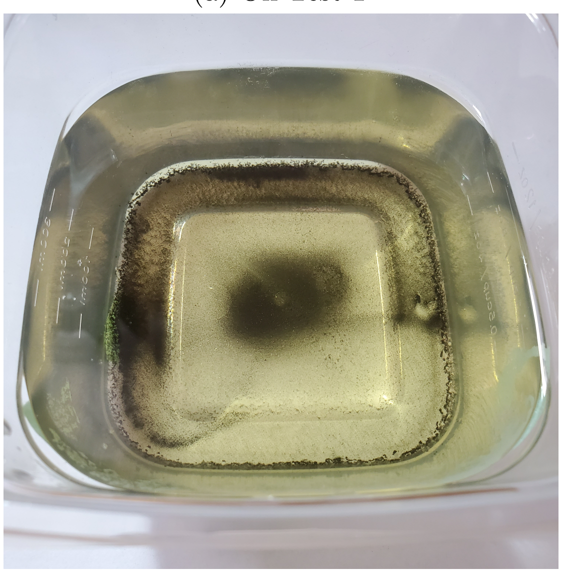

(c) Oil Test 3

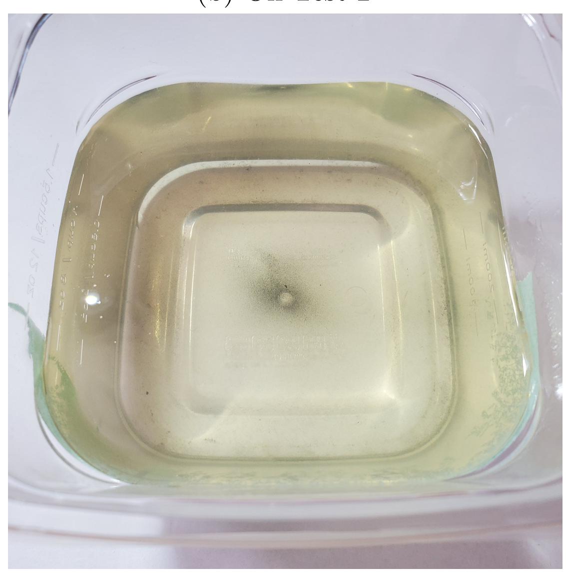

(d) Oil Test 4

Figure 6.12: Oil samples of tests, after sufficiently long settling time.

Chapter 7

Proposed Vehicle Testing

This chapter discusses a proposed vehicle testing plan, encompassing the remainder of vehicle integration. The plan will be high level in nature, and will not discuss specific individual testing plans. The plan also strives to be as realistic as possible. The MARC space contains numerous testing facilities including engine and electric motor dynamometers. While in a normal vehicle production plan each component would be thoroughly tested individually before vehicle integration, the tight timelines of the EMC do not allow such testing to occur. Additionally, not all of the components in the vehicle require that level of testing to achieve reasonable confidence in their functionality. For example, the ICE is a new GM component, and therefore it is reasonably to assume it is fully functional as a stand alone component. Testing for the ICE should focus on control via the team systems, as well as integration with other components such as the BAS.

The competition has previously released a recommended testing glide path, which can be seen in Table 7.1. This gives an outline for what full vehicle testing should be completed by what time. Each time period is given a recommended amount of total testing, as well as a goal for a continuous drive without breakdown. The impact of COVID-19 will effect the timing of this glide path. It is the author's recommendation that the MAC team adopt a milestone approach for Year 3 of the competition, using the continuous testing distances as goals. When the vehicle can successfully achieve an 80 km continuous test, the team can consider itself having reached the original goal for Year 2 development. This should continue for as long as is necessary. It is very possible that a firm timeline may not be possible to define until 2021 or later, and so this method can help ground the team in the original competition goals.

Table 7.1: Testing glide path given to teams by competition organizers.

Period	**Testing Distance (km)(mi)**	**Continuous Distance (km)(mi)**
Year 2 Spring	241 (150)	80 (50)
Year 3 Fall	805 (500)	161 (100)
Year 3 Spring	1609 (1000)	322 (200)
Year 4 Fall	805 (500)	N/A
Year 4 Spring	3219 (2000)	483 (300)

7.1 AVL Four Wheel Dynamometer

One system the MAC team has access to that is completely unique is the four wheel AVL dynamometer with linked driving simulator. This system entails a four wheel independent dynamometer setup, enabling testing of four wheel drive vehicles as well as the simulation of dynamic road loads. Connected to the dynamometer is a full size vehicle simulator, enabling a human driver to interact with a virtual environment such as a track or city street, and for the inputs and corresponding loads to be transferred to the dynamometer. The four wheel dynamometer is a perfect test bed for the MAC team vehicle to perform introductory vehicle integration tests, as well as longer continuous driving tests. The unique new vehicle timeline due to COVID-19 can even be used to the advantage of the team in this scenario. Normally the vehicle would need to be completely integrated, driveline and interior, by Year 2 competition where it would be evaluated. As Year 3 competition will be in May of 2021, the vehicle can now be tested as a bare shell and powertrain for a significant portion of that time.

Once both powertrains are integrated, the vehicle should be put onto the four wheel dynamometer and run through several low load tests. This will be the first time either powertrain will be operated under load, and therefore a gradual approach should be taken to torque delivery through the systems. This should be increased until a full power run from both systems can be done reliably, with no breakdowns from any components.

Once the systems are confirmed to be able to output their full loads, longer term testing using the competition drive cycles should be performed. This can be used to first ensure that the two powertrains are being properly controlled. The separation of the testing loads will provide a low risk environment to ensure both systems are outputting the correct torque commands in order to function as a cohesive vehicle. Once the controls system is deemed reliable, the first long distance test can be performed, corresponding to the Year 2 80 km continuous drive. Gearbox oil should be replaced after each set of tests, monitoring for particulate matter which would suggest excessive gear wear. At this point the vehicle will be reliable enough to replace all of the interior components, without fear of having to remove them again to troubleshoot wire harnesses.

At this point the vehicle can also be transitioned to the outdoor dynamic vehicle testing of the following section. However, it is the author's recommendation that the continuous driving distances be performed on this testing apparatus for several reasons. Normally the EcoCAR student vehicles are only deemed road worthy at competition, and any changes to the vehicle renders them unworthy until another official competition inspection. This system can bypass that limitation by allowing long distance testing be done in a controlled environment where no road worthiness is required. Testing done in this environment is also completely repeatable, allowing accurate comparisons of fuel consumption between tests for control system development. Additionally, the nature of the system allows many different driving scenarios to be explored through use of the simulator. This could be leveraged to have a more varied testing environment than what would be possible on-road near the university. Both Year 3 continuous distances should be attempted on the dynamometer before Year 3 competition.

7.2 Dynamic Vehicle Testing

Certain vehicle testing parameters are significantly easier to test on-road. These include practice runs of competition events such as acceleration time and braking distance. Additionally, it will be advantageous to do drive tests where the suspension is loaded, in order to investigate the effects on NVH from real road loads. Finally, the CAV sub team will need testing for radar detections from real vehicle data, although this section will focus on aspects of powertrain testing specifically.

7.2.1 On-Site Testing

The MAC team does not have extensive closed course testing area. The most useful testing area available is the parking lot of MARC. Figure 7.1 shows a proposed testing loop of the parking lot system, totalling approximately 950 m per lap. This can be used as a repeatable testing area for suspension and ride height modifications. It is inevitable that the new weight distribution of the vehicle will require new springs to be fitted, in order to maintain suspension compliance. Additionally, the rear springs will need to be sized in order to maintain competition mandated ground clearance.

This can be measured at vehicle rest, however departure angles can be tested on the parking lot ramp. The new rear sway bar can also be tested around this loop.

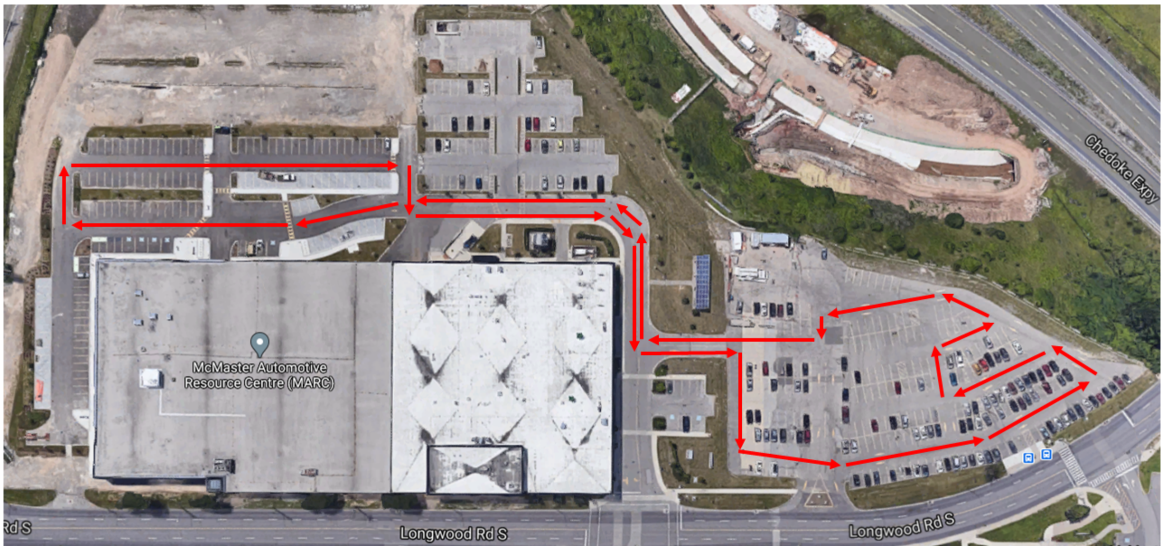

Figure 7.1: MARC parking lot 950 m proposed test loop.

The MARC parking lot is not large enough to safely conduct performance testing. For these circumstances it is advised the team move to McMaster's Lot M. This is a large parking lot that the team has used in the past for acceleration and braking distance tests. The university can close this lot over the weekend, providing an empty and therefore safe space to conduct these tests. A figure of eight test could also be conducted here, for further testing of the suspension and new rear sway bar.

7.2.2 EcoCAR Competition Testing

Year end competition has several vehicle dynamic events. The team does not control these tests, but can take a proactive approach to them. Some of the tests can be simulated in advance at McMaster, to ensure good results at competition. These include all acceleration tests such as 0 to 60 mph time, as well as endurance driving tests such as E&EC. Ensuring the vehicle can complete exact competition events will provide a higher overall points average.

Competition can also be a grueling endeavor for team vehicles. The testing density over the week is higher than most student vehicles see on a regular basis. To combat this, a high amount of preventative maintenance should be done at year end competitions to ensure the vehicle continues to run effectively. This includes frequent rear gearbox oil changes, as well as inspecting the internals via camera scope for signs of damage. Visual inspections of all torque transfer components should be done before and after each competition event, looking for cracks or other signs of fatigue. Steps should be taken to run the car in a reduced functionality state if any signs of fatigue are found.

Chapter 8

Conclusions and Future Work

8.1 Thesis Summary and Conclusions

As global automotive markets shift towards increased levels of electrification, the EcoCAR Mobility Challenge seeks to train future engineers in order to meet those goals. This thesis has outlined McMaster University's efforts towards that competition over the last two years, focusing on the mechanical design and integration of the team vehicle. This began with a thorough investigation of the MAC team architecture, and the design decisions that brought the team to choose it. Vehicle and team goals for the competition were outlined, as well as a full set of Vehicle Technical Specifications.

This was followed by a look at the design process for both the front and rear powertrains. The front powertrain is a mainly OEM system, allowing increased durability and reliability. This will be used as the main power source for the vehicle. The rear powertrain is the more aggressive of the two systems in terms of scope. Most components are custom machined, with the main driveline being designed by the author from the ground up. This tailored system allows the MAC team to better achieve its goals for the vehicle, including a completely stock trunk capacity. The system was evaluated using several Finite Element Analysis studies, confirming that it has sufficiently high safety factors in order to survive competition events.

The current vehicle status was discussed, detailing what integration work has been done on the vehicle. This includes the installation of the new powercube, and disassembly of vehicle interior and rear end. Work still to be done was outlined at a high level, including the integration of both hybrid systems, the BAS and rear powertrain. Some initial results from bench tests of the EM and gearbox were also discussed, as well as a high level testing plan for the future.

Overall the vehicle design presented in this work meets the requirements the MAC team set out. Vehicle integration has been hampered by the COVID-19 pandemic, but as work begins to resume the author is confident that the team can finish the vehicle and perform well at Year 3 competition. It is expected that when the vehicle reaches its full potential at the end of Year 4, it will become the most successful EcoCAR vehicle in McMaster's history.

8.2 Future Work

Future work in terms of vehicle integration has already been documented in this thesis. Focusing on areas of possible vehicle improvement via mechanical design, once basic functionality has been reached, several projects can be identified. The first is the redesign of the front side engine mount. This mount has significant potential for weight reduction, as well as possibly incorporating idler pulley mounts into its design. The cooling of the rear powertrain is also an area of possible improvement. The current system using radiators at the front of the vehicle causes significant tubing losses running to the rear. A compact system integrated into the rear skid plate should be pursued, for increased system efficiency.

Future work on the subject of Parallel Through-The-Road hybrid vehicle architectures should focus towards their use in electrifying existing FWD platforms, similar to the student vehicle in this thesis. Manufacturers can utilise this architecture to electrify large amounts of existing fleets, helping bridge the gap towards a fully electric future.

Appendices

Appendix A

Technical Drawings

All drawings in this section were produced by the author, and are of components designed or significantly modified by the author. Most drawings are ANSI size B, 11 in x 17 in, and have therefore been shrunken to fit as figures here.

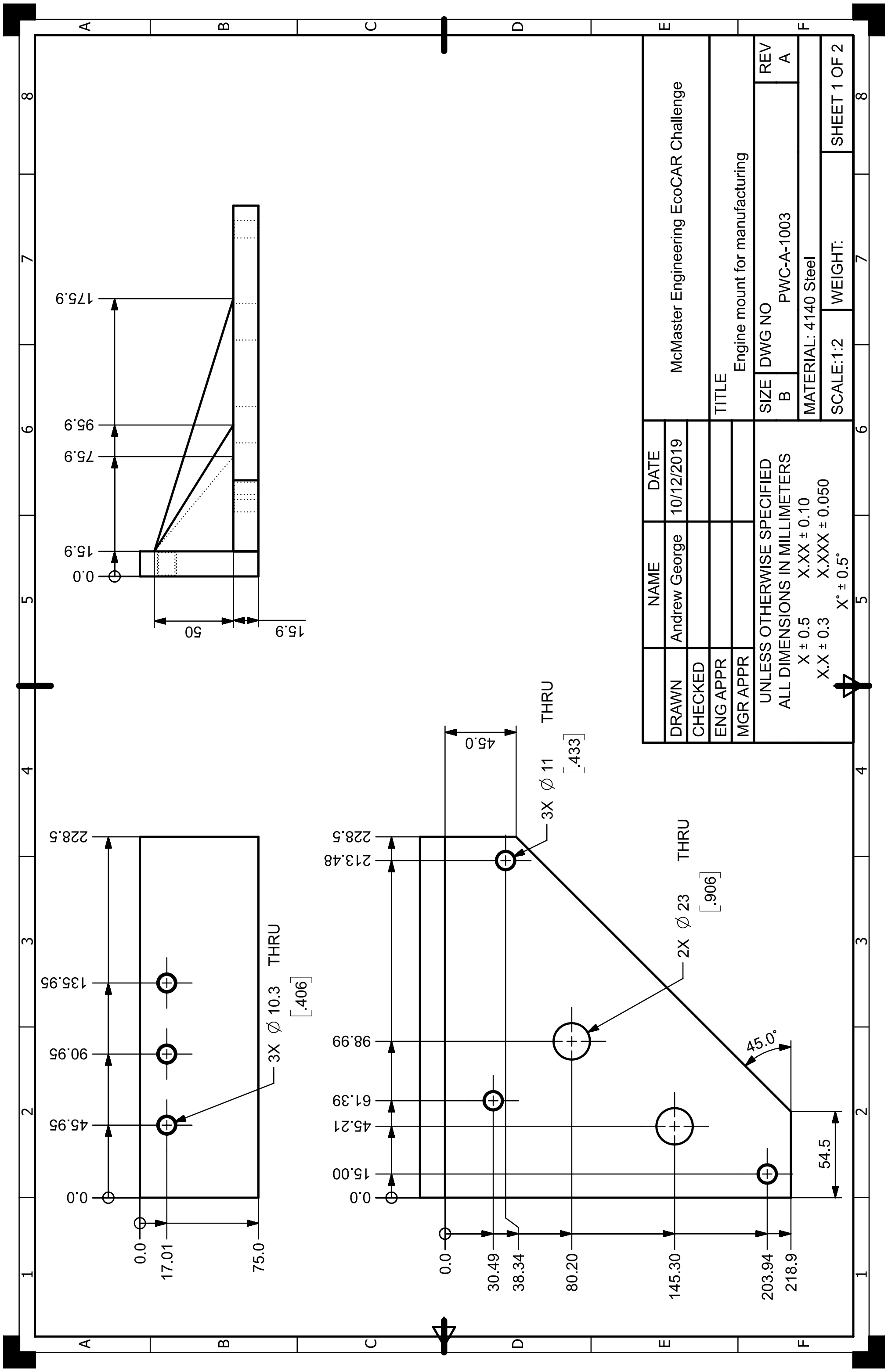

Figure A.1: Front Engine Mount Sheet 1 of 2

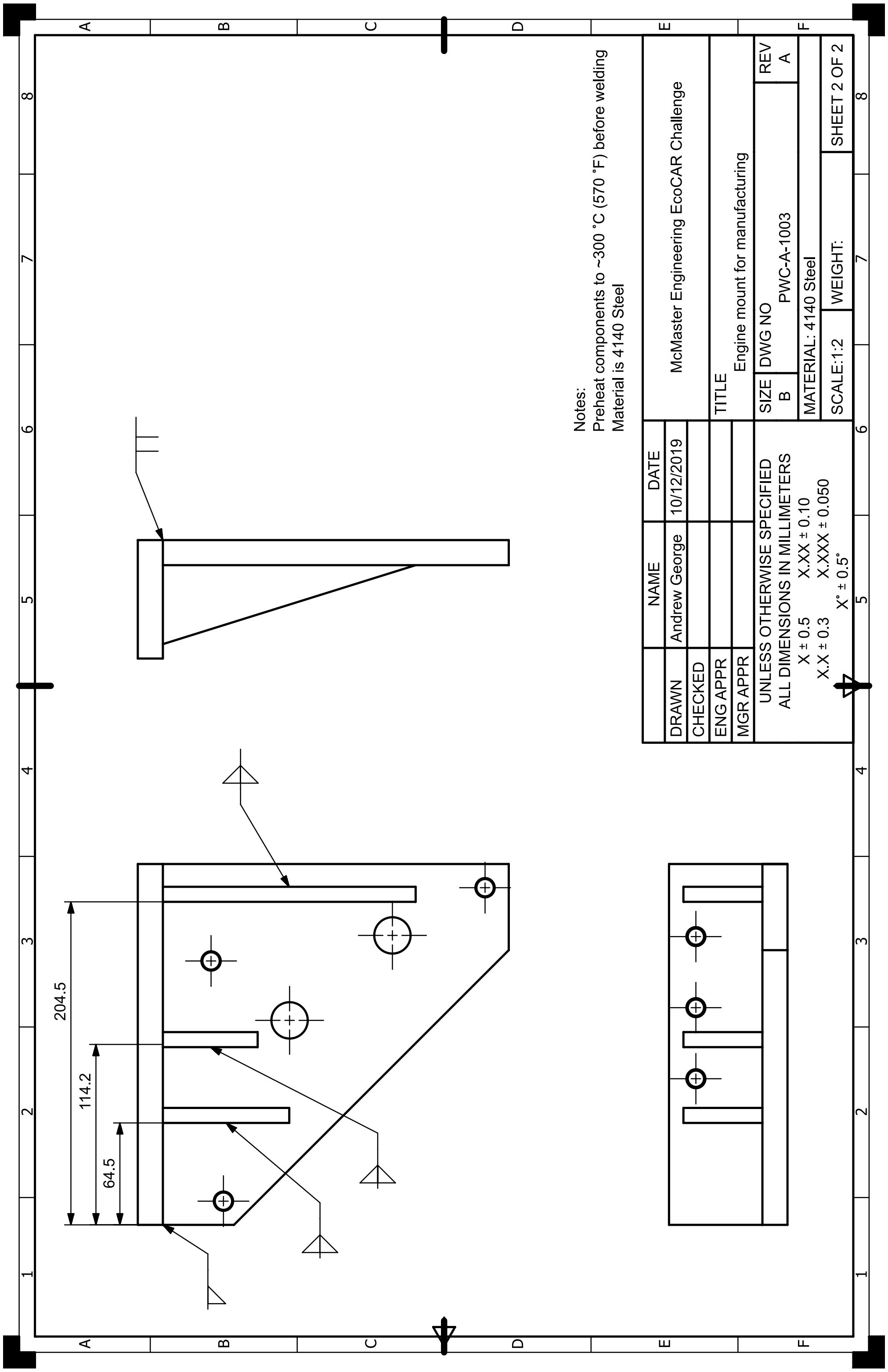

Figure A.2: Front Engine Mount Sheet 2 of 2

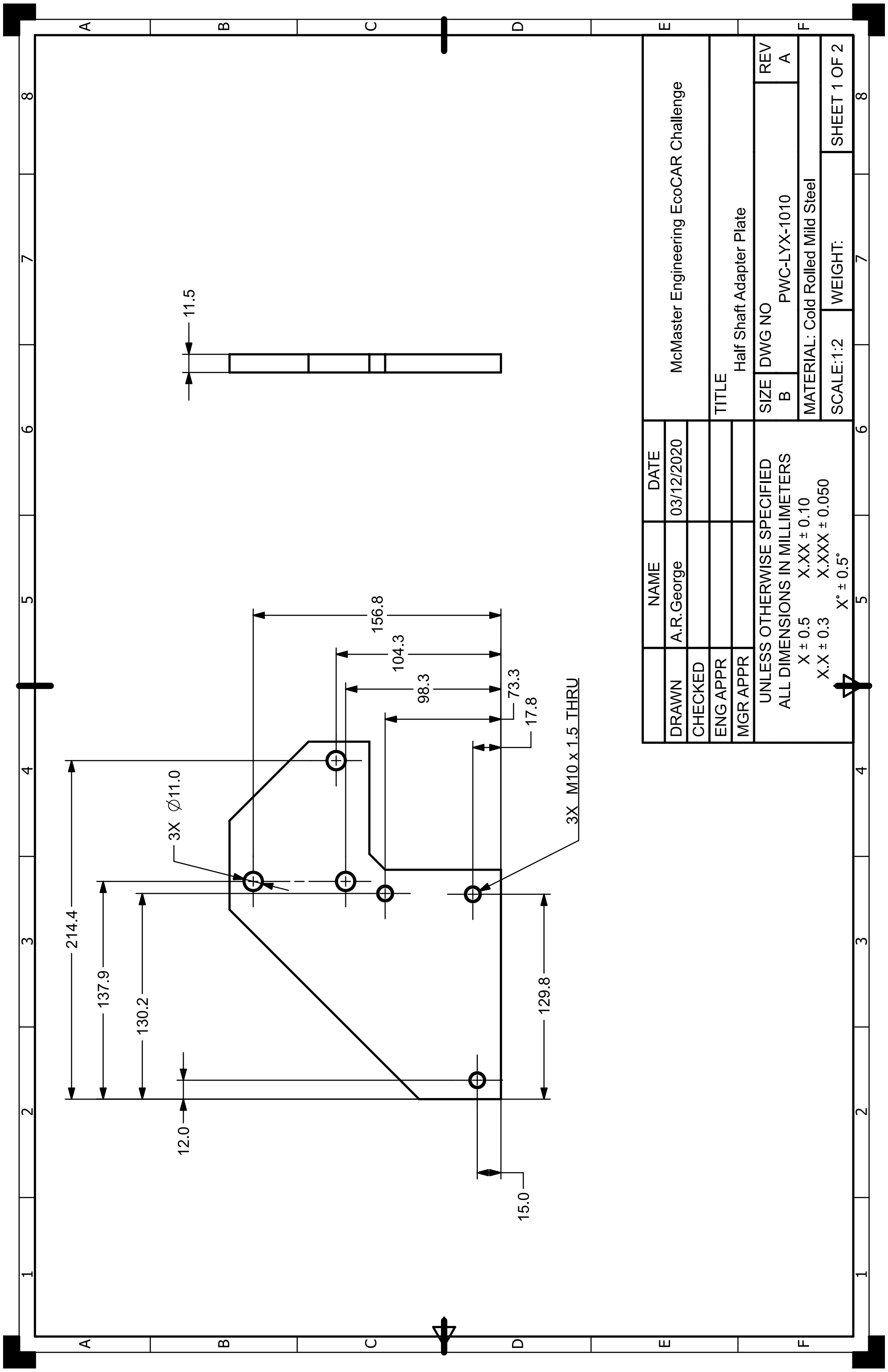

Figure A.3: Half Shaft Adapter Plate Sheet 1 of 2

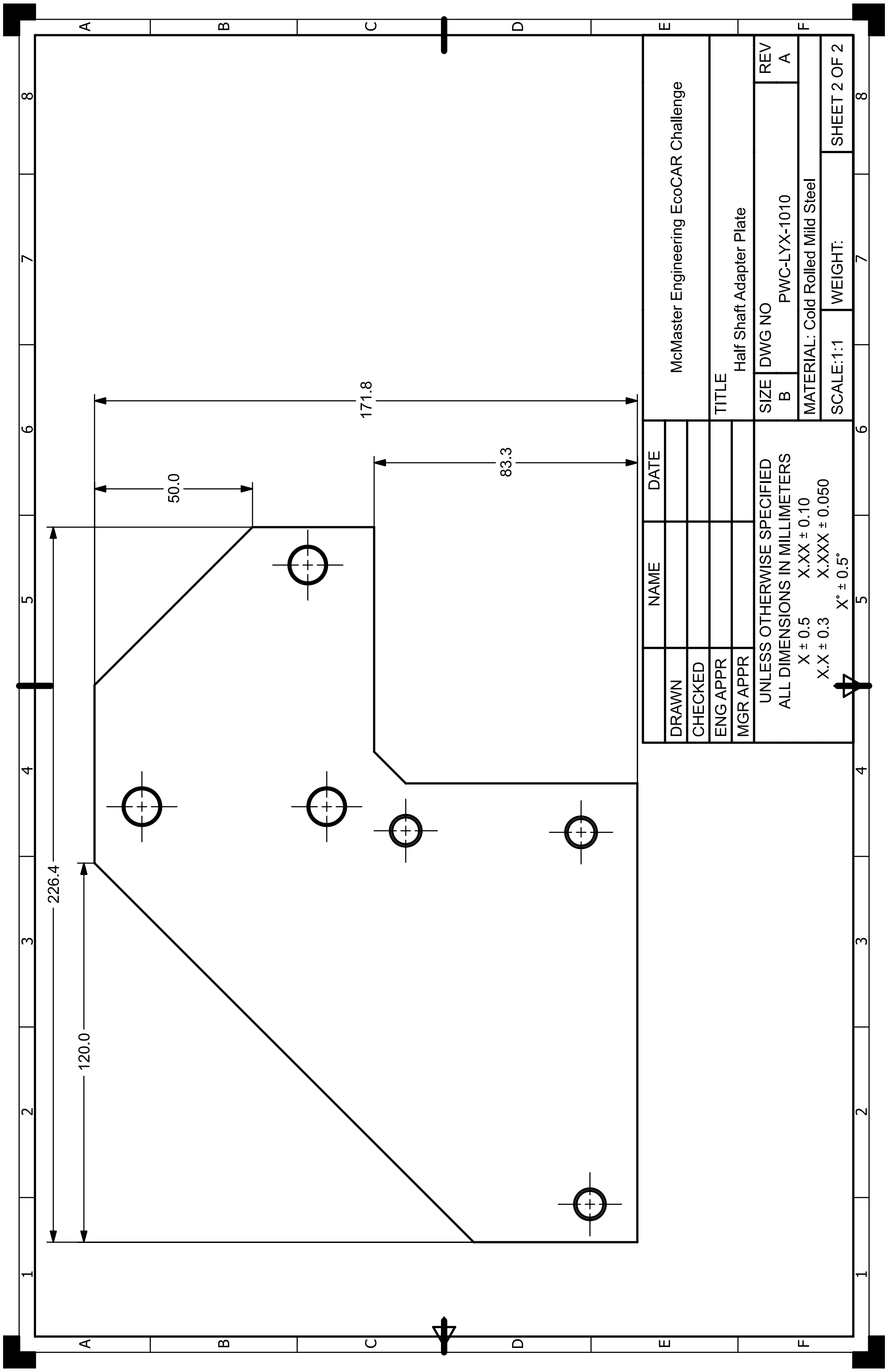

Figure A.4: Half Shaft Adapter Plate Sheet 2 of 2

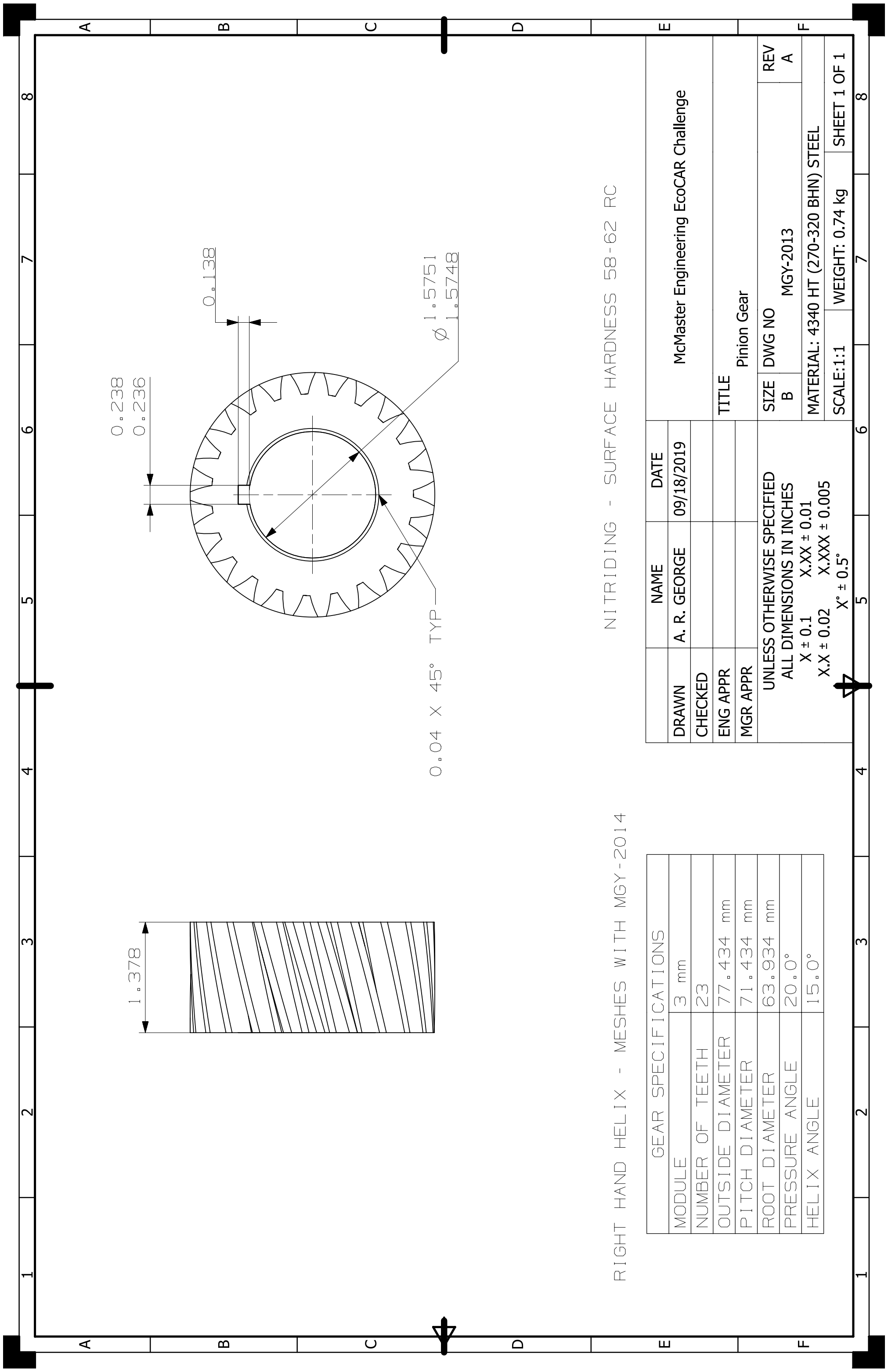

Figure A.5: Pinion Gear

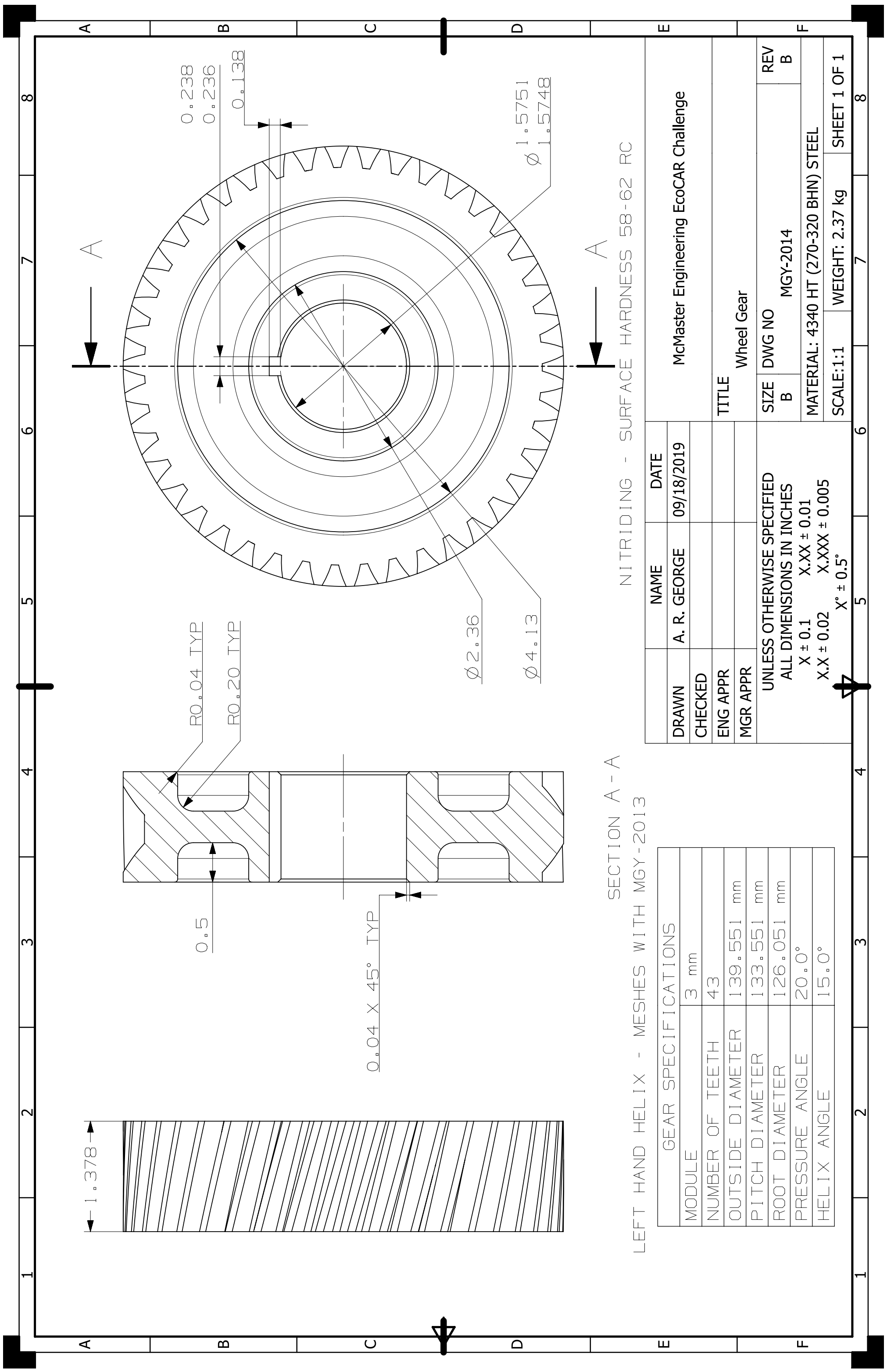

Figure A.6: Wheel Gear

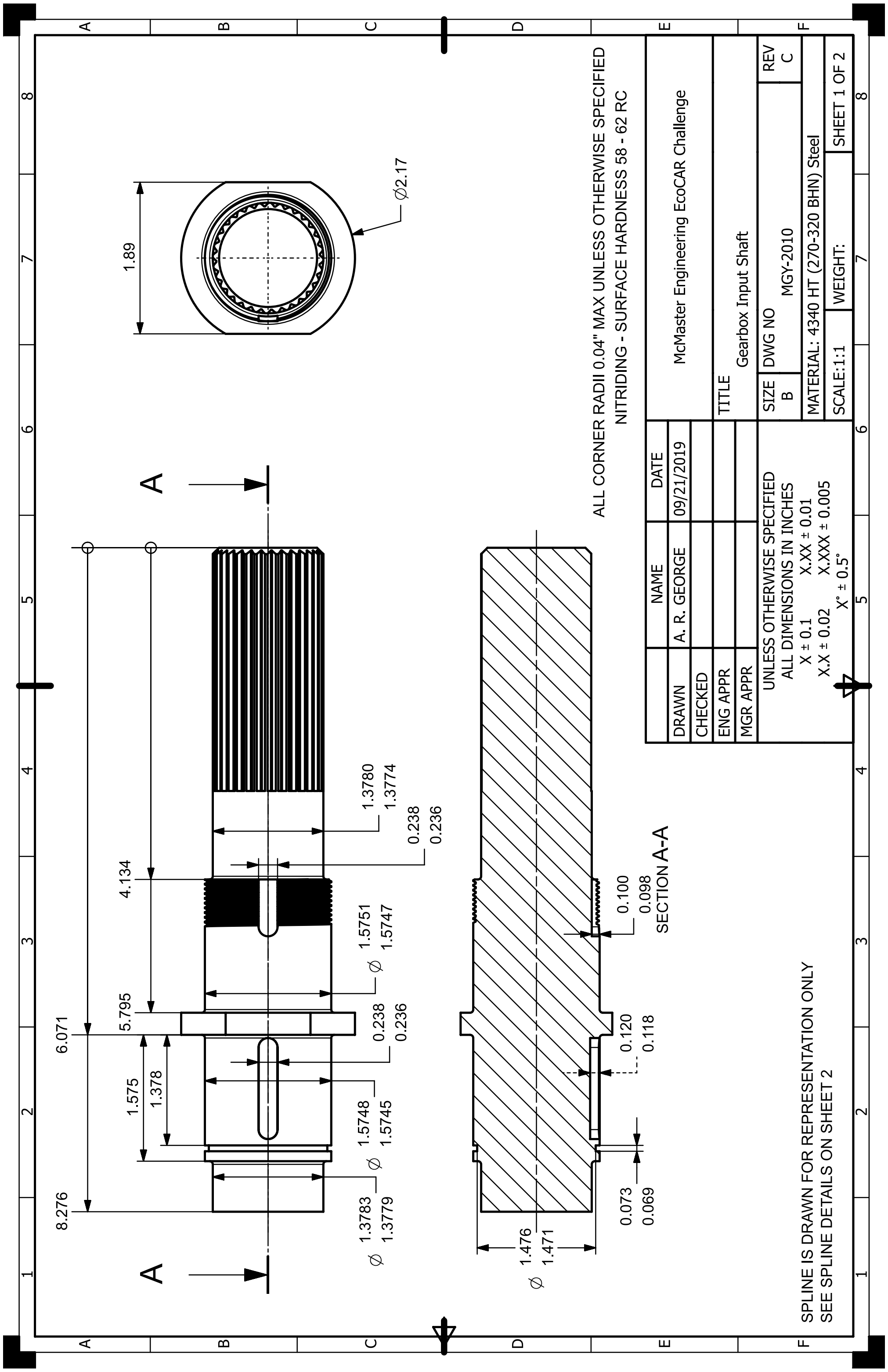

Figure A.7: Pinion Gear Shaft Sheet 1 of 2

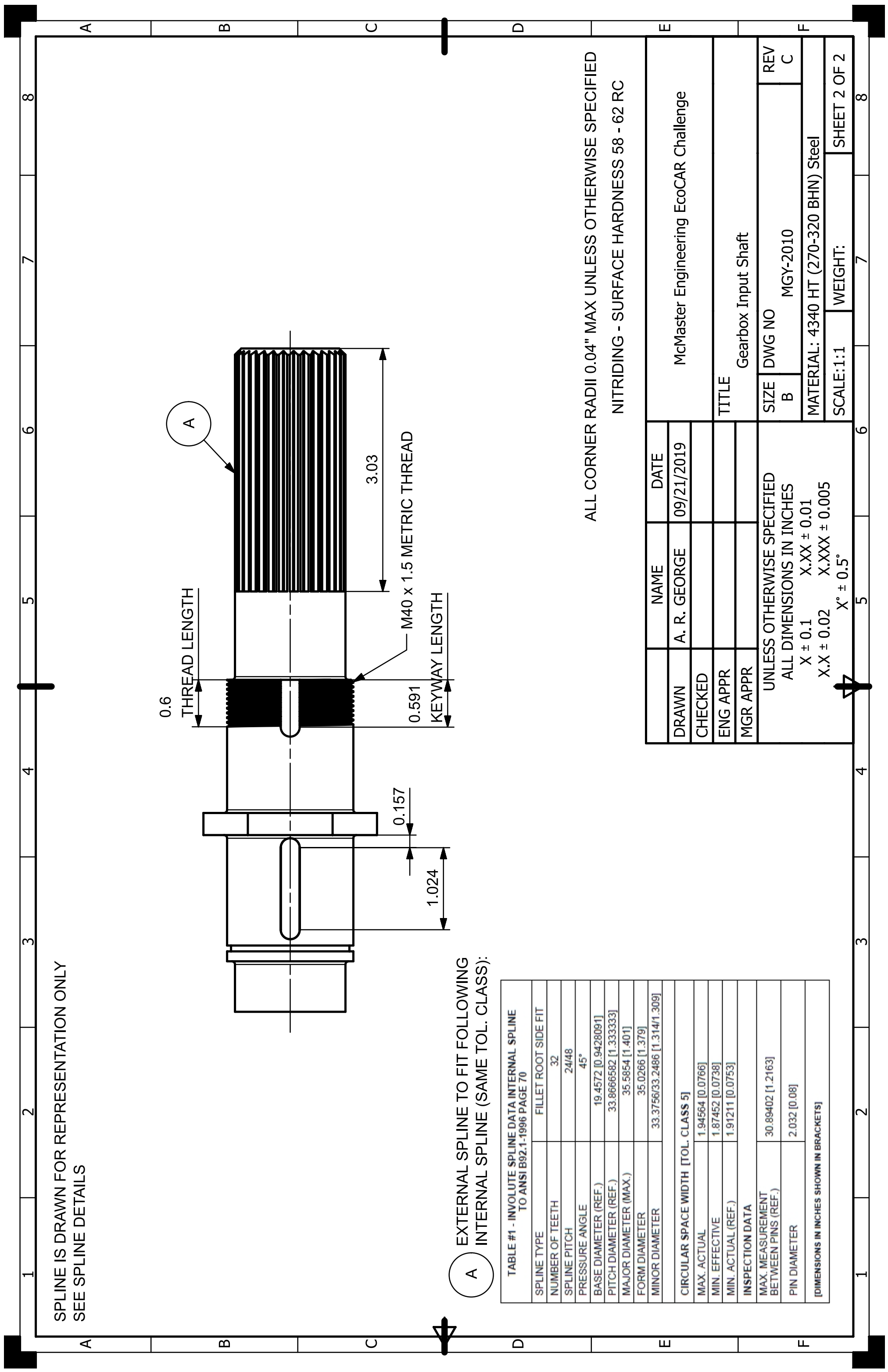

Figure A.8: Pinion Gear Shaft Sheet 2 of 2

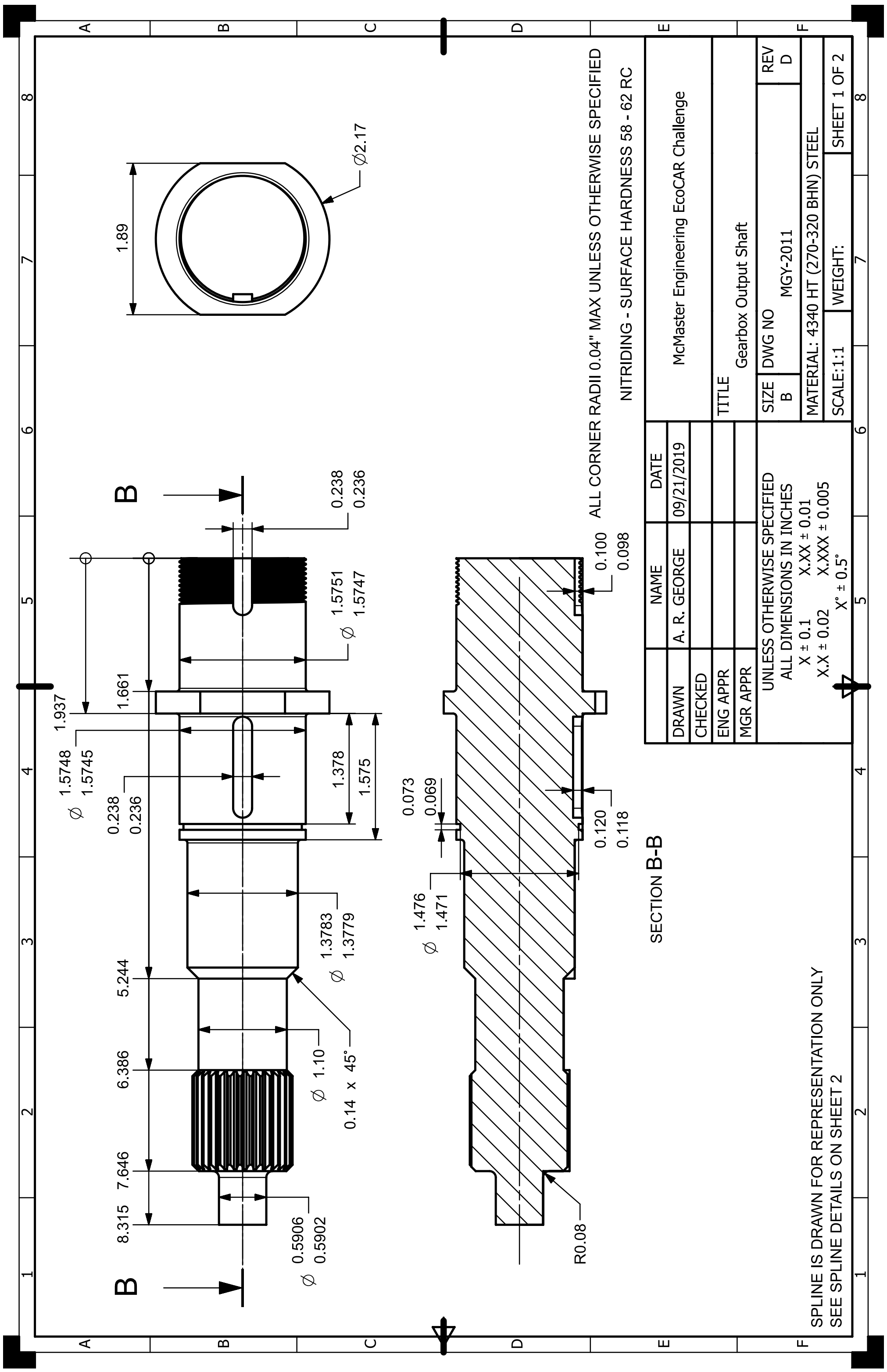

Figure A.9: Wheel Gear Shaft Sheet 1 of 2

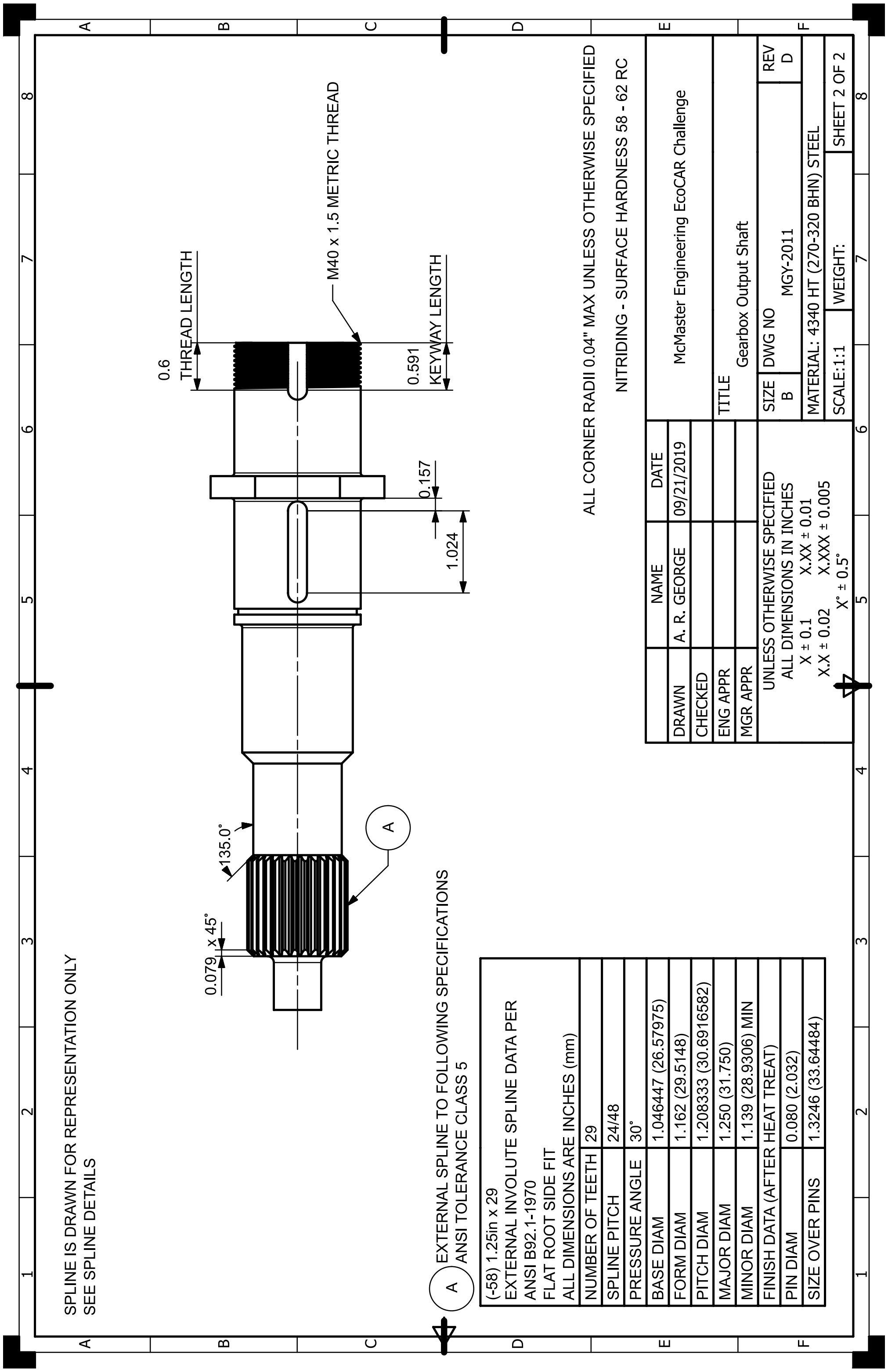

Figure A.10: Wheel Gear Shaft Sheet 2 of 2

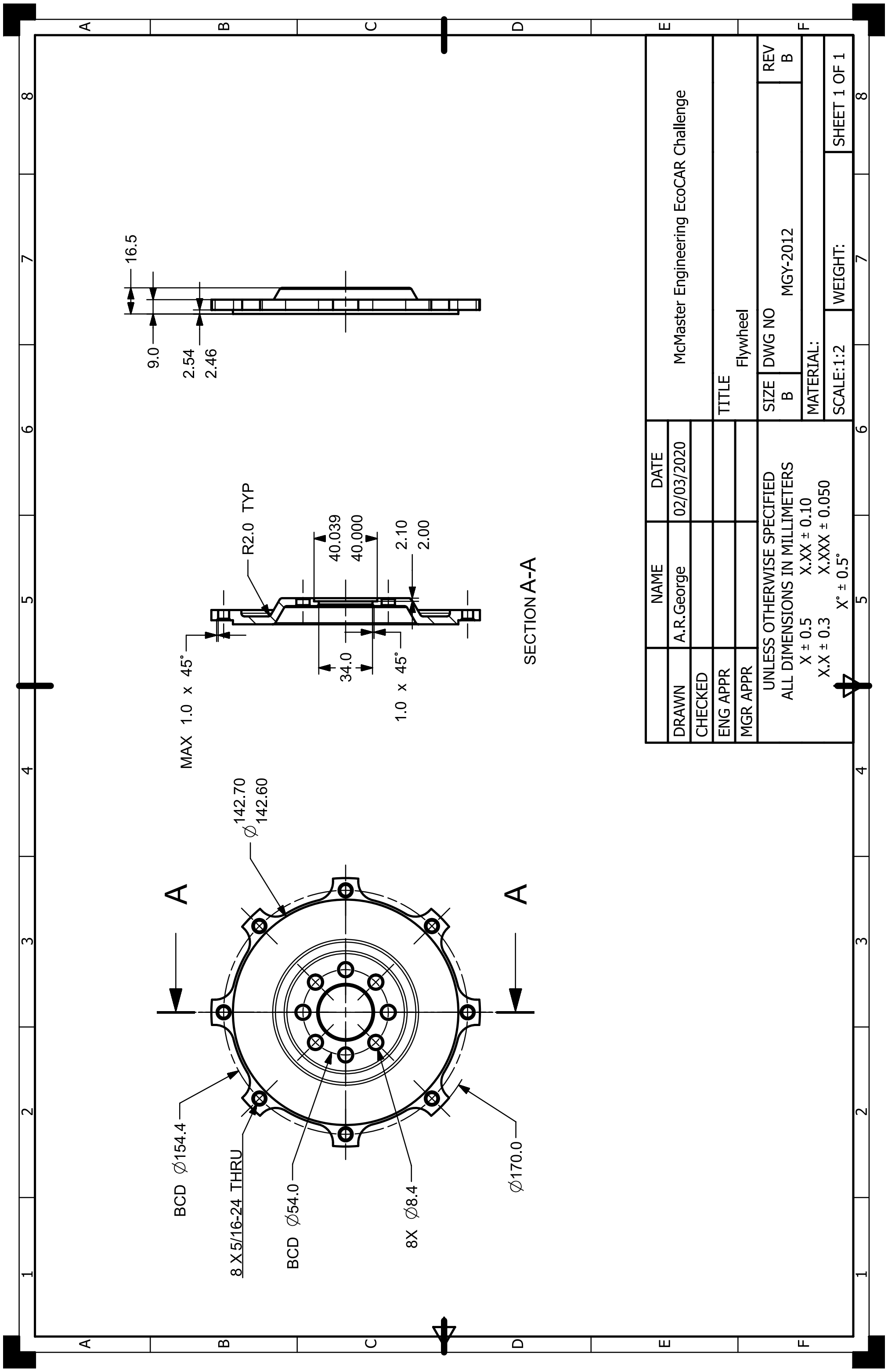

Figure A.11: Flywheel

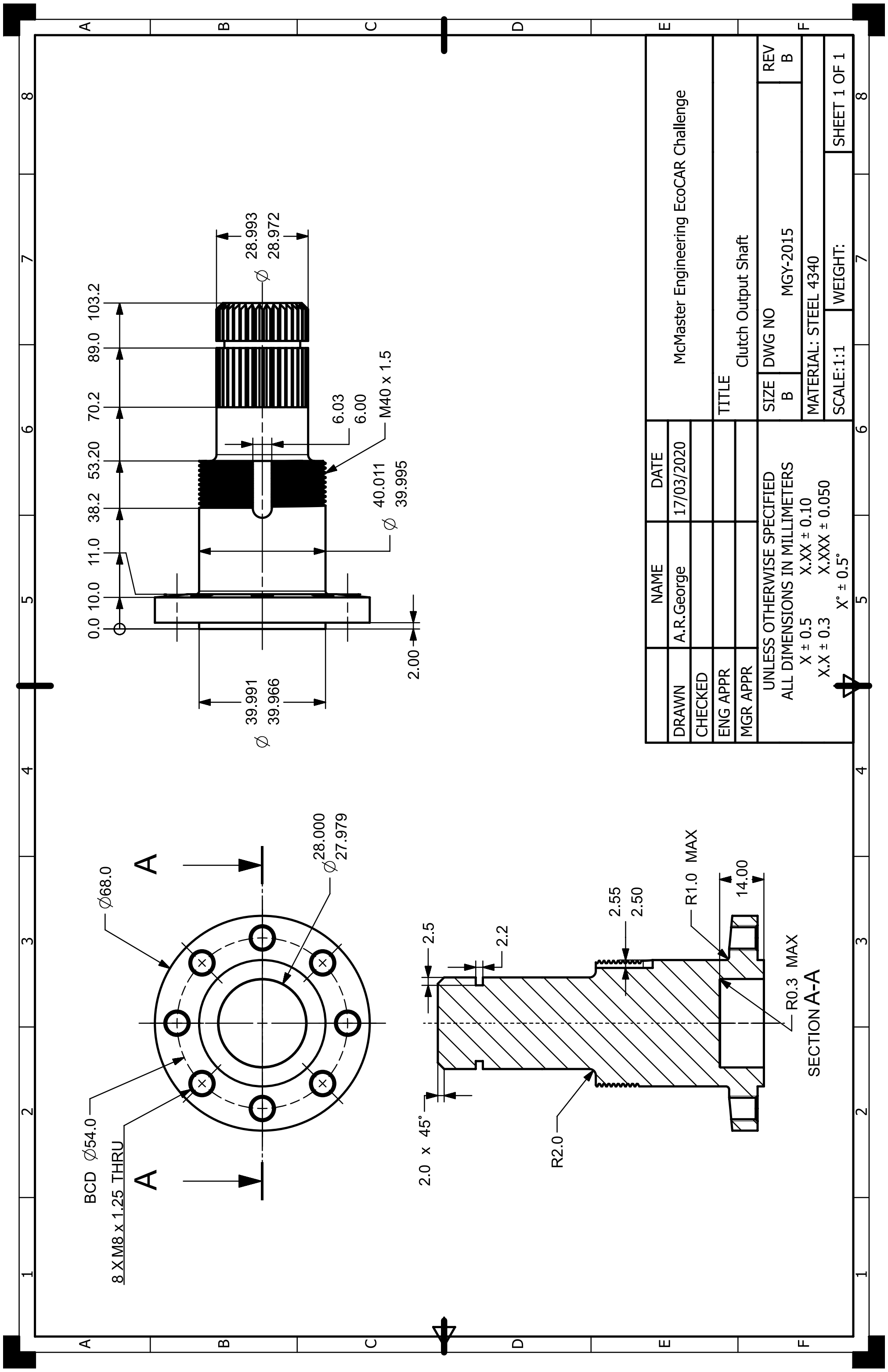

Figure A.12: Clutch Output Shaft

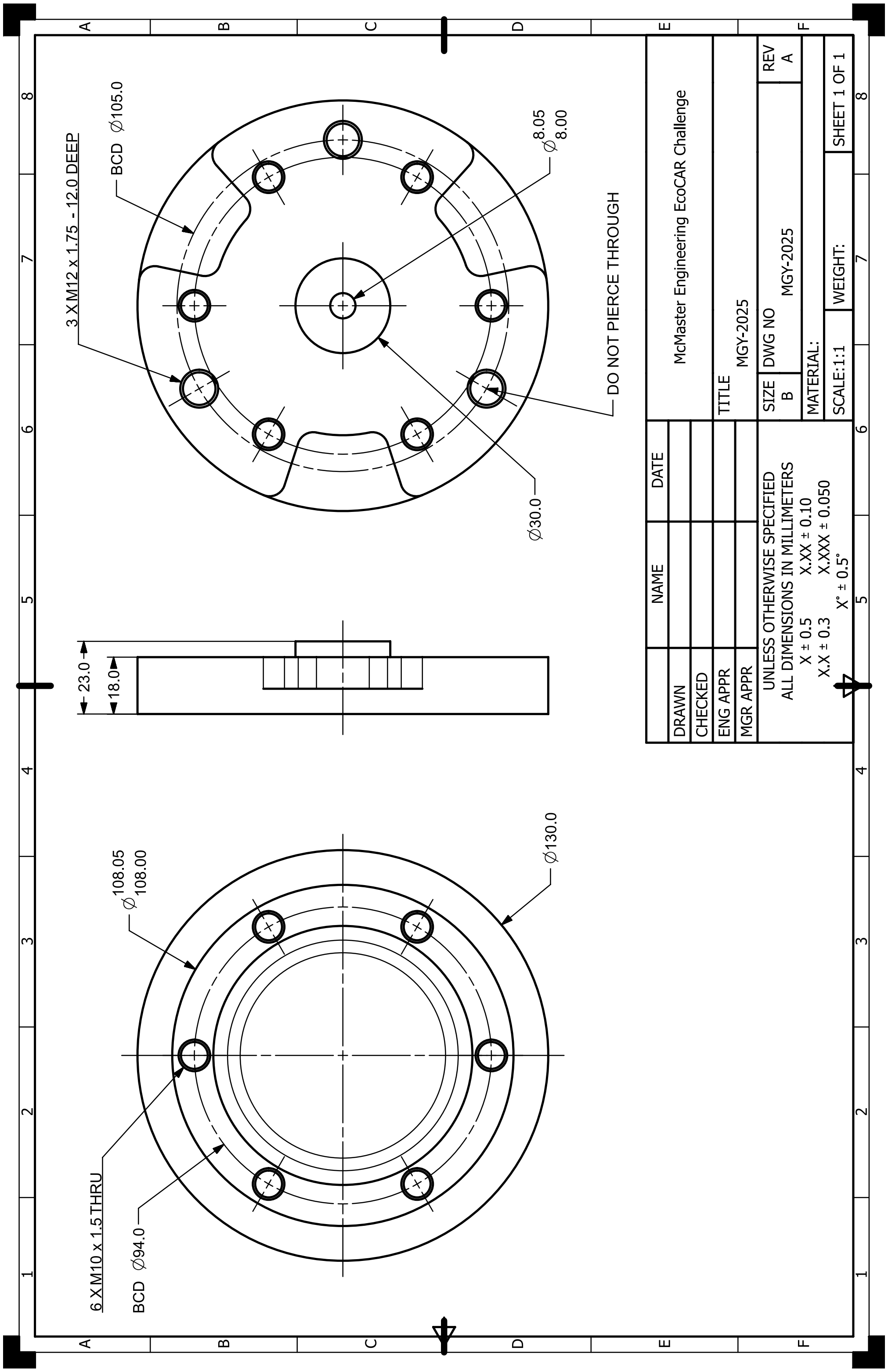

Figure A.13: CV to Differential Adapter

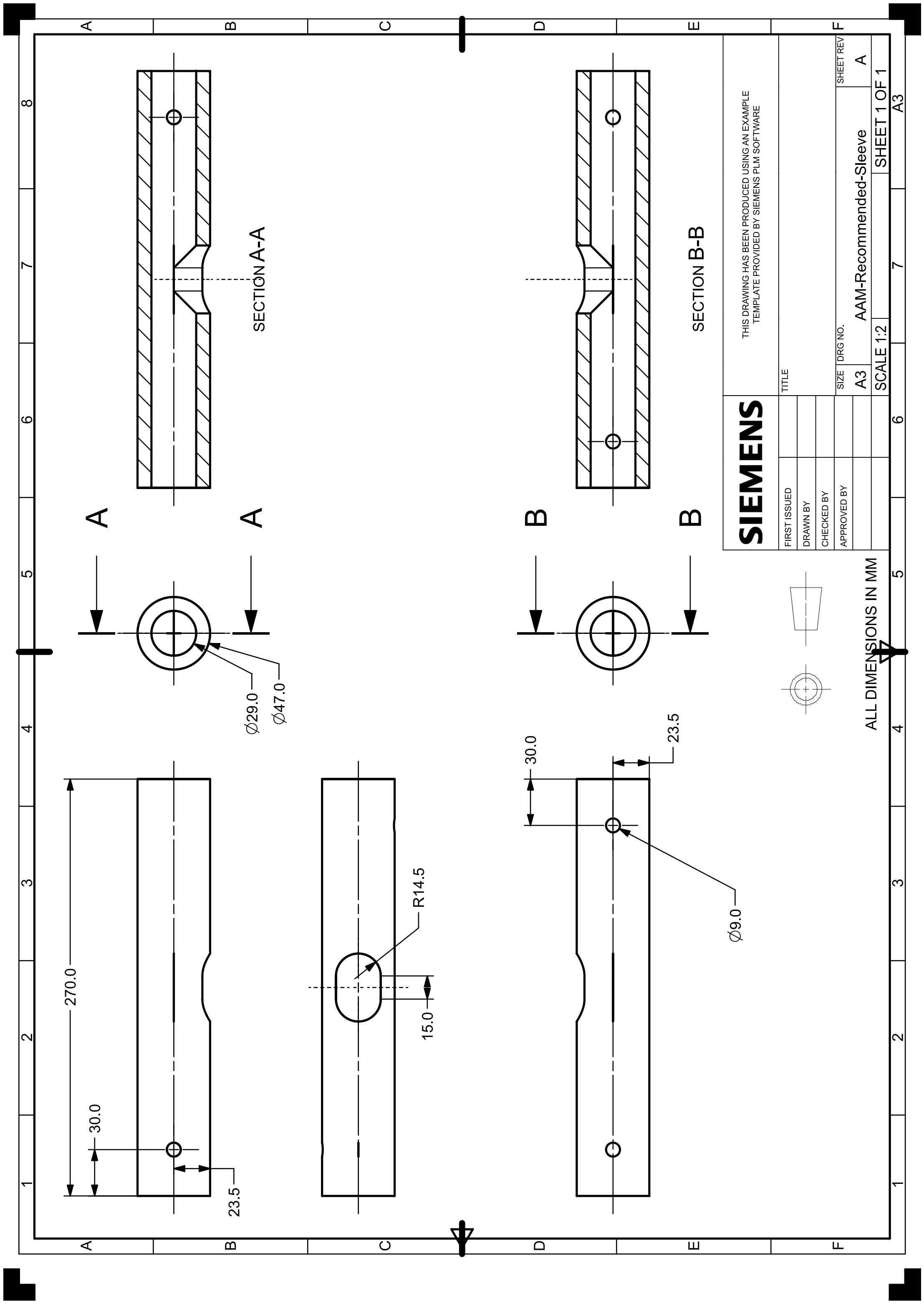

Figure A.14: Half Shaft Sleeve for Welded Joint

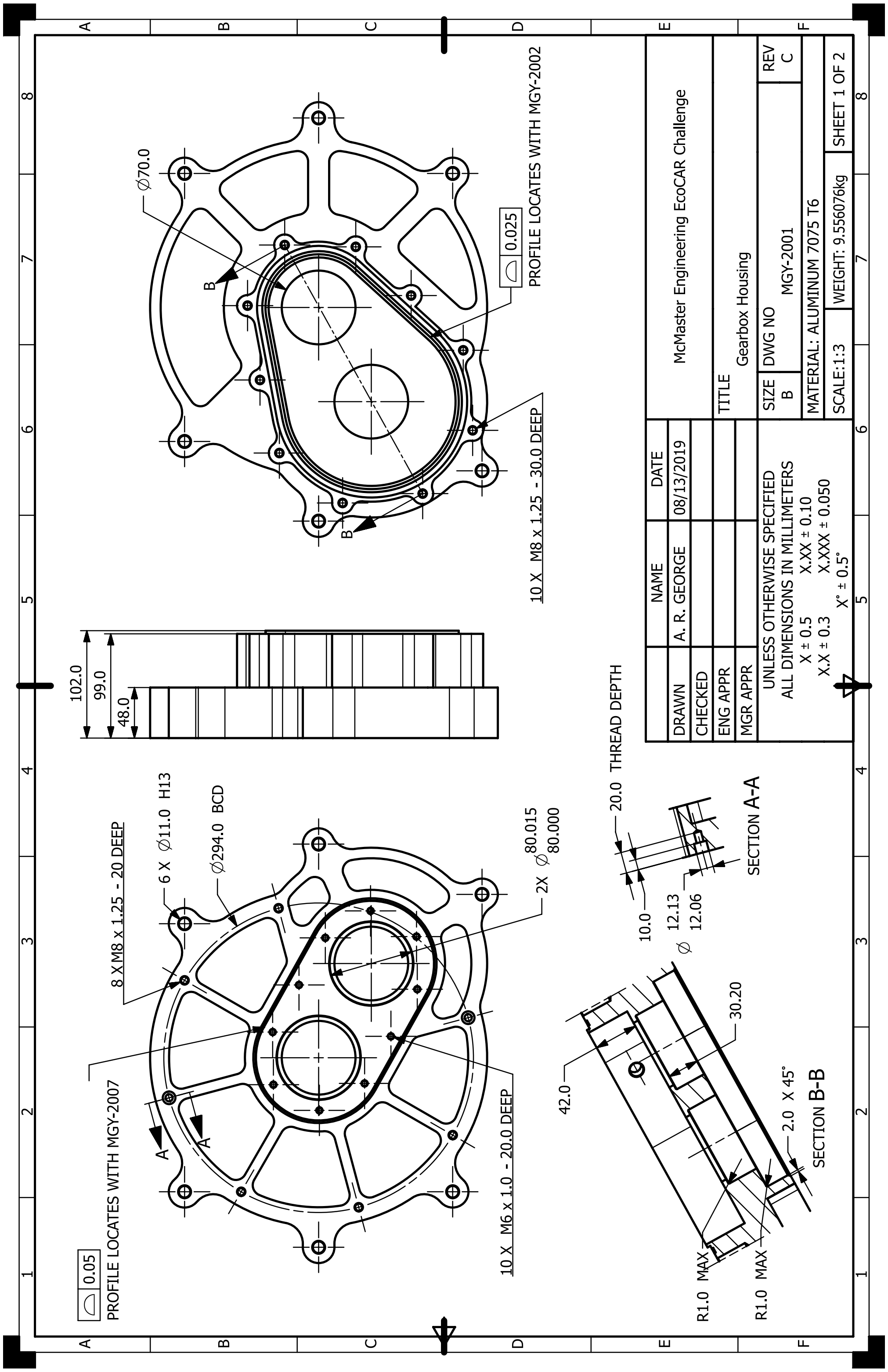

Figure A.15: Main Gearbox Casing Sheet 1 of 2

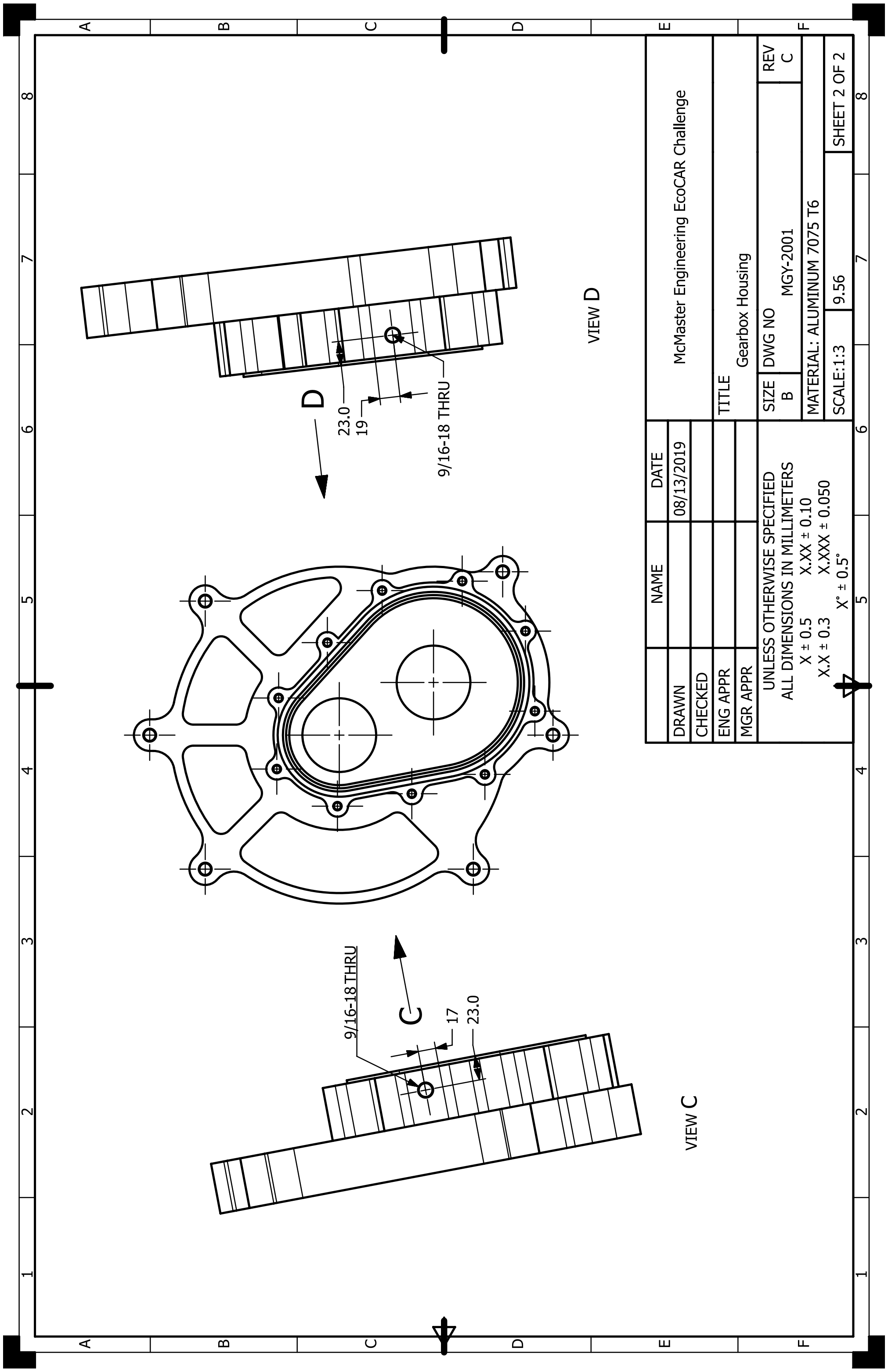

Figure A.16: Main Gearbox Casing Sheet 2 of 2

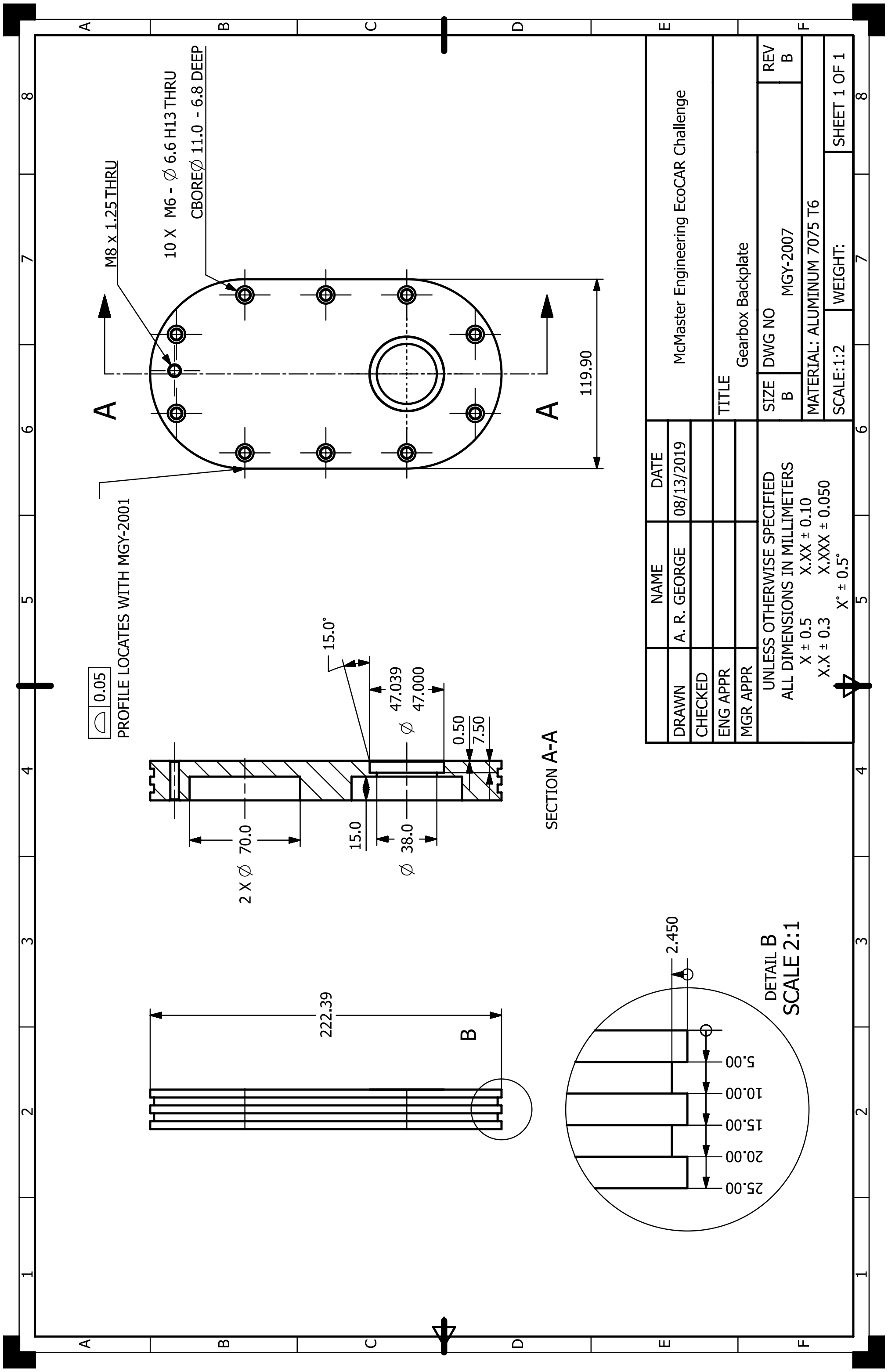

Figure A.17: Gear Housing Rear Cover

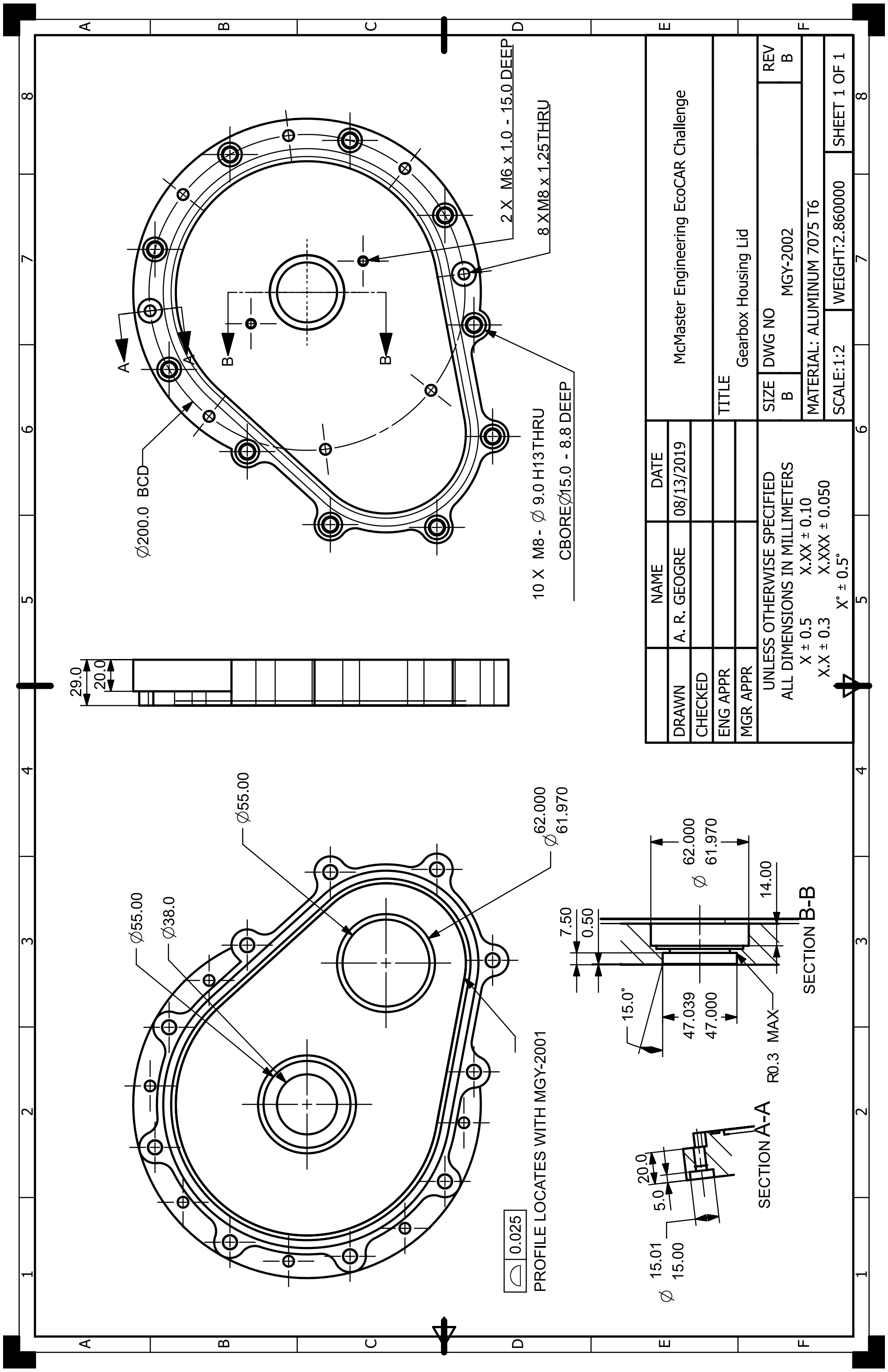

Figure A.18: Gear Housing Lid

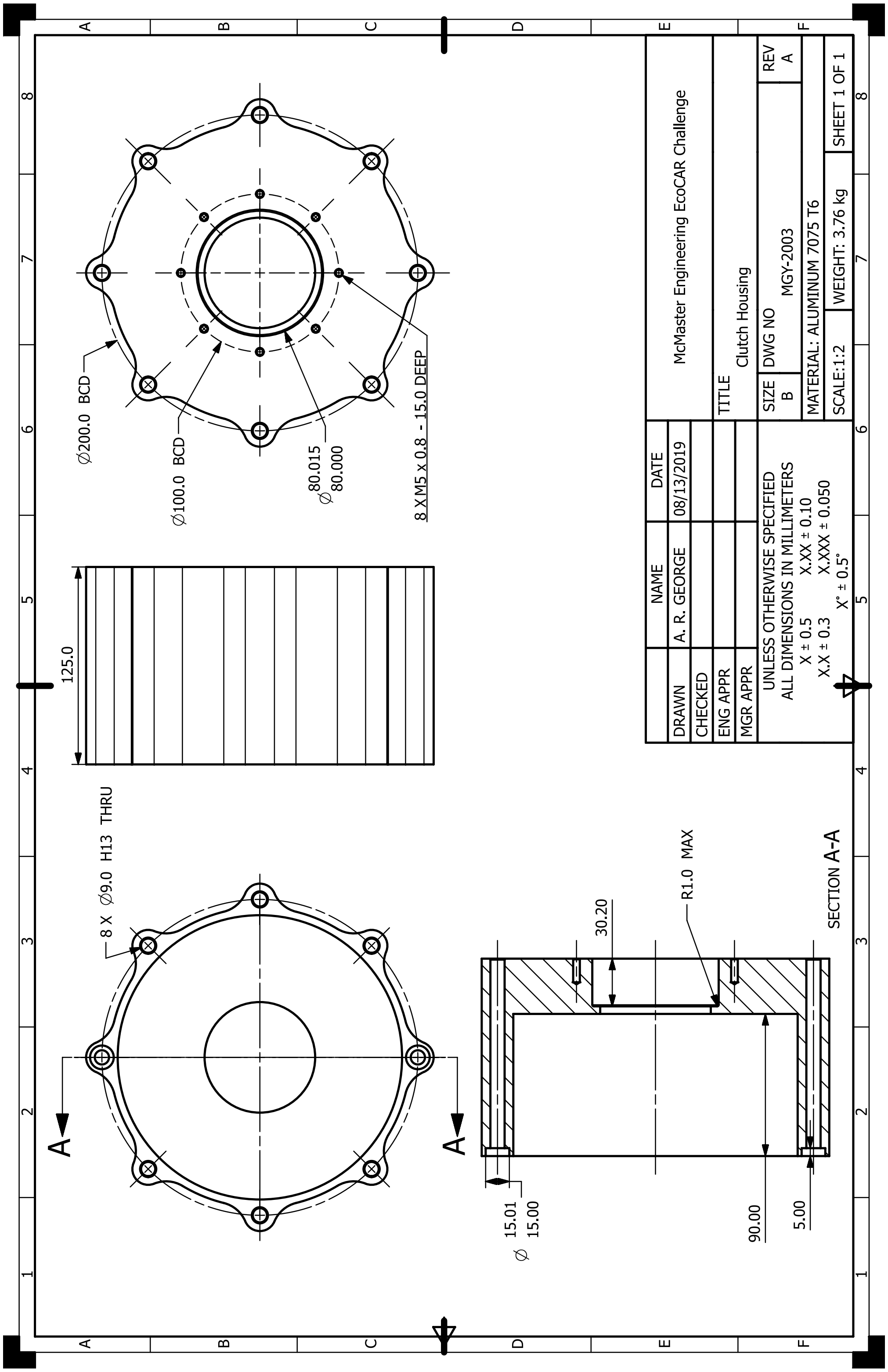

Figure A.19: Clutch Housing

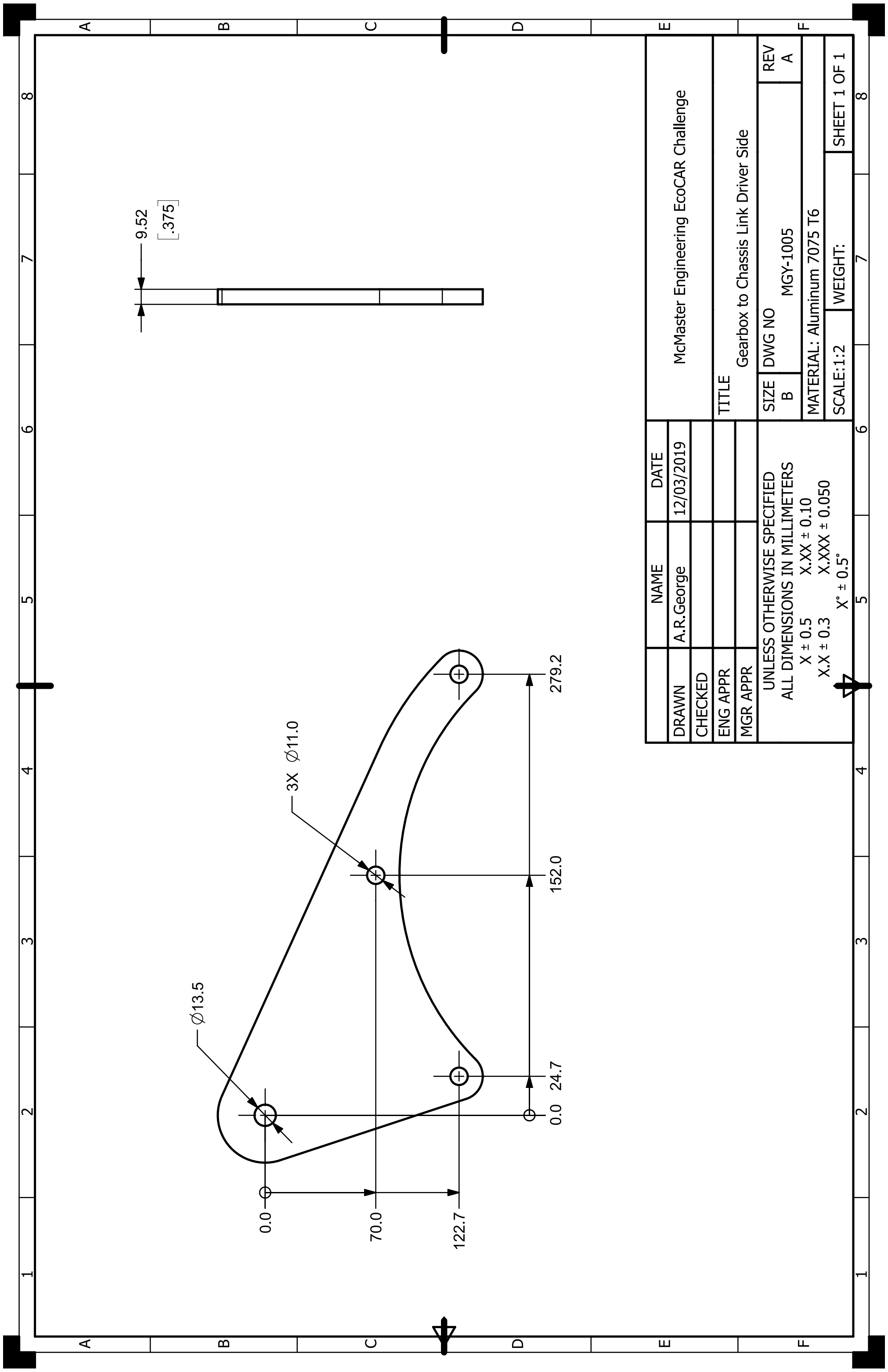

Figure A.20: Gearbox to Chassis Link Driver Side

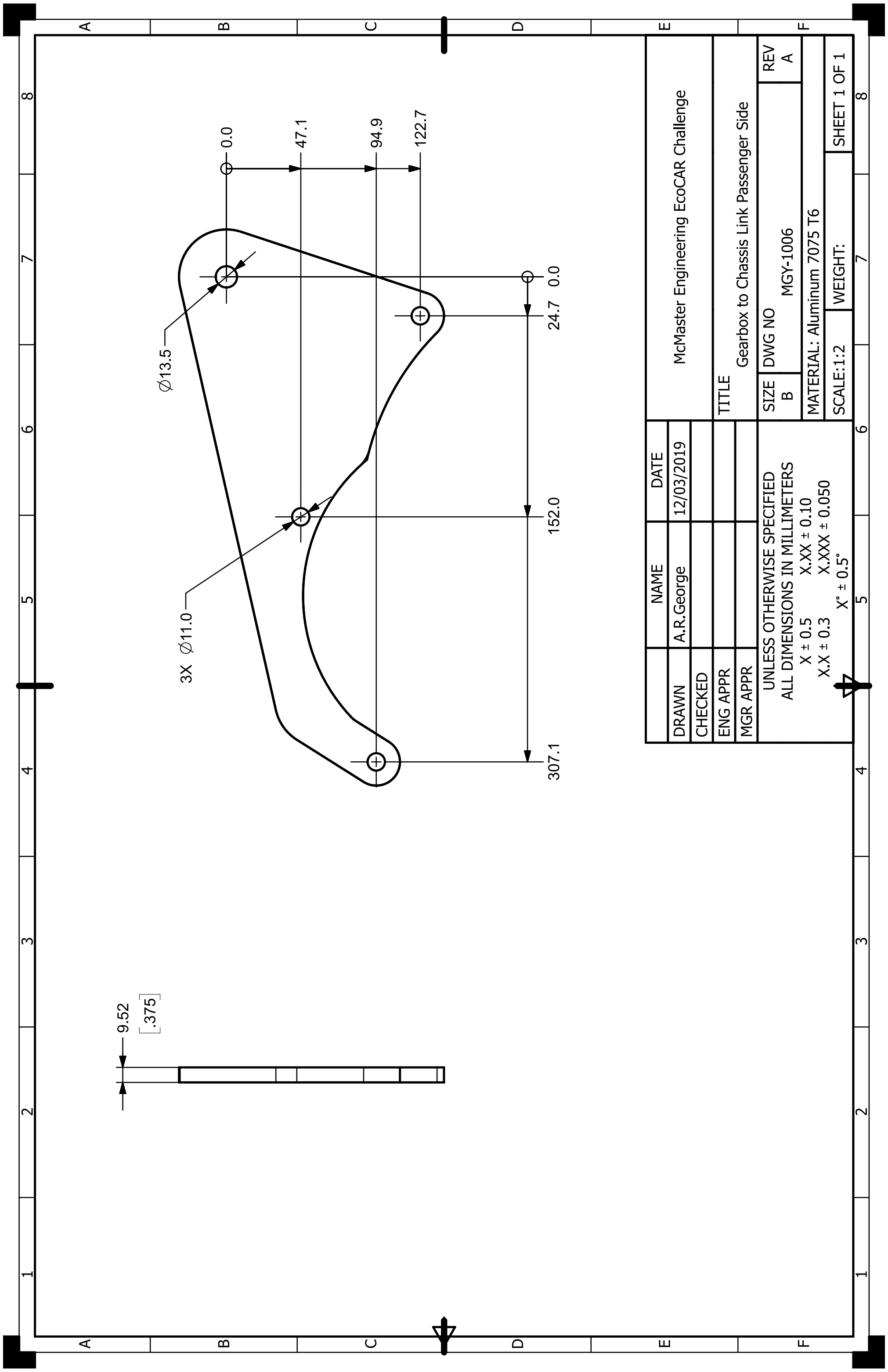

Figure A.21: Gearbox to Chassis Link Passenger Side

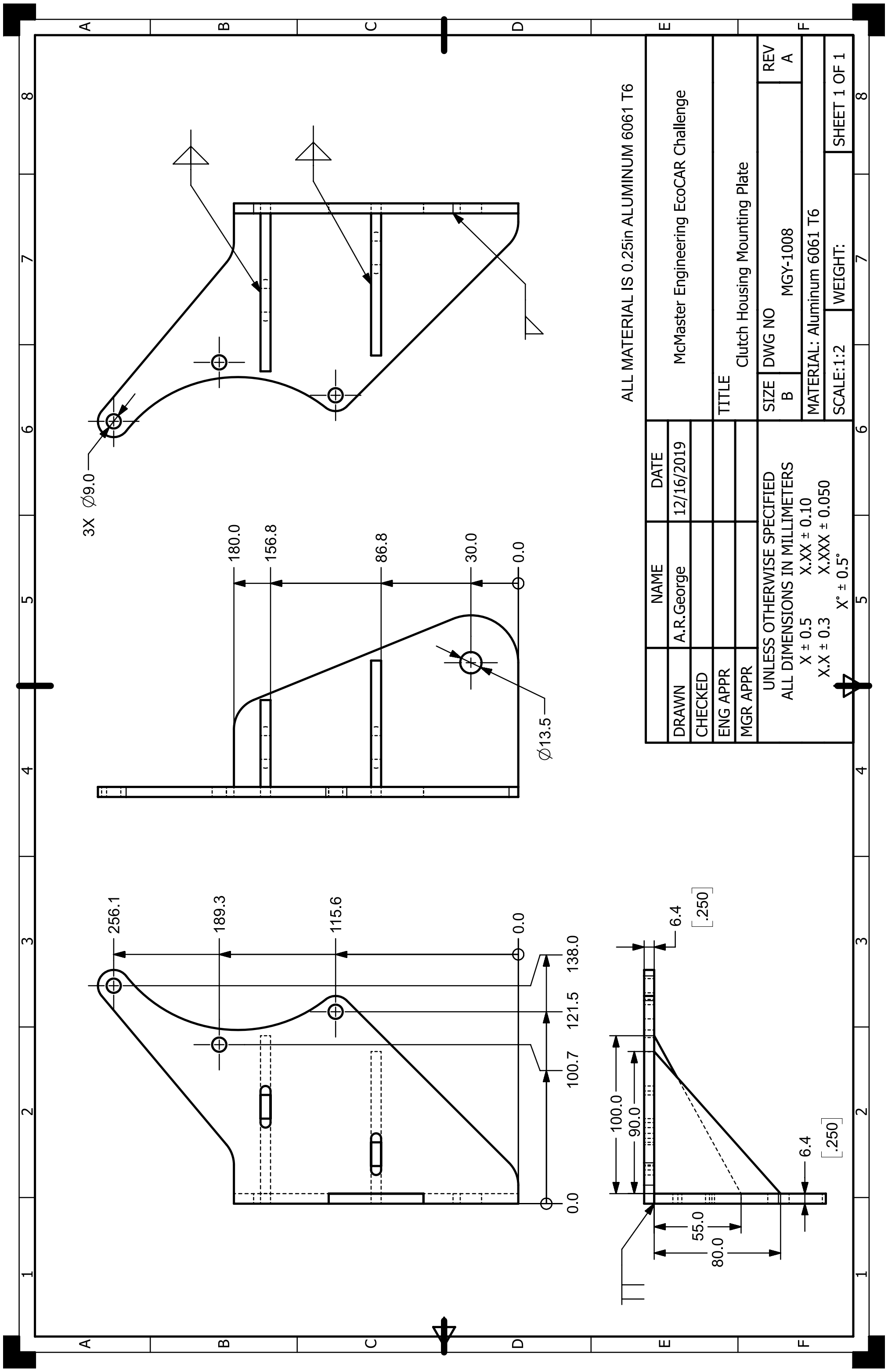

Figure A.22: Clutch Housing to Chassis Link Driver Side

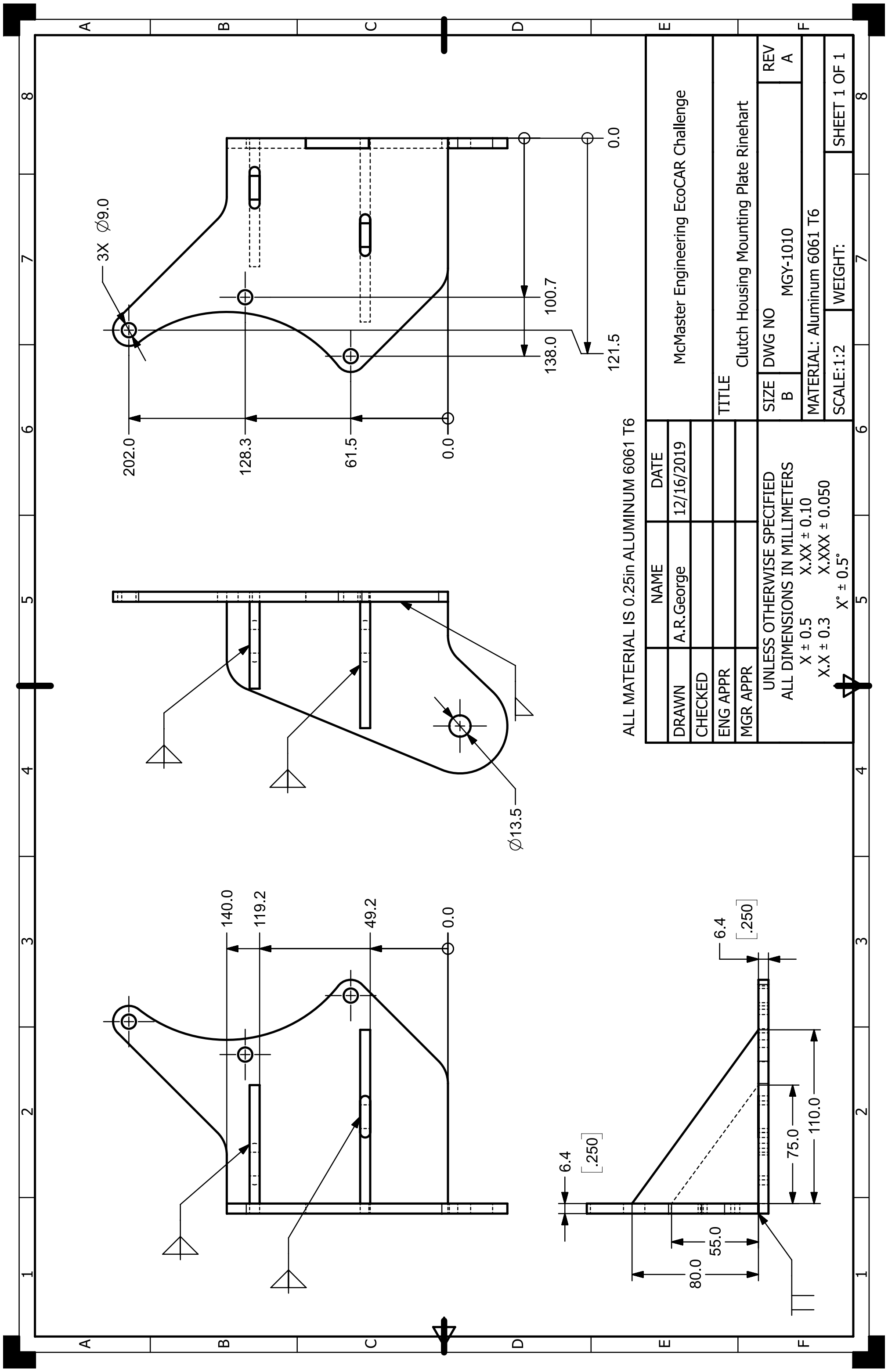

Figure A.23: Clutch Housing to Chassis Link Passenger Side

Appendix B

Gear Analysis

Table B.1: Summary of ISO 6336 design factors.

Factor	**Pinion**	**Wheel**	**Description**
			K-Factors
K_A	1.000	1.000	Application factor
K_V	1.060	1.060	Internal dynamic factor Subcritical Range
$K_{F\beta}$	1.275	1.275	Face load factor for tooth root
$K_{H\beta}$	1.349	1.349	Face load factor for contact
$K_{F\alpha}$	1.059	1.059	Transverse load factor for tooth root
$K_{H\alpha}$	1.059	1.059	Transverse load factor for contact
			Z-Factors for Contact Stress
Z_H	2.420	2.420	Zone Factor
Z_E	189.812	189.812	Elasticity Factor
Z_ε	0.795	0.795	Contact Ratio Factor
Z_β	1.035	1.035	Helix Angle Factor
Z_B	1.000	1.000	Single Pair Tooth Contact Factor Pinion
Z_D	1.000	1.000	Single Pair Tooth Contact Factor Wheel
			Z-Factors for Allowable Contact Stress
Z_{NT}	1.000	1.000	Life Factors, need SN Curve
Z_L	1.021	1.021	Lubricant Viscosity Factor
C_{Z_L}	0.905	0.905	
Z_v	1.003	1.003	Velocity and Lubricant Factor
C_{Z_v}	0.925	0.925	
Z_R	1.000	1.000	Surface Roughness Lubricant Factor
Z_W	1.000	1.000	Work Hardening Factor
Z_X	1.000	1.000	Size Factor
			Y-Factors for Bending Stress
Y_F	1.420	1.286	Form factor
Y_S	1.907	2.048	Stress Concentration Factor
Y_β	0.875	0.875	Helix Angle Factor
Y_B	1.000	1.000	Rim Thickness Factor
Y_DT	1.000	1.000	Deep Tooth Factor
			Y-Factors for Allowable Bending Stress
Y_{ST}	1.000	1.000	Stress Correction Factor
Y_{NT}	0.850	0.850	Life Factor - 0.85-1
$Y_{\delta relT}$	0.993	0.996	Relative Notch Sensitivity Factor
Y_{RrelT}	0.900	0.900	Relative Surface Factor
Y_X	1.000	1.000	Size Factor (1 for M_n <5)

Appendix C

Gearbox Assembly Photos

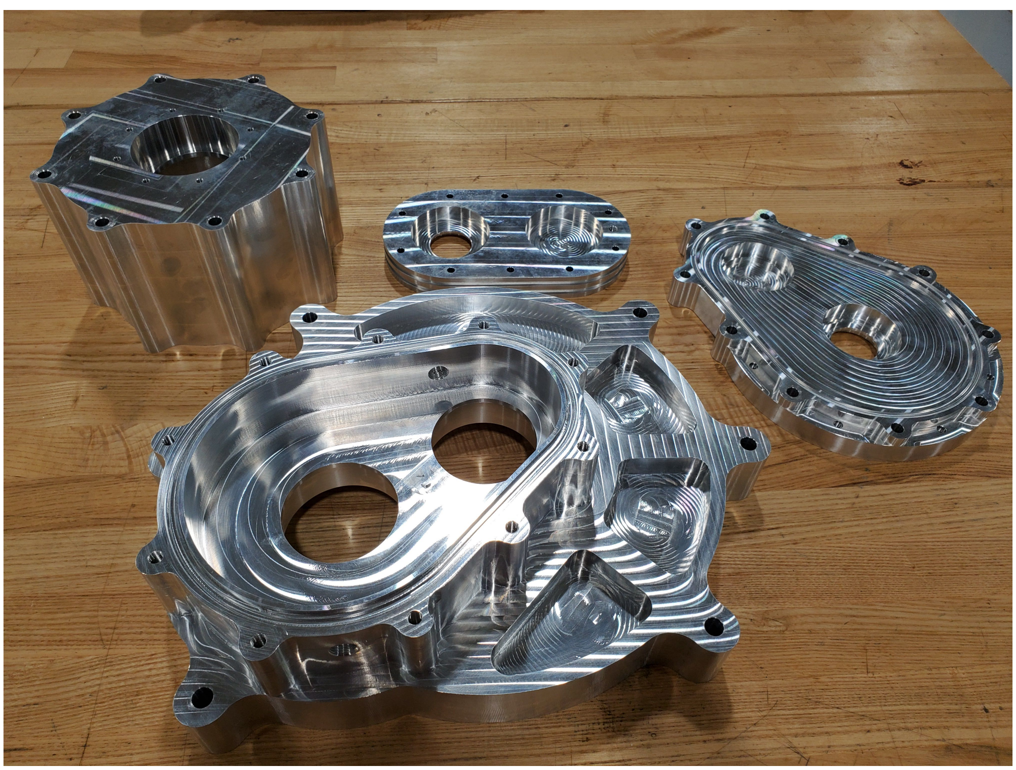

Figure C.1: Housing components as received from MERQ Inc.

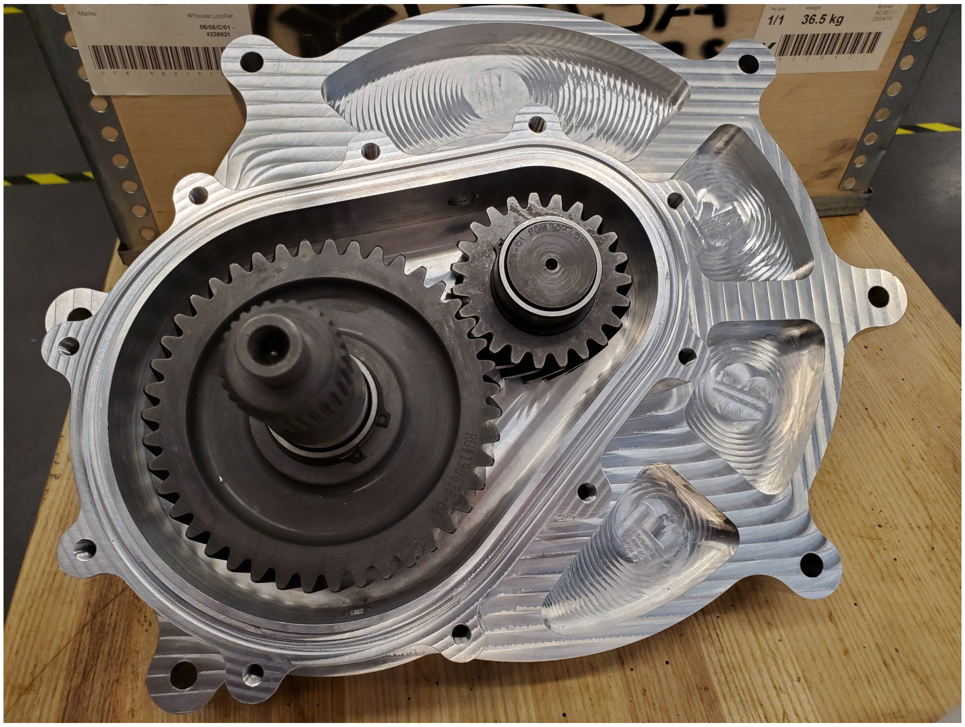

Figure C.2: Gear housing with assembled shafts fitted.

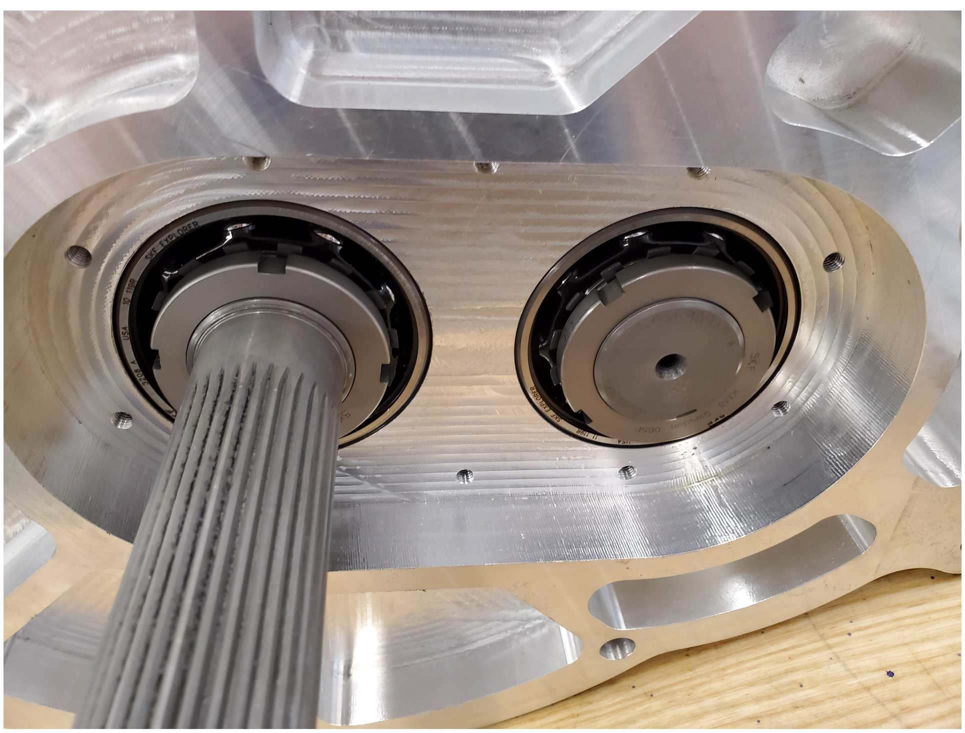

Figure C.3: Bearings assembled in housing, view from rear.

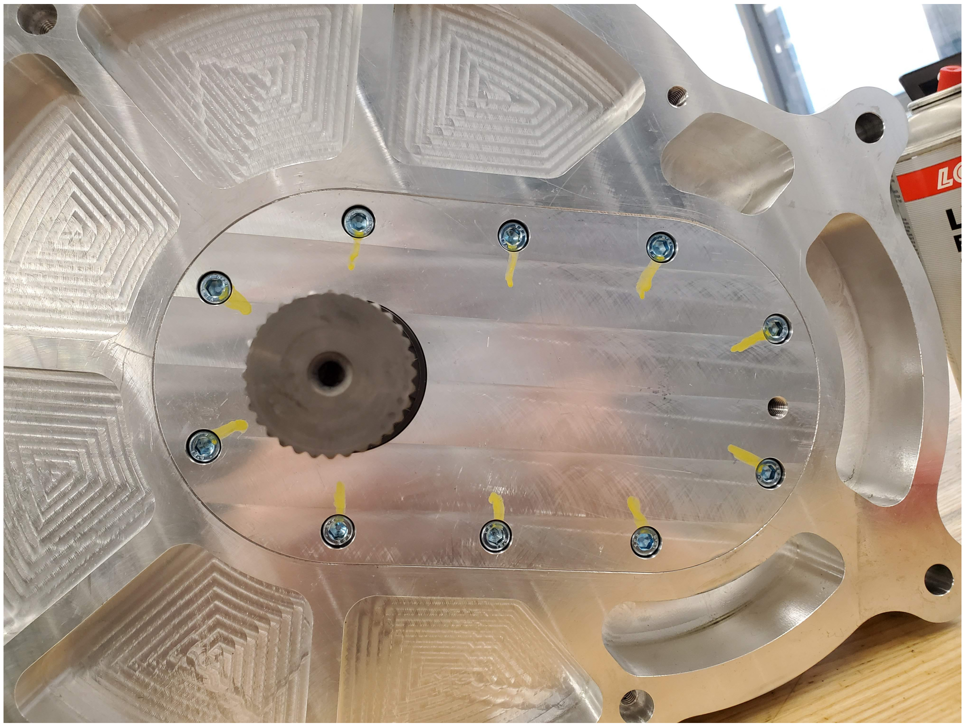

Figure C.4: Rear cover installed with torque stripes.

Figure C.5: Silicone placement in sealant groove.

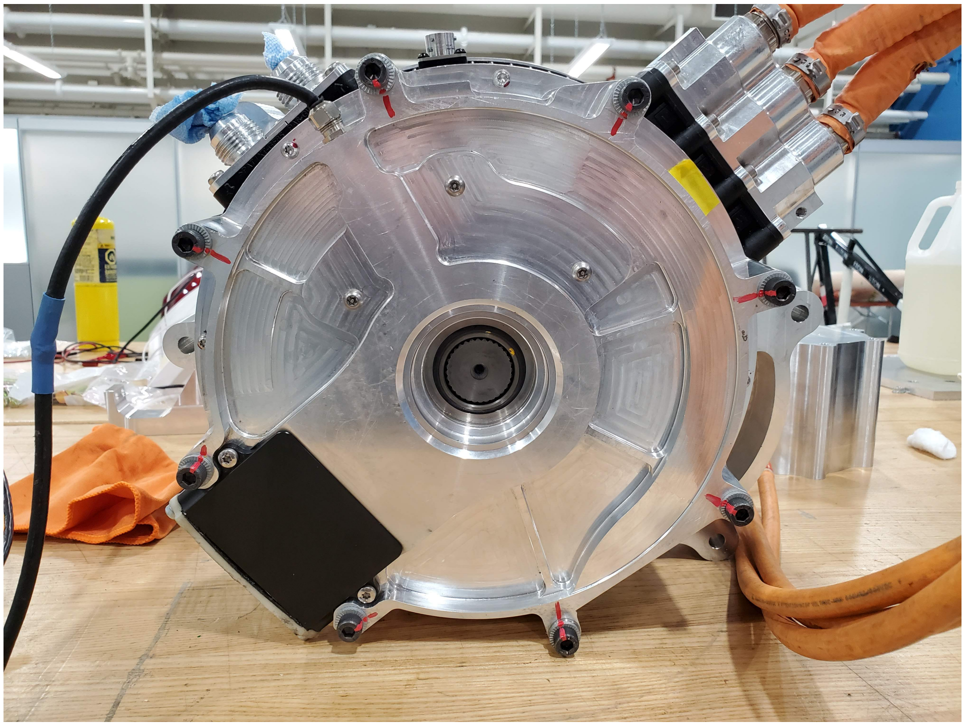

Figure C.6: Fully assembled gear housing, rear view of YASA P400.

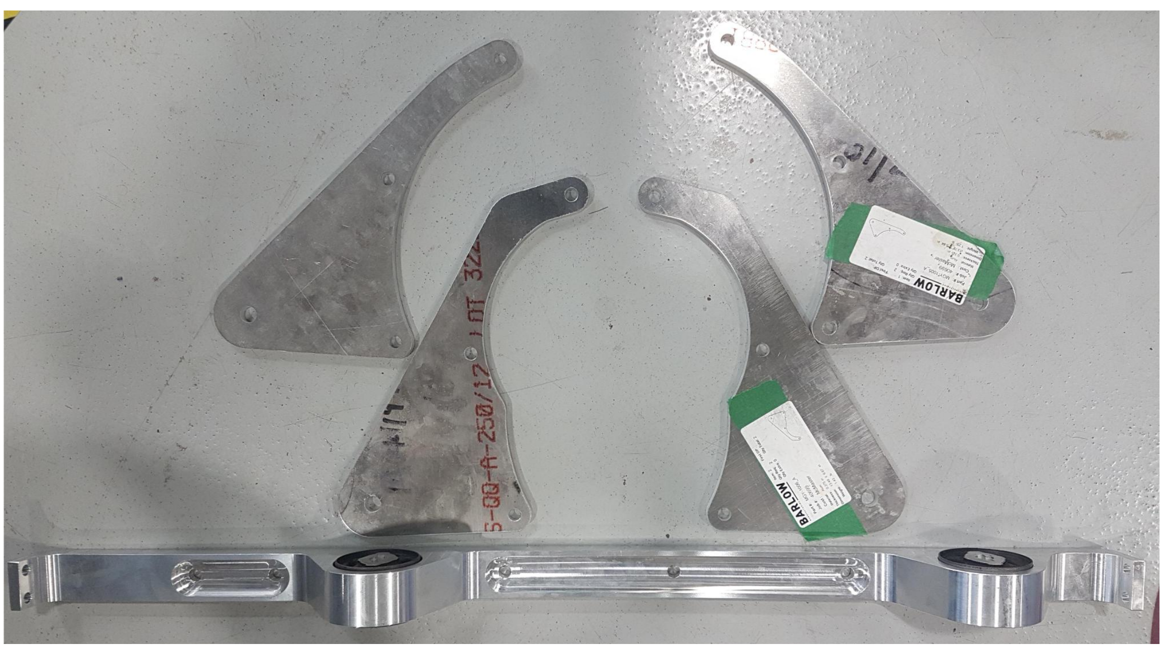

Figure C.7: Rear gearbox mounting system.

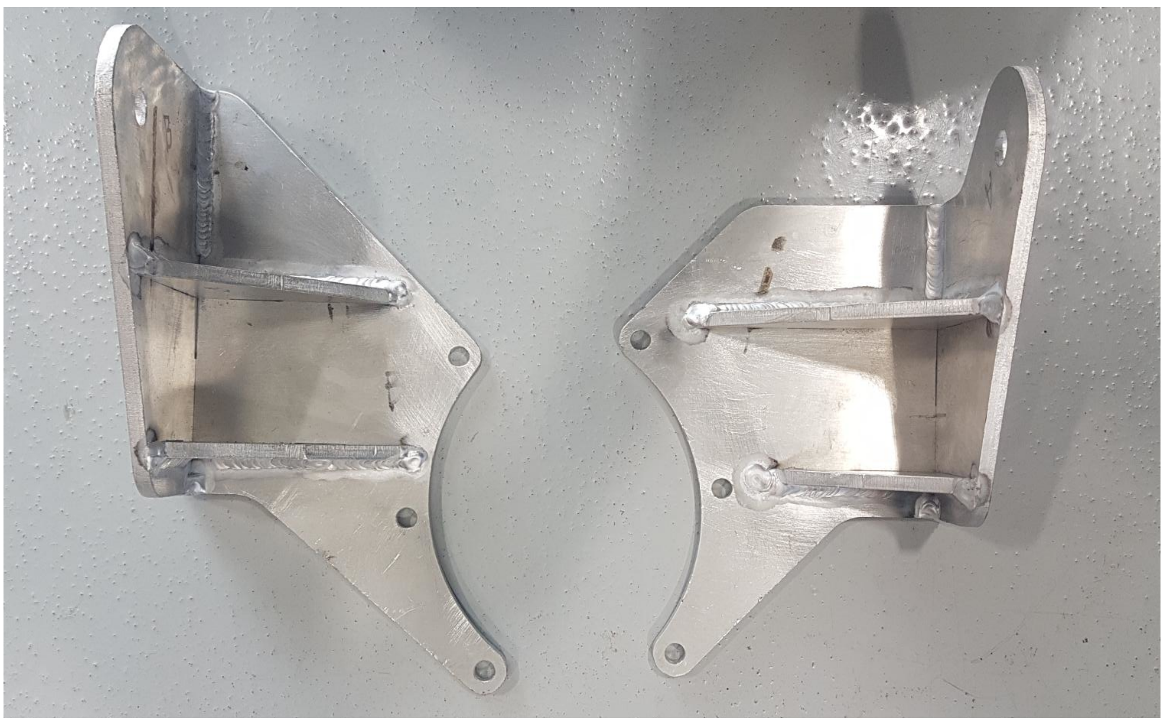

Figure C.8: Front gearbox mounting system.

References

[1] United States Environmental Protection Agency, "Fast Facts US Transportation Greenhouse Gas Emissions 1990 - 2017", Tech. Rep. June, 2019 (cit. on p. 1).

[2] U.S. Department of Energy, *Alternative Fuels Data Center: Maps and Data - Light-Duty AFV, HEV, and Diesel Model Offerings, by Fuel Type*. [Online]. Available: `https://afdc.energy.gov/data/` (visited on 04/30/2020) (cit. on p. 2).

[3] C. Tulumba, *Overall U.S Auto Industry Sales Figures — GCBC*. [Online]. Available: `https://www.goodcarbadcar.net/usa-auto-industry-total-sales-figures/` (visited on 05/01/2020) (cit. on p. 2).

[4] Statistics Canada, *New Motor Vehicle Registrations Data Visualization Tool*. [Online]. Available: `https://www150.statcan.gc.ca/n1/pub/71-607-x/71-607-x2019028-eng.htm` (visited on 04/30/2020) (cit. on p. 2).

[5] M. Wayland, *GM to spend $20 billion on new electric, autonomous vehicles*, 2020. [Online]. Available: `https://www.cnbc.com/2020/03/04/gm-to-spend-20-billion-on-new-electric-autonomous-vehicles.html` (visited on 04/30/2020) (cit. on p. 2).

[6] N. Carey and J. White, *Ford plans $11 billion investment, 40 electrified vehicles by 2022 - Reuters*, 2018. [Online]. Available: https://www.reuters.com/article/us-autoshow-detroit-ford-motor/ford-plans-11-billion-investment-40-electrified-vehicles-by-2022-idUSKBN1F30YZ (visited on 04/30/2020) (cit. on p. 2).

[7] Office of the Press Secretary, *Obama Administration Finalizes Historic 54.5 MPG Fuel Efficiency Standards — whitehouse.gov*. [Online]. Available: https://obamawhitehouse.archives.gov/the-press-office/2012/08/28/obama-administration-finalizes-historic-545-mpg-fuel-efficiency-standard (visited on 04/26/2020) (cit. on p. 2).

[8] O. US EPA, "The Safer Affordable Fuel Efficient (SAFE) Vehicles Final Rule for Model Years 2021-2026", (cit. on p. 3).

[9] B. Dennis and J. Eilperin, *California and other states sue Trump administration for the right to require more fuel-efficient cars - The Washington Post*. [Online]. Available: https://www.washingtonpost.com/climate-environment/2019/11/15/california-nearly-two-dozen-other-states-sue-trump-administration-right-require-more-fuel-efficient-cars/ (visited on 05/01/2020) (cit. on p. 3).

[10] Government of Canada, *40 CFR § 86.1818-12 - Greenhouse gas emission standards for light-duty vehicles, light-duty trucks, and medium-duty passenger vehicles. — CFR — US Law — LII / Legal Information Institute*. [Online]. Available: https://www.law.cornell.edu/cfr/text/40/86.1818-12 (visited on 05/01/2020) (cit. on p. 3).

[11] ——, *Summary of comments on the light-duty vehicle discussion paper - Canada.ca*, 2019. [Online]. Available: https://www.canada.ca/en/environment-

climate-change/services/canadian-environmental-protection-act-registry/summary-discussion-passenger-auto-light-truck-emissions-regulations.html%7B%5C#%7Dtoc13 (visited on 05/01/2020) (cit. on p. 3).

[12] Environment and Climate Change Canada, "Discussion paper on the mid-term evaluation of the Passenger Automobile and Light Truck Greenhouse Gas Emission Regulations", Tech. Rep. September, 2018, pp. 1–9 (cit. on p. 3).

[13] SAE International, "Taxonomy and Definitions for Terms Related to Driving Automation Systems for On-Road Motor Vehicles", *SAE International*, no. J3016, 2018. [Online]. Available: https://www.sae.org/standards/content/j3016%7B%5C_%7D201806/ (cit. on p. 3).

[14] Ecolane, *Ride-hailing vs. ride-sharing: The key difference and why it matters.* 2018. [Online]. Available: https://www.ecolane.com/blog/ride-hailing-vs.-ride-sharing-the-key-difference-and-why-it-matters (visited on 05/04/2020) (cit. on p. 4).

[15] P. Jittrapirom, V. Caiati, A. M. Feneri, S. Ebrahimigharehbaghi, M. J. Alonso-González, and J. Narayan, "Mobility as a service: A critical review of definitions, assessments of schemes, and key challenges", *Urban Planning*, vol. 2, no. 2, pp. 13–25, 2017, ISSN: 21837635. DOI: 10.17645/up.v2i2.931 (cit. on p. 4).

[16] A.V.T.C., *COMPETITIONSAVTC I ADVANCED VEHICLE TECHNOLOGY COMPETITIONS*. [Online]. Available: https://avtcseries.org/avtc-history/competitions/ (visited on 05/03/2020) (cit. on p. 4).

[17] D. Demuro, *SUV vs. Crossover: What's the Difference? - Autotrader*, 2019. [Online]. Available: https://www.autotrader.com/car-shopping/suv-vs-crossover-whats-difference-215843 (visited on 05/03/2020) (cit. on p. 5).

[18] U.S. Energy Information Administration, *Crossover utility vehicles overtake cars as the most popular light-duty vehicle type - Today in Energy - U.S. Energy Information Administration (EIA)*, 2018. [Online]. Available: https://www.eia.gov/todayinenergy/detail.php?id=36674 (visited on 05/02/2020) (cit. on p. 5).

[19] W. Hackmann, "Electrical Traction Drives : HEV E-Drive Development and Products", Tech. Rep., 2012 (cit. on p. 8).

[20] Magna, *Powertrain Electrification – etelligentDrive Solutions*, 2017. [Online]. Available: http://electrification.magna.com/powertrain-electrification/ (visited on 05/15/2020) (cit. on p. 8).

[21] S. Cropley, *Volvo XC40 examined in detail ahead of Geneva debut — Autocar*. [Online]. Available: https://www.autocar.co.uk/car-news/concept-cars/volvo-xc40-examined-detail-ahead-geneva-debut (visited on 05/30/2020) (cit. on p. 10).

[22] B. Bilgin, P. Magne, P. Malysz, Y. Yang, V. Pantelic, M. Preindl, A. Korobkine, W. Jiang, M. Lawford, and A. Emadi, "Making the Case for Electrified Transportation", *IEEE Transactions on Transportation Electrification*, vol. 1, no. 1, pp. 4–17, 2015, ISSN: 23327782. DOI: 10.1109/TTE.2015.2437338 (cit. on p. 10).

[23] M. Kintner-Meyer, K. Schneider, and R. Pratt, "Impacts Assessment of Plug-in Hybrid Vehicles on electric utilities and regional U.S. Power Grids", *Federal Energy Regulatory Commission*, pp. 1–20, 2007, ISSN: 1098-6596. DOI: 10.1017/CBO9781107415324.004. arXiv: arXiv:1011.1669v3. [Online]. Available: http://citeseerx.ist.psu.edu/viewdoc/download?doi=10.1.1.105.663%7B%5C&%7Drep=rep1%7B%5C&%7Dtype=pdf%7B%5C%%7D0Ahttps:

//www.ferc.gov/about/com-mem/5-24-07-technical-analy-wellinghoff.pdf (cit. on p. 12).

[24] Q. Gong, S. Midlam-Mohler, V. Marano, and G. Rizzoni, "Study of PEV charging on residential distribution transformer life", *IEEE Transactions on Smart Grid*, vol. 3, no. 1, pp. 404–412, 2012, ISSN: 19493053. DOI: 10.1109/TSG.2011.2163650 (cit. on p. 13).

[25] S. A. Zulkifli, N. Saad, S. Mohd, and A. R. A. Aziz, "Split-parallel in-wheel-motor retrofit hybrid electric vehicle", *2012 IEEE International Power Engineering and Optimization Conference, PEOCO 2012 - Conference Proceedings*, no. June, pp. 11–16, 2012. DOI: 10.1109/PEOCO.2012.6230915 (cit. on p. 13).

[26] S. A. Zulkifli, S. Mohd, N. Saad, and A. R. Aziz, "Split-parallel through-the-road hybrid electric vehicle: Operation, power flow and control modes", in *2015 IEEE Transportation Electrification Conference and Expo, ITEC 2015*, IEEE, Jun. 2015, pp. 1–7, ISBN: 9781467367417. DOI: 10.1109/ITEC.2015.7165774. [Online]. Available: http://ieeexplore.ieee.org/document/7165774/ (cit. on p. 13).

[27] S. A. Zulkifli, S. Mohd, N. Saad, and A. R. A. Aziz, "Operation, power flow, system architecture and control challenges of split-parallel through-the-road hybrid electric vehicle", *2015 10th Asian Control Conference: Emerging Control Techniques for a Sustainable World, ASCC 2015*, 2015. DOI: 10.1109/ASCC.2015.7244637 (cit. on p. 13).

[28] ——, "Operation and Control of Split-Parallel, Through-The-Road Hyrbid with In-Wheel Motors", vol. 11, no. June, pp. 2793–2808, 2015 (cit. on p. 13).

[29] C. Pisanti, G. Rizzo, and V. Marano, "Energy management of through-the-road parallel hybrid vehicles", *IFAC Proceedings Volumes (IFAC-PapersOnline)*,

vol. 19, pp. 2118–2124, 2014, ISSN: 14746670. DOI: 10.3182/20140824-6-ZA-1003.02494 (cit. on p. 14).

[30] G. Rizzo, C. Pisanti, M. D'Agostino, and M. Naddeo, "Driver intention analysis for a through-the-road solar hybridized car", *SAE Technical Papers*, vol. 6, 2013, ISSN: 26883627. DOI: 10.4271/2013-24-0079 (cit. on p. 14).

[31] E. Galvagno, D. Morina, A. Sorniotti, and M. Velardocchia, "Drivability analysis of through-the-road-parallel hybrid vehicles", *Meccanica*, vol. 48, no. 2, pp. 351–366, 2012, ISSN: 00256455. DOI: 10.1007/s11012-012-9606-6 (cit. on p. 14).

[32] R. Finesso, E. Spessa, and M. Venditti, "Optimization of the layout and control strategy for parallel through-the-road hybrid electric vehicles", *SAE Technical Papers*, vol. 1, 2014, ISSN: 26883627. DOI: 10.4271/2014-01-1798 (cit. on pp. 14, 15).

[33] J. Hall, M. Bassett, S. Borman, T. Lucas, and A. Whitehead, "Through-the-Road Parallel Hybrid with In-Wheel Motors", *SAE Technical Papers*, 2016, ISSN: 01487191. DOI: 10.4271/2016-01-1160 (cit. on p. 15).

[34] M. Young, G. M. Molen, D. Oglesby, K. Crawford, K. Walp, R. Lewis, C. Whitt, and S. Phillips, "The design and development of a through-the-road parallel diesel electric hybrid", *VPPC 2007 - Proceedings of the 2007 IEEE Vehicle Power and Propulsion Conference*, pp. 511–518, 2007. DOI: 10.1109/VPPC.2007.4544178 (cit. on pp. 15, 16).

[35] D. K. Mehr, M. Michalak, S. Erlien, and G. R. Bower, "Optimization and testing of a through the road parallel, hybrid-electric, crossover sports utility vehicle", *SAE Technical Papers*, pp. 1–14, 2009, ISSN: 26883627. DOI: 10.4271/2009-01-1318 (cit. on pp. 15, 16).

[36] H. M. Moore, B. W. Belt, C. Rhoades, A. Vora, H. Wu, P. Meckl, V. Motevalli, G. Shaver, O. Wasynczuk, and H. Zhang, "Designing a parallel-through-the-road plug-in hybrid electric vehicle", *SAE Technical Papers*, vol. 9, 2012, ISSN: 26883627. DOI: 10.4271/2012-01-1763 (cit. on p. 16).

[37] BMW, *BMW i8 Coupe and i8 Roadster — Features and Pricing — BMW USA*, 2020. [Online]. Available: https://www.bmwusa.com/vehicles/bmwi/i8/pricing-features.html (visited on 05/14/2020) (cit. on p. 17).

[38] E. Tingwall, *2017 Acura NSX Supercar Full Test – Review – Car and Driver*. [Online]. Available: https://www.caranddriver.com/reviews/a15098793/2017-acura-nsx-supercar-full-test-review/ (visited on 05/14/2020) (cit. on p. 17).

[39] M. Creyaufmueller, "Press information", Tech. Rep., 2013. [Online]. Available: https://presse.porsche.de/presskits%7B%5C_%7Duntil%7B%5C_%7D2015/products/2013/spyder/text/presskit/918%7B%5C_%7DSpyder%7B%5C_%7DFahrvorstellung%7B%5C_%7DEN6%7B%5C_%7Dhp.pdf (cit. on p. 17).

[40] S. Siler, *2016 Volvo XC90 T8 Plug-In Hybrid: 400 hp, 59 MPGe – News – Car and Driver*, 2014. [Online]. Available: https://www.caranddriver.com/news/a15359346/2016-volvo-xc90-t8-plug-in-hybrid-powertrain-detailed-400-hp-and-59-mpge/ (visited on 05/14/2020) (cit. on p. 17).

[41] Volvo, *All about our Plug-In Hybrid Cars (PHEV) — Volvo Cars*, 2020. [Online]. Available: https://www.volvocars.com/intl/why-volvo/human-innovation/electrification/plug-in-hybrids (visited on 05/14/2020) (cit. on p. 17).

[42] McMaster Engineering EcoCAR Team, "EcoCAR 3 Architecture Study", Tech. Rep., 2018 (cit. on pp. 19–21).

[43] ——, "EcoCAR 3 Closeout Report Survey", Tech. Rep., 2018 (cit. on p. 19).

[44] Argonne National Labratory, "EcoCAR Mobility Challenge Non-Year-Specific Rules Rev. H", 2020 (cit. on pp. 22, 25).

[45] Ontario Ministry of Finance, "Ontario Fact Sheet", no. May, p. 1, 2020 (cit. on p. 28).

[46] T. Harris, *28 per cent of Toronto households don't have a car — including many suburban homes. Here's how they make it work — The Star*, 2018. [Online]. Available: https://www.thestar.com/news/gta/2018/07/18/28-per-cent-of-toronto-households-dont-have-a-car-including-many-suburban-homes-heres-how-they-make-it-work.html (visited on 06/01/2020) (cit. on p. 28).

[47] R. Carrick, *Suburban living is more expensive than you may think - The Globe and Mail*, 2016. [Online]. Available: https://www.theglobeandmail.com/real-estate/mortgages-and-rates/thinking-of-buying-a-suburban-home-dont-forget-the-commuting-costs/article29202895/ (visited on 06/01/2020) (cit. on p. 28).

[48] McMaster Engineering EcoCAR Team, "Target Market and Vehicle Technical Specification Selection Report", 2018 (cit. on pp. 28, 29).

[49] D. Petramala, M. S. Researcher, F. Clayton, A. Butler, A. Mackaay, A. Quigg, and E. Quigg, "Millennials in the Greater Toronto and Hamilton Area: A Generation Stuck in Apartments?", Centre for Urban Research and Land Developement Ryerson University, Tech. Rep., 2018. [Online]. Available: https://www.ryerson.ca/content/dam/cur/pdfs/policycommentaries/CUR%7B%5C_%7DResearch%7B%5C_%7DReport%7B%5C_%7DMillennial%7B%5C_

%7DHousing%7B%5C_%7DGTHA%7B%5C_%7DMay%7B%5C_%7D22.pdf (cit. on pp. 28, 29).

[50] YASA, "YASA 400 Axial Flux Electric Motor", Tech. Rep., 2014 (cit. on p. 33).

[51] Plettenberg Motoren, *Motors*. [Online]. Available: https://plettenberg-motoren.net/en/products/motor-solutions/motors (visited on 06/26/2020) (cit. on p. 33).

[52] D. S. Kibalama, "Design and Implementation of a Belted Alternator Starter System for the OSU EcoCAR 3 Vehicle", 2017. [Online]. Available: https://etd.ohiolink.edu/pg%7B%5C_%7D10?::NO:10:P10%7B%5C_%7DETD%7B%5C_%7DSUBID:151537 (cit. on p. 33).

[53] Bosch, *Bosch SMG 180/120 electric motor: compact powerhouse - Bosch Media Service*. [Online]. Available: https://www.bosch-presse.de/pressportal/de/en/bosch-smg-180-120-electric-motor-compact-powerhouse-42158.html (visited on 06/26/2020) (cit. on p. 34).

[54] AAM, *Electric Drive Technology by AAM*. [Online]. Available: https://www.aam.com/what-we-do/our-technologies/electric-drive-technology (visited on 06/26/2020) (cit. on p. 34).

[55] K. Niste, "Volvo Cars , Plug-In Hybrid Concept Development", 2009 (cit. on p. 34).

[56] Argonne National Labratory, "EcoCAR Mobility Challenge Y1 Event Rules Rev L", Tech. Rep., 2019 (cit. on pp. 36, 40).

[57] Davies Craig, *EWP80*. [Online]. Available: https://daviescraig.com.au/product/ewp80-12v-80lpm21gpm-remote-electric-water-pump-8105/

`ewp80-electric-water-pump-12v-8105` (visited on 07/08/2020) (cit. on p. 46).

[58] ISO, "BS ISO 6336-2:2006 Calculation of load capacity of spur and helical gears — Part 2: Calculation of surface durability (pitting)", 2006 (cit. on p. 59).

[59] ——, "BS ISO 6336-3:2006 Calculation of load capacity of spur and helical gears — Part 3: Calculation of tooth bending strength", 2006 (cit. on p. 59).

[60] SKF Group, "Rolling Bearings Catalogue", 2018. [Online]. Available: `skf.com/go/17000` (cit. on pp. 68, 69).

[61] R. Lau, "Design , Implementation , and Testing of a High-Power Electrified Powertrain for an American Muscle Car", 2017 (cit. on p. 70).